5-2023

Starch Granule and Crystalline Structures with Relation to Enzyme Digestibility

Ana Isabel Gonzalez Conde
University of Arkansas-Fayetteville

Starch Granule and Crystalline Structures with Relation to Enzyme Digestibility

A dissertation submitted in partial fulfillment
of the requirements for the degree of
Doctor of Philosophy in Food Science

by

Ana Gonzalez Conde
Universidad de Córdoba
Bachelor of Science in Food Engineering, 2014
University of Arkansas
Master of Science in Food Science, 2017

May 2023
University of Arkansas

This dissertation is approved for recommendation to the Graduate Council.

_____
Ya-Jane Wang, PhD
Dissertation Director

_____
Sun-Ok Lee, PhD
Committee Member

_____
Ali Ubeyitogullari, PhD
Committee Member

_____
Suresh Kumar, PhD
Committee Member

_____
Xianghong Qian, PhD
Committee Member

ABSTRACT

Porous starch produced by enzyme hydrolysis has attracted much attention for its adsorption and delivery properties. Porous starch has been successfully prepared from A-type starch, but not from B-type and C-type starches, which is partly attributed to the surface and crystalline structure. The present study aimed to characterize the role of the crystalline structure and the structure-function relationship impacting the susceptibility of starch with different crystalline polymorphs to amylase digestion. The starches were subjected to chemical modification (acid hydrolysis or surface gelatinization), physical modification (heat-moisture treatment, HMT, or high-pressure processing, HPP) or their combinations prior to amylase digestion, and the physiochemical properties of the resultant starches were characterized. Both acid hydrolysis and surface gelatinization removed densely packed crystallites to improve amylase binding and the digestion degree, resulting in the formation of a porous structure in potato starch. Combined acid hydrolysis and HMT reduced the amylase digestion degree of all three starches by increasing their thermal stability and crystallinity from hydrolyzed starch chains that reorganized into more thermally stable structures. The strong electrostatic interaction of sodium sulfate with water molecules decreased the gelatinization degree during HPP, and generally decreased the α-amylase digestion degree compared to HPP in water for all three starches. However, the competition for the water in the starch crystallites and the restricted association of gelatinized starch from reduced free water in sodium sulfate allowed the formation a porous structure in corn and potato starches and their partial transition to a C-like polymorph. The results demonstrate that the combination of chemical or physical modification and alpha-amylase digestion was capable of producing porous starch from B-type starches. This study will

help develop porous starch with new properties for applications in food, pharmaceutical and agricultural industries.

ACKNOWLEGMENTS

I would have not been able to complete this degree without the guidance and mentoring of Dr. Ya-Jane Wang. Her support, patience, and work ethic made me believe I could continue and achieve great things. Thanks to Dr. Wang, I understood the value of scientific thinking and how constant self-challenge can overcome any fear.

Secondly, I would like to recognize Dr. Lee, Dr. Ubeyitogullari, Dr. Kumar, and Dr. Qian for their constant support and guidance.

My most sincere appreciation to the carbohydrate chemistry laboratory former and current members, Jia-Rong Jinn, Michelle Opong Siao, Pam Wunthunyarat, and Anne Janasch. I could not have asked for a better team. Thank you for listening during the hard times and encouraging me to keep going.

All my love and thanks to Evelyn and Bronson Stilwell, Charles and Carol Axtell, and Doug and Tammy Tyler, which adopted me as a daughter and a friend, showing that love has many forms and is beyond cultural differences.

To my friends, Hernando, Mayra, Bailey, Trent, Delmy, Sara, Shilpa, Inah, Carlos, Ragita, Hans, and John. Thank you for your support and constant cheering every step of the way.

Finally but not least important, Mom, Dad, Anto, Carlos, and Ryan. You are my inspiration and greatest motivation. Your constant effort and understanding got me through the hard and the good times. I could not have asked for better role models. You gave me the best of everything, love, patience, kindness, and a home.

TABLE OF CONTENTS

LIST OF TABLES

LIST OF FIGURES

LIST OF SUPPLEMENTAL MATERIAL

LIST OF PAPERS

Gonzalez, A., & Wang, Y.-J. (2020). Enhancing the formation of porous potato starch by combining $\boldsymbol{\alpha}$-amylase or glucoamylase digestion with acid hydrolysis. *Starch – Stärke*, 72, 1900269. Published. (Chapter 3).

Gonzalez, A., & Wang, Y.-J. (2021). Surface removal enhances the formation of a porous structure in potato starch. *Starch – Stärke, 73*, 2000261. Published. (Chapter 4).

Gonzalez, A., & Wang, Y.-J. (2023). Effects of acid hydrolysis level prior to heat-moisture treatment on properties of starches with different crystalline polymorphs**.** Submitted. (Chapter 5).

Gonzalez, A., & Wang, Y.-J. (2023). Effects of suspension media on the properties of high pressure treated starches with different crystalline polymorphs. To be submitted. (Chapter 6).

CHAPTER 1

INTRODUCTION

Porous starch has received increasing attention because of its absorption and protection ability in many food and pharmaceutical applications. Porous starch has been prepared from A-type starches using amylase digestion or combinations of amylase digestion and physical or chemical treatments but has not been prepared from B-type or C-type starches. The differences in the susceptibility to enzyme digestion among starches and consequentially in the formation of porous starch have been attributed to their differences in granule surface structure, amylopectin chain length distribution, and crystalline type (Gallant et al., 1992).

Starch is classified as A-, B-, or C-type according to the crystalline structure, and in general native A-type starch granules exhibit a greater susceptibility to amylases than B- and C-type starch granules (Jane, Wong, and McPherson. 1997; Planchot, Colonna, and Buleon, 1997). It has been shown that the surface of A-type starch granules, such as common corn, comprises characteristic micropores and channels that facilitate enzyme binding and mobility through the granules and thus enhance the digestion rate (Fannon, Huber, and BeMiller, 1992; Huber and BeMiller, 1997). In contrast, B-type starch granules, such as potato, are devoid of surface channels and micropores and display considerably lower susceptibility to amylases (Gallant, Bouchet, Buleon, and Perez, 1992). B-type starches are characterized by the presence of a larger proportion of long amylopectin chains and consequentially a more perfect crystalline structure, whereas A-type starches comprise a larger proportion of shorter chains that are more susceptible to amylase digestion. C-type starches display a molecular structure and susceptibility to amylase digestion between that of A- and B-type starches (Dhital, Shrestha, and Gidley, 2010; Shrestha et al., 2012).

The combination of chemical or physical treatments such as acid hydrolysis, heat-moisture treatment, or high-pressure processing, with enzyme digestion has been shown to influence the formation of a porous structure in A-type starches (Latip, Samsudin, Utra, and Alias, 2021). However, there is little information available about the effect of combined treatments on the surface and crystalline structure of different polymorphs. It was hypothesized that improving the digestibility of starch by chemical, physical methods, or their combination would promote the formation of a porous structure in B and C-type starches and at the same time provide a better understanding of their differences in molecular/granular structures contributing to their different responses. The dissertation is presented in a "published/to-be submitted papers" format, where each chapter is a stand-alone paper that has been published, in review, or in preparation for submission to a peer-reviewed journal. The objectives of this dissertation included as follows:

1. Chapter 3… To enhance the formation of porous potato starch by combining α-amylase or glucoamylase digestion with acid hydrolysis.
2. Chapter 4… To evaluate the effect of surface removal to enhance the formation of a porous structure in potato starch.
3. Chapter 5… To examine the effects of acid hydrolysis level prior to heat-moisture treatment on properties of starches with different crystalline polymorphs.
4. Chapter 6… To investigate the effects of suspension media on high pressure treated starches with different crystalline polymorphs.

REFERENCES

Cai, L., & Shi, Y. (2013). Self-assembly of short linear chains to A- and B-type starch spherulites and their enzymatic digestibility. *Journal of Agricultural and Food Chemistry, 61*, 10787–10797.

Cai, L., & Shi, Y. (2014). Preparation, structure, and digestibility of crystalline A- and B-type aggregates from debranched waxy starches. *Carbohydrate Polymers, 105*, 341–350.

Dhital, S., Shrestha, A. K., & Gidley, M. J. (2010). Relationship between granule size and in vitro digestibility of maize and potato starches. *Carbohydrate Polymers, 82*, 480–488.

Fannon, J., Hauber, R., & Bemiller, J. (1992). Surface pores of starch granules. *Cereal Chemistry, 69*, 284–288.

Gallant, D., Bouchet, B., Buleon, A., & Perez, S. (1992). Physical characteristics of starch granules and susceptibility to enzymatic degradation. *European Journal of Clinical Nutrition, 46*, S3–S16.

Huber, K., & BeMiller, J. (1997). Visualization of channels and cavities of corn and sorghum starch granules. *Cereal Chemistry, 74*, 537–541.

Jane, J., Wong, K., & McPherson, A. E. (1997). Branch-structure difference in starches of A- and B-type X-ray patterns revealed by their naegeli dextrins. *Carbohydrate Research, 300*, 219–227.

Latip, D.N. H., Samsudin, H., Utra, U., & Alias, A.K. (2021). Modification methods toward the production of porous starch: a review. *Critical Reviews in Food Science and Nutrition, 61*, 2841–2862.

Pan, D., & Jane, J. (2000). Internal structure of normal maize starch granules revealed by chemical surface gelatinization. *Biomacromolecules, 1*, 126–132.

Planchot, V., Colonna, P., & Buleon, A. (1997). Enzymatic hydrolysis of α-glucan crystallites. *Carbohydrate Research, 298*, 319–326.

Shrestha, A. K., Blazek, J., Flanagan, B. M., Dhital, S., Larroque, O., Morell, M. K., Gilbert E., & Gidley, M. J. (2012). Molecular, mesoscopic and microscopic structure evolution during amylase digestion of maize starch granules. *Carbohydrate Polymers, 90*, 23–33.

Srichuwong, S., Isono, N., Mishima, T., & Hisamatsu, M. (2005). Structure of lintnerized starch is related to X-ray diffraction pattern and susceptibility to acid and enzyme hydrolysis of starch granules. *International Journal of Biological Macromolecules, 37*, 115–121.

CHAPTER 2

LITERATURE REVIEW

2.1 Starch components and organization

Starch properties are governed by its composition and structural organization, with the botanical source greatly affecting the size, shape, and fine structure of the granule. Starch granules have a multiscale structure as depicted in Figure 2.1. The building blocks of starch are anhydroglucose units that form two distinct structures, amylose and amylopectin. Amylose is an essentially linear polymer of glucose linked through α-(1→4) glucosidic linkages, whereas amylopectin has a backbone of α-(1→4) glucosidic linkages and ~5.0% branches linked through α-(1→6) glucosidic linkages. Depending on the botanical source, starch comprises 1-2% of other components, e.g. lipids, proteins, and minerals, which greatly affect starch physicochemical properties (Tester, Karkalas, and Qi, 2004; Jane, 2009).

Regardless of the botanical source, native starch granules consist of growth rings that display an alternating distribution of crystalline and amorphous originating from the hilum towards the surface. The semi-crystalline nature of the growth rings is made up of blocklets, which in turn are organized by amylose and amylopectin into crystalline and amorphous lamellae with a repeat distance of 9-11 nm regardless of the starch type. The crystalline lamellae are composed of cluster of amylopectin chains forming double helical configurations, whereas the amorphous lamellae comprise mainly amylopectin branch points and amylose (Jenkins and Donald, 1995; Gallant, Bouchet, and Baldwin, 1997; Tester, Karkalas, and Qi, 2004; Vandeputte and Delcour, 2004; Pérez and Bertoft, 2010).

2.1.1 Amylopectin

Amylopectin is a large molecule with a molecular weight between 10^7-10^9 g/mol and an average degree of polymerization by number (DP_n) 9600-15,900. In contrast to amylose, a greater variability is observed in amylopectin in terms of unit chain length (CL) and branching pattern. The structure of amylopectin has been described as a cluster of interconnected individual chains classified in terms of their location and CL (Figure 2.2). The most external chains, i.e A chains, are linked to B-chains through α-(1→6) glucosidic linkages. The B-chains can be linked to other B-chains when they are across 1, 2, and 3 clusters, respectively, are classified from B1 to B3. The average DP in anhydroglucose unit of A chains is 6-12, whereas, for B1, B2, B3, the average DP is 13-24, 25-36, and >37, respectively. The chain carries the only reducing group in amylopectin is termed C chain (Hizukuri, 1985, 1986; Morrison and Karkalas, 1990; Hanashiro, Abe, and Hizukuri, 1996).

2.1.2 Amylose

The molecular weight of amylose is approximately 10^5-10^6 g/mol DP_n between 324–4,920 (Morrison and Karkalas, 1990). The amylose content is affected by the botanical source and ranges from 0% in waxy starches to > 40% in high-amylose starches. The amylose content is also affected by the granule size within the same type of starch, with larger granules characterized by a greater amylose content. Amylose is synthesized after amylopectin synthesis and can be found in both the amorphous and crystalline regions of the granule (Jane, Xu, Radosavljevic, and Seib., 1992; Kasemsuwan and Jane, 1994; Tatge, Marshall, Martin, Edwards, and Smith,1999). In addition, amylose is not evenly distributed in the granule. Jane and Shen

(1993) and Pan and Jane (2000) showed that a greater concentration of amylose was present towards the granule periphery using surface gelatinization.

2.2 Crystalline structure

The external amylopectin chains form double helices that arrange into crystalline structures. Four types of crystalline structures, A-, B-, C-, and V-type, have been identified using X-ray diffractometry, with native starches containing between 15 to 45% of relative crystallinity (Zobel, 1988). The differences among these structures are ascribed to the water content, the packing of the double helices, and the geometry of the single cell units as illustrated in Figure 2.3. The A-type structure is characterized by a relatively compact organization with less water content (8 water molecules per unit) with strong peaks at reflection angles (2θ) 15.3°, 17.1°, 18.2°, and 23.5°, and it is generally found in cereal starches. In contrast, the B-type structures has a more open arrangement (hexagonal cell units) with 36 water molecules and diffraction peaks at 5.59°, 14.4°, 17.2°, 22.4°, and 24.0° (Figure 2.4), and is characteristic of tubers and high amylose starches (Hizukuri, Kaneko, and Takeda, 1983). The C-type polymorph has been suggested to be a combination of the A- and B-type crystallites with strong diffraction peaks at 3.73°, 15.3°, 17.3°, and 23.5°, and is typically found in legumes. The V-type is only observed when amylose forms inclusion complexes with non-polar molecules and some organic solvents, and displays strong peaks at 7.8°, 13.5°, and 20.9°. The A-type pattern is associated with an average CL of approximately 26, the average CL for the B-type is approximately 36, and an intermediate CL of 28 has been associated with the C-type (Imberty and Perez, 1988; Zobel, 1988).

2.3 Mechanisms of starch digestion by enzymes

Starch-hydrolyzing enzymes are used to analyze starch structure as well as for industrial production of glucose, maltose, oligosaccharides, and modified starches, with the most common enzymes being α-amylase, β-amylase, and glucoamylase (Haki and Rakshit, 2013). The extent and susceptibility of starch granules to enzyme digestion are governed by factors such as starch botanical source, enzyme origin, temperature, pH, and enzyme and substrate concentration. The enzymatic hydrolysis of starch granules is a heterogeneous reaction that involves the diffusion of the enzyme to the solid granule surface, followed by the adsorption onto the granule surface, and finally the degradation of starch chains. The average size of a starch granule is approximately 3000 times larger than that of amylase, offering many sites for the adsorption. Nevertheless, the enzyme adsorption onto the granule surface could be non-specific, thus hydrolysis only occurs when consecutive glucose molecules are perfectly accommodated into the enzyme active site (Payan, 1980; Leloup, Colonna, and Ring, 1991; Colonna, Leloup, and Buleon, 1992).

2.3.1 Alpha-amylase

Alpha-amylase is an endo-hydrolyzing enzyme present in animals, plants, and microorganisms, and its action concentrates in the α-(1→4) glucosidic linkages of amylose and amylopectin internal chains. The hydrolysis pattern of α-amylase follows three distinct mechanisms, single chain, multichain, and multiple attacks, which depend on the origin of the enzyme and its active site spatial configuration. In the single chain attack mechanism, the enzyme hydrolyzes starch chains in a “zipper” towards until the end of the chain. In the multichain and multiple action attack mechanisms, the enzyme hydrolyzes one bond and multiple α-(1→4) glucosidic bonds per active encounter, respectively (Robyt and French, 1967).

2.3.2 Beta-Amylase

The known β-amylases are primarily isolated from plant sources such as sweet potato, soybean, barley, and wheat, and have an exo-hydrolyzing α-(1→4) glucosidic linkages mechanism that changes the configuration of the anomeric carbon. The hydrolysis proceeds from the non-reducing end, and because the enzyme cannot bypass α-(1→6) linkages, the hydrolysis of amylopectin yields approximately equal amounts of maltose and β-limit dextrin (Xie, Liu, and Cui, 2005).

2.3.3 Glucoamylase

Glucoamylase is an exo-acting enzyme that can hydrolyze both α-(1→4) and α-(1→6) glucosidic linkages, with the hydrolysis of α-(1→4) linkages being preferred. The enzyme action results in the complete conversion of starch to D-glucose through a multi-chain mechanism. The mechanism of hydrolysis requires that the remaining starch chain leaves the active site after the first cleavage before glucose can be released. The most common glucoamylases are isolated from fungi such as *Aspergillus niger* and *A. awamori.*, and germinated grains (Meagher, Nikolov, Reilly, 1989; Robyt, 2009).

2.4 Factors affecting starch digestibility

The mechanisms limiting the enzymatic digestion of starches can be classified into two groups: firstly, naturally present barriers such as proteins, lipids, and cell walls that prevent enzyme binding to starch granule, and secondly, starch granule multi-scale structure that prevents or delays the hydrolytic action of enzymes after the biding (Dhital, Warren, Butterworth, Ellis, and Gidley, 2017). The bran layer components in whole grains serve as

natural barriers to prevent enzyme diffusion and effective binding, and consequentially to reduce enzymatic digestion (Bird, Lopez-Rubio, Shrestha, and Gidley 2009). Among starch granule features and structure, the granule morphology (Brewer, Cai, and Shi, 2012; Shrestha et al., 2012), the arrangement of crystalline and amorphous structures (Planchot, Colonna, Gallant, and Bouchet, 1995), the blocklets size (Gallant, Bouchet, and Baldwin, 1997), amylose and amylopectin structure (Jane et al., 1997; Srichuwong et al., 2005), and the type and perfection of crystallites exert great influences in the extent and rate of enzyme digestion (Jane, Wong, and McPherson, 1997; Gallant, Bouchet, and Baldwin, 1997; McCleary and Monaghan, 2002). However, the intercorrelation among the granule structures makes the underlying mechanism behind starch digestion difficult to elucidate (Bird, Lopez-Rubio, Shrestha, and Gidley., 2009).

2.4.1 Granule morphology

Starch granules vary in size even for the same source, and size is known to be an important factor controlling the digestion rate of native starch granules. Starch granules range from <3 μm to >100 μm in size, and both unimodal and bimodal distributions are observed (Tester, Karkalas, and Qi, 2004). Franco do Rio Preto, and Ciacco (1992) studied the susceptibility of corn and cassava starches to α-amylase and glucoamylase digestion in relation to their sizes by separating starch granules into three fractions. They found that granules larger than 16 μm displayed a lower hydrolysis than those smaller than 10 μm and that the hydrolysis pattern varied with granule size as well. Larger granules showed evident corrosion on the surface mainly in the axial axis, whereas smaller granules displayed surface corrosion with subsequentially solubilization of the granule.

The initial rate of hydrolysis of corn, potato, and rice starches was found to be inversely proportional to the granule size in the order rice > corn > potato when treated with porcine pancreatic α-amylase (Kong, Kim, Kim, and Kim, 2003). Dhital, Shrestha, and Gidley (2010) fractionated potato and common corn starch granules into five and four fractions, respectively, and observed that larger potato starch granules displayed a hydrolysis rate three times lower than that of smaller granules. Smaller granules of corn starch were digested to a greater extent than larger ones, but the difference was not as broad as for the fractionated potato starch granules. Tahir, Ellis, and Butterworth (2010) studied the kinetic parameters of the digestion by α-amylase of wheat, potato, and rice starches in relation to their surface area, and suggested that granules with large diameter provide smaller surface area per unit weight, and therefore are poor substrates regarding the catalytic efficiency. Similarly, Warren, Royall, Gaisford, Butterworth, and Ellis (2011) observed that potato starch smaller surface area compared to common corn, wheat, waxy rice decreases the digestion efficiency, additionally they suggested that high gelatinization enthalpies were associated with low enzyme binding/adsorption because of the greater proportion of packed crystalline material that rendered enzyme access to glucan chains.

2.4.2 Granule surface pores and channels

Unlike tuber starches, cereal starches possess pores and channels which function is associated with the regulation of the enzymatic conversion of starch into glucose during the germination of seed or starch granule synthesis (Fannon et al, 1993), as revealed b by confocal laser scanning microscopy (CLSM) (Figure 2.5). The presence of pores and channels was reported to contribute to the increase in surface area of A-type starches (Fannon, Hubber, and Bemiller, 1992; Fannon, Shull, and Bemiller, 1993; Hubber and BeMiller, 1997), therefore A-

type starches such as common corn are more susceptible to enzymatic degradation than B-type starches such as potato starch. The channels range from 0.007 to 0.1 μm, and the pores openings are in the range of 0.1 to 0.3 μm, which would allow enzymes such as α-amylase to diffuse into starch granules (Payan et al., 1980; Planchot and Colonna, 1995).

The action pattern of amylases in A-type starches, which display pores and channels, is commonly known as "inside out" because of the easy access of to the disorganized hilum area. Scanning electron microscopy (SEM) photographs of waxy and common starches treated with α-amylase showed a layered structure with a porous-like appearance as a result of the endo-erosion. For starches lacking pores and channels, the action pattern is described as "exo pitting" or "outside in" because the enzyme cannot pass the impermeable surface, therefore its adsorption takes place on the granule surface where the enzyme tries to break through in order to diffuse into the granule, resulting in granule breakage (Gallant, Bouchet, Buleon, and Pérez, 1992; Helbert, Schulein, and Henrissat, 1996; Sarikaya, Higasa, Adachi, and Mikami, 2000). O'Brien and Wang (2002) compared the hydrolysis pattern of α-amylase and glucoamylase on common corn and potato starch granules and observed that regardless the enzyme type, common corn displayed a defined and more homogeneous porous structure distribution, as well as a greater hydrolysis degree. On the other hand, potato starch granules did not exhibit an evident porous structure but rather collapsed granules and lower hydrolysis degree (Figure 2.6).

2.4.3 Crystalline structure

Starch crystalline structure is the result of a specific configuration of glucan chains and is largely influenced by amylose and amylopectin chain lengths as well as their distribution within the granule. In general A-type starches, such as common corn, are more susceptible to enzymatic

hydrolysis compared to B- and C-type starches, such as potato and pea starch, respectively (Colonna, Leloup, and Buleon, 1992; Gallant, Bouchet, Buleon, and Pérez, 1992; Planchot, Colonna, and Buleon, 1997).

The enzymatic hydrolysis of native starch granules occurs in two stages, an initial fast hydrolysis of the amorphous regions, followed by a slower hydrolysis of the crystalline regions of the granule (Franco, Ciacco, and Tavares, 1988; Hoover and Vasanthan, 1993). The average chain length of amylopectin from A-, B-, and C-type starches is in the DP ranges of 19-28, 29-31, and 25-27, respectively. The amylopectin of B-type starches comprises a greater proportion of B2 and B3 chains, and a lower proportion of A and B1 chains (Hizukuri, Kaneko, and Takeda, 1983; Hizukuri 1985). The longer chains extend through multiple crystals, and the branching points are clustered in the amorphous lamellae; hence the crystalline structure of B-type starch granules is more stable and resistant toward enzymatic hydrolysis. In contrast, the enzymatic susceptibility of A-type starches has been linked to the greater proportion of short amylopectin chains and the least stable crystalline lamellae, product of the scattered distribution of the branching points (McPherson and Jane, 1999; Jane et al., 1999).

Gérard, Colonna, P., Buléon, and Planchot (2001) analyzed the enzyme susceptibility of corn starch mutants that covered a range of granules with A-, B-, and V-type allomorphs, and observed that even though the granules differed in amylose content and relative crystallinity, granules with B-type starches were evidently more resistant to the hydrolytic activity of porcine pancreatic α-amylase. After 5 h of hydrolysis, A-type granules reached more than 70% hydrolysis, whereas B-type and C-type granules reached approximately 35% and 60% hydrolysis, respectively. Analysis of the hydrolysis products of the digested B-type starches showed that the residues were a mixture of amorphous material and B-type crystallites. They

suggested that the enzyme susceptibility of B-type starches depended not only on the type of crystallites but on the distribution of those crystallites within the granule. Similar results were observed by Ratnayake, Hoover, Shahidi, Perera, and Jane (2001) when C-type (A- and B-type mixture) field pea starches with a greater proportion of B-type crystallites displayed a lower hydrolysis extent.

Gallant, Bouchet, and Buleon (1992) suggested that alongside the type of crystalline structure, the thick surface layer, product of stacked blocklets as observed by SEM, is involved in the resistance to enzyme digestion of B-type starches. Baldwin, Adler, Davies, and Melia (1998) studied the surface structure of potato and wheat starches using atomic force microscopy (AFM) and low voltage scanning electron microscopy (LVSEM) and also concluded that potato starch comprised larger (200-500 nm) and more perfectly organized blocklets towards the surface, compared to the smaller blocklets of wheat starch. The differences in blocklet size and distribution have been associated with the susceptibility of native starches to enzyme digestion. Lin et al. (2006) observed that the α-amylase hydrolysis of lotus rhizome starch, a C-type starch, resulted in granules with a hollow interior, which was concentrated in one end of the granule. This action pattern was suggested to be the product of the fast hydrolysis of loosely packed crystalline lamellae and small blocklets towards the center of the granule, whereas the periphery containing a tightly packed larger blocklets showed little erosion, similar to the digestion of potato starch.

2.4.4 Gelatinization and Retrogradation

When starch is gelatinized, the granule structure transitions from a semi-crystalline state to an amorphous state. Over time and as the temperature decreases, the amorphous structure is

transformed into a more ordered state, which is termed retrogradation (Figure 2.7). During retrogradation, starch chains present as random coils reassociate to become A- or B-type crystallites depending on the temperature and the average chain length; chains with DP 12-13 will yield the A-type polymorph when recrystallized at ~50°C, while chains of DP >13 result in B-type crystallites at crystallization temperatures 2-25°C (Cai and Shi, 2013), which are very stable and correlate with increased resistance to enzymatic hydrolysis (Gidley and Bulpin, 1987; Gidley et al., 1995; Eerlingen and Delcour, 1995)

Jane and Robyt (1984) showed that the digestion of retrograded amylose with α-amylase from *Bacillus subtilis* resulted in amylodextrins with an average DP of 50. The length of the enzyme resistant residues was correlated with the number of binding subsites of α-amylase due to its inability to hydrolyze glucose units close to the crystalline regions. Witt, Gidley, and Gilbert (2010) investigated the susceptibility to α-amylase digestion of debranched waxy, common, and high-amylose corn starches, and observed that a remnant fraction of linear dextrins (DP 50) was involved in the reduced digestibility properties of the high amylose starches due to the formation of a highly organized crystalline structure that is not accessible to the enzyme. Teng, Witt, Wang, Li, and Hasjim (2016) observed a similar structure in the remaining dextrins of native waxy corn, common corn, high-amylose, and potato starch that were subjected to similar digestion conditions.

2.5 Surface gelatinization

Chemical surface gelatinization is a technique that has been used to analyze the internal structure of common corn and potato starches using salts of different concentrations. The most commonly used salts are lithium chloride (LiCl) and calcium chloride ($CaCl_2$), and both have

been shown to cause the gelatinization of the granules from the periphery towards the interior. Jane (1993) suggested that the mechanism of starch gelatinization in salt solution involves two effects: structure-making and structure-breaking effects on water, and the electrostatic interaction between the salt ions and starch hydroxyl groups. Hydrogen bonds between water molecules are promoted by the high charge density of the ions, hence the diffusion of water through the granule is retarded. The increase in electrostatic interactions increases the solution viscosity, which contributes to the decreased diffusion of the salt solution, resulting in the preferred gelatinization of the granule surface due to the significant heat generated by the high concentration of ions and their attraction to starch -OH groups. The rate and extent of surface gelatinization depend on the botanical source of starch and the amylose/amylopectin composition, although the exact location of the salt attack on the granule is not clear. Koch and Jane (2000) used 4 M $CaCl_2$ solution to induce 50-70% chemical surface gelatinization of potato, waxy potato, sweet potato, common corn, high amylose corn, waxy corn, wheat, normal barley, high-amylose barley, waxy barley, and rice starches. Normal potato, waxy potato, sweet potato, corn, and high amylose corn starches displayed an evenly gelatinized surface, whereas wheat, barley, and high-amylose barley starches were gelatinized at specific parts of the granules. The analysis of the gelatinized fractions and the remaining granules demonstrated that amylose tended to be located towards the surface of the granules and that the amylopectin chains distribution was non-uniform, with longer B-chains located in the granule core (Pan and Jane, 2000; Kuakpetoon and Wang, 2007).

The surface gelatinization of potato and waxy potato starches, both displaying B-type crystalline structure resulted in granules with a shell-like structure (Figure 2.8), although the remaining granules of waxy potato starch appeared smoother than normal potato starch granules. Huang et al. (2014) suggested, based on SEM and AFM observations of the remaining granules,

that the structural packing of waxy potato starch was ordered with smaller and more uniform blocklets with similar distribution on the surface and near the hilum, whereas normal potato starch displayed greater surface blocklets, and the distribution is significantly different from that of the inner granule structure.

More recently, Bartz, Zavareze, and Dias (2017) used surface gelatinization with LiCl to analyze internal structural changes in potato starch granules after heat-moisture treatment. They observed that at 24% moisture content the proportion of amylose was greater at the granule periphery, but granules treated at 12, 15, 18, and 21% moisture displayed greater amylose content towards the granule core. The relative crystallinity of the surface gelatinized starches treated at lower moisture contents increased after 30% surface removal, whereas that of the surface gelatinized starch treated at 24% moisture granules only showed an increase in the periphery. The results suggested that the heat-moisture treatment had a significant effect in starch structure and that chemical surface gelatinization provided evidence of the changes in the internal structures of the granule. Although surface gelatinization can elucidate starch structure and properties, there are no available reports on the enzyme digestibility of surface gelatinized starch.

2.6 Acid hydrolysis

Acid treatment of starches has been used to produce modified starch, glucose syrup, low molecular weight dextrins, nanoparticles and nanocrystals from starch. Traditionally when sulfuric acid (H_2SO_4) is used, the final products are known as low molecular weight Nägeli dextrins (Nägeli, 1874), but when hydrochloric acid (HCl) is used, lintnerized starches are produced (Lintner, 1886). Depending on the extent of the acid hydrolysis, intact A or B-type

crystallites that are resistant to acid attack will be produced. During acid hydrolysis, the hydroxonium ion (H_3O^+) first attacks the oxygen present in α-(1→4) glucosidic linkage, and then an unstable high-energy carbocation is generated after the carbon-oxygen electron transference between bonds takes place. Finally, the unstable carbocation reacts with water, a Lewis base is generated, and the hydroxyl group is regenerated (Figure 2.9).

It is generally recognized that starch solubilization in acid follows a two-stage process. The first stage exhibits a relatively fast hydrolysis rate in which the amorphous regions of the granules are degraded; the second stage corresponds to the hydrolysis of the crystalline regions at a slower hydrolysis rate (Mussulman and Wagoner, 1968). The slower hydrolysis rate of the crystalline regions is associated with the denser packaging of double helices in the crystalline lamellae which prevents the acid-ion penetration. Furthermore, the crystalline arrangement keeps the glucosyl units locked in a chair conformation, and for the hydrolysis to take place a change from chair to half-chair configuration is required (Kainuma and French, 1971; Hoover, 2000). The time to achieve partial or complete hydrolysis depends on the botanical source, but in general is considered a lengthy process, and as the hydrolysis progresses the relative crystallinity of the products tends to increase.

The effect of acid hydrolysis on starch properties depends on the extent of the treatment and the type of starch. The differences in susceptibility to acid hydrolysis among starches have been partly attributed to their differences in the distribution of α-(1→6) glucosidic linkages between the amorphous and crystalline regions (Jane, Wong, and McPherson, 1997) and the extent of starch chain interactions within the amorphous and crystalline domains of the granule (Hoover, Swamidas, and Vasanthan, 1993). Jane, Wong, and McPherson (1997) characterized the Näegeli dextrins and debranched Näegeli dextrins of A-type and B-type starches and

concluded that the A-type starches had branch points distributed in both amorphous and crystalline regions, whereas the B-type starch displayed branch points clustered in the amorphous region. Because of this distribution, the branch linkages present in the crystalline region were protected during the acid hydrolysis, but those present in the amorphous region were more susceptible to the acid hydrolysis. Hoover, Swamidas, and Vasanthan (1993) suggested that the extent of acid hydrolysis is affected by the interactions of starch chains in both the amorphous and crystalline lamellae, after they compared a number of separate studies in which the extent of acid hydrolysis of different legume starches (Biliaderis, Grant, and Vose, 1981; Hoover, Rorke, and Martin, 1991) did not correlate with amylose contents ranging from 28.5% to 64%.

Srichuwong, Isono, Mishsima, and Hisamatsu (2005) studied the α-amylase digestion of the residues of A-, B-, and C-type starches after they were hydrolyzed by 2.2 M HCl at 35°C for 12 days. They found that the susceptibility to α-amylase digestion followed the order A- > C- > B-type starches, and α-amylolysis was enhanced by the acid treatment. They hypothesized that the acid hydrolyzed the α-(1→6) branching points and intercluster chains of the amorphous lamellae, thus increasing the access of α-amylase to the internal structures of the crystallites. Furthermore, they hypothesized the resistance of both acid residues and native B-type granules to α-amylolysis was related to the greater proportion of long chains and the clustered distribution of branching points in the amorphous lamellae of B-type crystallites. A similar trend was reported by Zhang, Venkatachalam, and Hamaker (2006) using a combination of α-amylase and glucoamylase on acid-hydrolyzed common corn (60%, 70%, and 85%) and potato (82%) starches. They observed increased digestion of all acid-hydrolyzed starches, with potato starch displaying an increase of ~44.0 percentage points.

Most studies (Srichuwong, Isono, Mishsima, and Hisamatsu, 2005; Zhang, Venkatachalam, and Hamaker, 2006; Espinosa-Solis, Sanchez-Ambriz, Hamaker, and Bello-Perez, 2011; Miao, Jiang, Zhang, Jin, and Mu, 2011; Ulbrich, Natan, and Flöter, 2014) have targeted a high degree of acid hydrolysis (>50%) to obtain crystalline residues that the granule structure was no longer present and did not emphasize the formation of a porous starch structure.

2.7 High pressure treatment

High pressure treatments, especially high hydrostatic pressure (HHP), can be traced back to 1899, when milk sanitation was accomplished by reducing the bacterial count applying 680 MPa for 10 min (Hoover, 1993). According to Katopo, Song, and Jane (2002), the application of HPP in starch research can be classified in three categories: treatments with lower pressures that do not induce gelatinization, treatment with low and high pressure in dry starches, and ultra-high pressure (UHP) treatment (>400 MPa) in starches with excess water.

The HHP treatment is classified as non-thermal modification method of starch and have attracted much attention because it can be used to produce physically modified starches and HHP-gelatinized starches, which display properties that are different from those of heat-gelatinized starches (Pei-Ling, Qing, Qun, Xiao-Song, and Ji-Hong, 2012). For instance, HHP-treated starches maintain the granule structure after the treatment (Stolt, Oinonen, and Autio, 2001) and display an increased content of slowly digestible starch fraction (Selmi, Marion, Perrier Cornet, Douzals, and Gervais, 2000). Various combinations of pressure, temperature, starch concentration, and holding times have been investigated to understand the mechanism behind the changes in the physicochemical properties of HHP-starch, with the majority of the studies focusing on starch-water suspension in excess water (30-99.6% w/w) where the main

effect is a pressure induced gelatinization (Liu, Selomulyo, and Zhou, 2008). During HHP in excess water, a reversible hydration of the amorphous regions takes place, while the crystalline structure undergoes irreversible disruption.

A water-wheat starch suspension (5% solids) was subjected to HHP treatment of 600 MPa at 25°C for 15 min, resulting in complete gelatinization of the suspended starch (Douzals, Perrier Cornet, Gervais, and Coquillet, 1998). Stolt, Oinonen, and Autio (2001) studied the kinetic of pressure induced gelatinization of barely starch at concentrations of 10 and 25% over a pressure range of 400 to 550 MPa, and concluded that the changes in granule microstructure, crystalline structure, and rheological properties were time and pressure dependent. The impact of HHP in starch granules also depends on the botanical origin and the crystalline structure (Rubens and Haremans, 2000). Cereal starches such as corn, wheat, and rice, which display the A-type crystalline structure, have been found to be highly sensitive to high pressure treatments.

In a range of 400-600 MPa, A-type starches displayed complete gelatinization at room temperature, whereas B-type starches such as potato starch require pressure levels of 650-1000 MPa to obtain similar gelatinization degrees (Bauer and Knorr, 2005; Kawai, Fukami, and Yamamoto, 2007). Furthermore, when subjected to UHP (>500 MPa), A-type crystalline structure was transformed into B-type crystalline structure when suspended in water, while B-type crystalline structure remained unchanged (Hibi, Matsumoto, and Hagiwara, 1993). Katopo, Song, and Jane (2002) subjected common corn and potato starches to a pressure of 690 MPa in dry powder form, 1:1 (v/w), 1:2 (v/w) water to starch suspension, and 1:1 (v/w) ethanol starch suspension for 5 min and 1 h. They observed the change of the crystalline structure of common corn starch from A- to B-type when water was used, as evidenced by the appearance of diffraction peaks at ~5.5° and the merge of the peaks at ~17.5°, but no change was observed

when ethanol was used. No change in the crystalline structure of potato starch was observed regardless of the type of suspension as depicted in Figure 2.10. The granular form of both starches was maintained, although the dry powder form starches displayed significant surface cracking compared to the starches in water and ethanol suspensions.

They suggested that the difference in susceptibility to pressure treatment between A- and B-type starches can be attributed to their differences in amylopectin structure and water content. The 36 water molecules in B-type starches fill up the channels within the localized crystalline unit cells, thus exerting a stabilizing effect of the structure. In contrast, the scattered distribution of branching points in A-type starches results in a flexible structure that allows the reconfiguration of the double helix to permit the introduction of water molecules during the HHP treatment, resulting in the observed transition from A- to B-type crystalline structure. These findings agree with the work of Hibi, Matsumoto, and Hagiwara (1993) and Rubens, Snauwaert, Heremans, and Stute (1999), which suggest that the greater water content in B-type starches reduces its compressibility and the importance of water as a plasticizer of starch molecules. Sevenou, Hill, and Farhat (2002) applied infrared spectroscopy and observed that potato starch and high amylose corn starches displayed a highly organized outer granule surface compared to common corn and waxy corn starches. Later Blaszczak, Valverde, and Fornal (2005) subjected a 10% (w/w) potato starch–water suspension to high pressure at 600 MPa for 3 min, and observed that broken granules displayed a highly condensed outer layer resistant to pressure treatment, whereas the interior displayed visible disrupted fibrillar structures as depicted in Figure. 2.11.

The starch susceptibility to enzyme digestion is also altered by HHP treatment. Mercier, Charbonnière Et, and Guilbot (1968) reported the digestibility of common corn, wheat, and potato starches that were HHP treated at 588.4 MPa was dependent on the moisture content with

potato starch displaying a greater resistance to digestion by α- and β-amylase. Hayashi and Hayashida (1989) subjected a 5% (w/w) starch suspension to high pressure at 490.33 MPa between 20 min and 17 h, and observed an increase in the susceptibility of corn and wheat starches to amylases, however, the increase was not as significant for potato starch. They attributed the lower digestibility of potato starch to a change in granule structure during extended HPP but did not elaborate what structures was involved. Later, Takahashi, Kawauchi, Suzuki, and Nakao (1994) observed significant increase in common corn starch digestibility by glucoamylase when starches were treated at pressures >400 MPa. They suggested that at pressure >400 MPa the granule interior becomes amorphous and thus the enzyme interacts more strongly with the disorganized structure. Recently, Shen et al. (2018) showed that at pressures <400 MPa the digestibility of high amylose corn starches was reduced, but as the pressure increased up to 600 MPa the digestibility increased. The data acquired through small-angle X-ray scattering (SAXS) and wide-angle X-ray scattering (WAXS) showed that an increase in the thickness of the amorphous lamellae took place as water molecules diffused in the helix between crystalline units, and that the HPP mainly affected the amylose amorphous background and the amylopectin amorphous lamellae. They suggested that at pressures <400 MPa the crystalline lamellae tighten, and the digestibility consequently decreased; in contrast at higher pressures the crystalline and amorphous lamellae are destroyed, thus resulting in an increased digestibility.

2.8 Heat-moisture treatment

Heat-moisture treatment (HMT) is a physical modification of starch, which comprises the heating of starch granules at moisture levels below 35% (w/w) and temperatures between 84-120°C over varying time periods. When subjected to HMT, starch granules morphology,

gelatinization properties, pasting properties, X-ray diffraction pattern, retrogradation properties, enzyme digestibility, and susceptibility to acid hydrolysis are greatly affected. The extent of change is dependent on the botanical source, with tuber starches such as potato starch being more susceptible to HMT than cereal and legume starches (Donovan, Lorenz, and Kulp, 1983: Hagiwara, Esaki, Kitamura, and Kuge, 1991; Hoover, Swamidas, and Vasanthan, 1993; Gunaratne and Hoover, 2002).

Studies on the morphology of HMT treated potato, sweet potato, yam, cassava, wheat, maize, rice, finger millet, and lentil starches showed that when the treatment was carried out at temperatures <110°C little to none changes on the granule surface or morphology were observed. In contrast, when temperatures ≥110°C were used, corn and potato starches displayed the formation of indentations and voids toward the center of the granules (Figure 2.12), and in some cases a slightly decreased birefringence was observed (Stute, 1992; Kawabata et al., 1994; Hoover and Vasanthan, 1994; Vermeylen, Goderis, and Delcour, 2006; Khunae, Tran, and Sirivongpaisal, 2007).

When tuber and high amylose starches are subjected to HMT, their diffraction pattern changes from B- to A-type or a mixture of A + B type diffraction pattern. However, cereal and legume starches do not display changes in their crystalline type when subjected to similar HMT conditions. Gunaratne and Hoover (2002) attributed the transition from B- to A- type to the dehydration process that takes place during HMT. They suggested the 36 water molecules located in the central channel of the B-type crystalline unit vaporized during HMT, therefore the doubles helices tend to move toward the central channel. Vermeylen, Goderis, and Delcour (2006) concluded that during the HMT potato starch double helices moved within the highly dense lamellae both laterally and along the helical axis according to the disappearance 0.6 mm^{-1}

scattering maximum in SAXS, which corresponds to the characteristic 5.6° X-ray diffraction peak of B-type starches, and that this movement resulted in the disturbance of the lamellar structure. The relative crystallinity has been reported to both increase and decrease depending on the temperature and moisture content during HMT. The decrease in relative crystallinity has been suggested to be the product of the disruption of hydrated water bridges and hydrogen bonds that keep the adjacent double helices linked, resulting in a rearrangement that disrupts the double helices oriented in the perfect crystalline array (Gunaratne and Hoover, 2002; Vermeylen, Goderis, and Delcour, 2006; Khunae, Tran, and Sirivongpaisal, 2007; Vieira and Sarmento, 2008).

Starch susceptibility to enzyme digestion is also affected by the HMT conditions. For instance, when wheat starch was subjected to HMT (100°C, 16 h) at two different moisture contents, 18% and 27%, the digestibility increased by 0.43% and 5.9%, respectively. Under the same HMT conditions the digestibility of potato starches increased only by 0.05% and 0.33%, respectively (Lorenz and Kulp, 1983). Hoover and Manuel (1996) reported that after HMT (100°C/16 h) at 30% moisture the susceptibility of field pea, wrinkle pea, pigeon pea, black bean, and lentil starches to digestion by porcine pancreatic α-amylase (PPA) increased in the range of 5.5% to 18.3%.Similarly, the digestibility of waxy and common corn starches by a mixture of PPA and glucoamylase was reported to decrease by 18.9% and 33%, respectively, after HMT (100°C/16 h) at 18% moisture content. When HMT (100°C/16 h) was conducted at 27% moisture, the digestibility of waxy and common corn starches increased by 19.4% and 15.6%, respectively (Franco, Ciacco, and Tavares, 1995). Gunaratne and Hoover (2002) suggested that after HMT the digestibility of B-type starches tends to increase because the disruption near the surface of the granules could facilitate the binding and catalytic activity of the

enzyme, and the dehydration that takes place in the lamellar structure leaves glucan chain available for digestion. They also mentioned that the digestibility of the A-type starches, including cassava, taro, and new coco yam, after HMT increased, but the increase was related to the interplay between disrupted double helices in the amorphous regions and the interaction taking place between amylose chains.

2.9 Porous starch

In recent years there is an increasing interest in porous starches and their application in the delivery of drugs and bioactive components. The term “porous starch” has been used to describe porous matrices produced through physical, chemical or enzymatic treatments (Sujka, Pankiewicz, Kowalski, Nowosad, and Noszczyk-Nowak, 2018). The amount and size of the pores determine the loading capacity of the starches, and thus starches containing more pores are preferred for adsorption and encapsulation. In this study, porous starches are defined as starches in a granule form for the adsorption of bioactive components and drugs.

Most studies in the application of porous starches as delivery system have focused in porous systems produced by destroying the granule and reforming the structure. A recent review by Qi and Tester (2019) summarizes the applications and some methods for production of porous starches, and the literature survey shows that there is lack of details in the relationship of starch structure with respect to the formation of porous structure and how this affect the adsorption and release properties of porous starches. In order to increase the pore size and volume or to create the porous structure, physical, chemical, and biological methods have been applied. One of the most common methods used to produce porous starch is the enzymatic treatment of starch granules with amylases, such as α-amylase and glucoamylase (Table 1.1), which have been

described as efficient and convenient due to the specificity and mild reaction conditions required by the enzymes (Dura, Błaszczak, and Rosell, 2014; Xie, Li, Chen, and Zhang, 2019).

Although there are several factors affecting the formation of a porous structure when using the enzymatic hydrolysis method, its efficiency and specificity make the process easy to control (Benavent-Gil and Rosell, 2017). The enzyme hydrolysis of cereal, roots, tuber, and legume starches has been investigated with respect to the degree of hydrolysis, enzyme adsorption in the granule and kinetic events (Gorinstein, 1993; Tahir, Ellis, and Butterworth, 2010; Butterworth, Warren, Grassby, Patel, and Ellis, 2012), the enzyme action pattern (Kerr, Cleveland, and Katzbeck,1951; Robyt and French, 1963; Baldwin et al., 2015), and the effect of physical and structural characteristic such as granule size (Dhital, Shrestha, and Gidley, 2010) and crystalline type on the hydrolysis extent as well as *in vitro* and *in vivo* digestibility properties (Lin et al., 2006; Zhang, Venkatachalam, and Hamaker, 2006).

For the production of porous starches, the direct hydrolysis of native starch granules at temperatures below the gelatinization temperature is the preferred method (Lacerda, Leite, Soares, and da Silveira, 2018). However, enzymatic treatments at the subgelatinization temperatures of starches are challenging because the native crystalline structure slows down enzyme adsorption, and the catalytic activity is restricted to loosely packed areas of the granules, which are amorphous in nature (Butterworth, Warren, Grassby, Patel, and Ellis, 2011). The most common enzymes used for starch modification are α-amylase, glucoamylase, and β-amylase, (Benavent-Gil and Rosell, 2017b,). Alpha-amylase, β-amyalse, and glucoamylase action mode were discussed earlier. Depending on the type of enzyme used or their combination different pattern of porous structure including pin-holes and sponge-like erosion will be observed (Lacerda, Leite, Soares, and da Silveira, 2018).

After treating common corn, high amylose maize, and waxy corn starches with glucoamylase from *Aspergillus sp.* K-27 at 40°C, Yamada et al. (1995) observed that the size of the granules did not change, while the amount and size of the pores increased with increasing the reaction time for common corn and waxy corn starches. A similar increase in pore size and pore number in common corn starch was observed by Chen and Zhang (2012) after digestion by glucoamylase (Figure 2.13). High amylose maize was found to be least susceptible to glucoamylase and did show enlarged pores. After analyzing the X-ray diffraction and differential scanning calorimetry (DSC) profiles, Yamada et al. (1995) suggested that the crystalline region of corn starch is more susceptible to enzymatic attack compared to its amorphous region. Zhao, Madson, and Whistler, (1996) observed that the treatment of common corn starch with glucoamylase resulted in porous starch with a large and empty central cavity, that when submerged in peppermint oil was able to uptake ~54% (w/w) of the oil.

2.10 REFERENCES

Arijaje, E., Wang, Y.-J., Shin, S., Shah, U., & Proctor, A. (2014). Effects of chemical and enzymatic modifications on starch-stearic acid complex formation. *Journal of Agricultural and Food Chemistry, 62*, 2963–2972.

Baldwin, A. J., Egan, D. L., Warren, F. J., Barker, P. D., Dobson, C. M., Butterworth, P. J., &Ellis, P. R. (2015). Investigating the mechanisms of amylolysis of starch granules by solution-state NMR. *Biomacromolecules, 16*, 1614–1621.

Baldwin, P. M., Adler, J., Davies, M. C., & Melia, C. D. (1998). High resolution imaging of starch granule surfaces by atomic force microscopy. *Journal of Cereal Science, 27*, 255–265.

Bartz, J., da Rosa Zavareze, E., & Dias, A. R. G. (2017). Study of heat-moisture treatment of potato starch granules by chemical surface gelatinization. *Journal of the Science of Food and Agriculture, 97,* 3114–3123.

Bauer, B. A. & Knorr, D. (2005). The impact of pressure, temperature and treatment time on starches: pressure-induced starch gelatinization as pressure time temperature indicator for high hydrostatic pressure processing. *Journal of Food Engineering, 68*, 329–334.

Bemiller, J. N., & Huber, K. C. (2015). Physical modification of food starch functionalities. *Annual Review of Food Science & Technology, 6*, 19.

Benavent-Gil, Y., & Rosell, C. (2017a) Comparison of porous starches obtained from different enzymes types and levels. *Carbohydrate Polymers,157*, 533–540.

Benavent-Gil, Y., & Rosell, C. M. (2017b). Morphological and physicochemical characterization of porous starches obtained from different botanical sources and amylolytic enzymes. *International Journal of Biological Macromolecules, 103*, 587–595.

Biliaderis, C. G., Grant, D. R., & Vose, J. R. (1981). Structural Characterization of Legume Starches. II. Studies on Acid-Treated Starches. *Cereal Chemistry, 58*, 502–507.

Blaszczak, W., Valverde, S., & Fornal, J. (2005). Effect of high pressure on the structure of potato starch. *Carbohydrate Polymers*, *59*, 377–383.

Bird, A. R., Lopez-Rubio, A., Shrestha, A. K., & Gidley, M. J. (2009). Resistant starch in vitro and in vivo: factors determining yield, structure, and physiological relevance. In *Modern biopolymer science*. S. Kasapis, I. T. Norton, & J. B. Ubbink Eds.; Elsevier Inc: pp. 449–510.

Brewer, L., Cai, L., & Shi, Y. (2012). Mechanism and enzymatic contribution to in vitro test method of digestion for maize starches differing in amylose content. *Journal of Agricultural and Food Chemistry, 60*, 4379–4387.

Butterworth, P. J., Warren, F. J., & Ellis, P. R. (2011). Human α-amylase and starch digestion: An interesting marriage. *Starch – Stärke, 63*, 395–405.

Butterworth, P. J., Warren, F. J., Grassby, T., Patel, H., & Ellis, P. R. (2012). Analysis of starch amylolysis using plots for first-order kinetics. *Carbohydrate Polymers, 87*, 2189–2197.

Cai, L., & Shi, Y. (2013). Self-assembly of short linear chains to A- and B-type starch spherulites and their enzymatic digestibility. *Journal of Agricultural and Food Chemistry, 61*, 10787–10797.

Chen, G., & Zhang, B. (2012). Hydrolysis of granular corn starch with controlled pore size. *Journal of Cereal Science, 56*, 316–320.

Colonna, P., Leloup, V., & Buleon, A. (1992). Limiting factors of starch hydrolysis. *European Journal of Clinical Nutrition, 46*, S17–S32.

Dhital, S., Shrestha, A. K., & Gidley, M. J. (2010). Relationship between granule size and in vitro digestibility of maize and potato starches. *Carbohydrate Polymers, 82*, 480–488.

Dhital, S., Warren, F. J., Butterworth, P. J., Ellis, P. R., & Gidley, M. J. (2017). Mechanisms of starch digestion by α-amylase-structural basis for kinetic properties. *Critical Reviews in Food Science and Nutrition, 57*, 875–892.

Donovan, J.W., Lorenz, K., & Kulp, K. (1983). Differential scanning calorimetry of heat-moisture treated wheat and potato starches. *Cereal Chemistry, 60*, 381–387.

Douzals, J.P., Perrier Cornet, J.M., Gervais, P., & Coquillet, J.C. (1998). High-pressure gelatinization of wheat starch and properties of pressure-induced gels. *Journal of Agricultural and Food Chemistry, 46*, 4824–4829.

Dubois, M., Gilles, K., Hamilton, J., Rebers, P., & Smith, F. (1956). Colorimetric Method for Determination of Sugars and Related Substances. *Analytical Chemistry, 28*, 350–356.

Dura, A., & Rosell, C. M. (2016). Physicochemical properties of corn starch modified with cyclodextrin glycosyltransferase. *International Journal of Biological Macromolecules, 87*, 466–472.

Dura, A., Błaszczak, & W., Rosell, C. M. (2014). Functionality of porous starch obtained by amylase or amyloglucosidase treatments. *Carbohydrate Polymers, 101*, 837–845.Eerlingen, R. C., & Delcour, J. A. (1995). Formation, analysis, structure and properties of type III enzyme resistant starch. *Journal of Cereal Science, 22*, 129–138.

Espinosa-Solis, V., Sanchez-Ambriz, S. L., Hamaker, B. R. & Bello-Perez, L. A. (2011). Fine structural characteristics related to digestion properties of acid-treated fruit starches. *Starch – Stärke, 63*, 712–727.

Fannon, J., Hauber, R., & Bemiller, J. (1992). Surface pores of starch granules. *Cereal Chemistry, 69*, 284–288.

Fannon, J., Shull, J., & Bemiller, J. (1993). Interior channels of starch granules. *Cereal Chemistry, 70*, 611–613.

Franco, C. M. L., Ciacco, C. F., & Tavares, D. Q. (1988). Studies on the susceptibility of granular cassava and corn starches to enzymatic attack. Part 2: Study of the granular structure of starch. *Starch – Stärke, 40*, 29–32.

Franco, C. M., do Rio Preto, S. J., & Ciacco, C. F. (1992), Factors that Affect the Enzymatic Degradation of Natural Starch Granules -Effect of the Size of the Granules. *Starch – Stärke, 44*, 422–426.

Franco, C.M.L., Ciacco, C.F., & Tavares, D.Q. (1995). Effect of the heat-moisture treatment on the enzymatic susceptibility of corn starch granules. *Starch – Stärke, 47*, 223–228.

Gallant, D. J., Bouchet, B., & Baldwin, P. M. (1997). Microscopy of starch: Evidence of a new level of granule organization. *Carbohydrate Polymers, 32*, 177–191.

Gallant, D.J, Bouchet, B., Buleon, A., & Pérez, S. (1992). Physical characteristics of starch granules and susceptibility to enzymatic degradation. *European Journal of Clinical Nutrition, 46*, S3–S16.

Gérard, C., Colonna, P., Buléon, A., & Planchot, V. (2001). Amylolysis of maize mutant starches. *Journal of the Science of Food and Agriculture, 81*, 1281–1287.

Gidley, M. J., & Bulpin, P. V. (1987). Crystallisation of maltooligosaccharides as models of the crystalline forms of starch: Minimum chain-length requirement for the formation of double helices. *Carbohydrate Research, 161*, 291–300.

Gidley, M. J., Cooke, D., Darke, A. H., Hoffmann, R. A., Russell, A. L., & Greenwell, P. (1995). Molecular order and structure in enzyme resistant retrograded starch. *Carbohydrate Polymers* 28, 23–31.

Gorinstein, S. (1993). Kinetic Studies During Enzyme Hydrolysis of Potato and Cassava Starches. *Starch – Stärke, 45*, 91–95.

Gunaratne, A., & Hoover, R. (2002). Effect of heat-moisture treatment on the structure and physicochemical properties of tuber and root starches. *Carbohydrate Polymers, 49*, 425–437.

Hagiwara, S., Esaki, K., Kitamura, S., & Kuge, T. (1991). Observation by photomicroscopic and X–ray diffraction method of heat–moisture treatment on starch granules. *Denpun Kaguku 38*, 241–247.

Haki, G. D., & Rakshit, S. K. (2003). *Developments in industrially important thermostable enzymes: A review*. OXFORD: Elsevier Ltd.

Hanashiro, I., Abe, J., & Hizukuri, S. (1996). A periodic distribution of the chain length of amylopectin as revealed by high-performance anion-exchange chromatography. *Carbohydrate Research, 283*, 151–159.

Hayashi, R., & Hayashida, A. (1989). Increased amylase digestibility of pressure-treated starch. *Agricultural and Biological Chemistry, 53, 2543–2544.*

Helbert, W., Schulein, M., & Henrissat, B. (1996). Electron microscopic investigation of the diffusion of bacillus licheniformis alpha-amylase into corn starch granules. *International Journal of Biological Macromolecules, 19*, 165–169.

Hibi, Y., Matsumoto, T., & Hagiwara, S. (1993). Effect of high pressure on the crystalline structure of various starch granules. *Cereal Chemistry, 70*, 671–676.

Hizukuri, S. (1985). Relationship between the distribution of the chain-length of amylopectin and the crystalline-structure of starch granules. *Carbohydrate Research, 141*, 295–306.

Hizukuri, S. (1986). Polymodal distribution of the chain lengths of amylopectins, and its significance. *Carbohydrate Research, 147*, 342–347.

Hizukuri, S., Kaneko, T., & Takeda, Y. (1983). Measurement of the chain length of amylopectin and its relevance to the origin of crystalline polymorphism of starch granules. *Biochimica Et Biophysica Acta (BBA) - General Subjects, 760*, 188–191.

Hizukuri, S., Takeda, Y., Shitaozono, T., Abe, J., Ohtakara, A., Takeda, C. & Suzuki, A. (1988), Structure and properties of water chestnut (*Trapa natans* L. var. *bispinosa* Makino) Starch. *Starch – Stärke, 40*, 165–171.

Hoover, D.G. (1993). Pressure effects on biological systems. *Food Technology*, *47*, 150-155.

Hoover, R. (2000). Acid-treated starches. *Food Reviews International, 16*, 369–392.

Hoover, R. (2010). The impact of heat-moisture treatment on molecular structures and properties of starches isolated from different botanical sources. *Critical Reviews in Food Science & Nutrition, 50*, 835–847.

Hoover, R., & Manuel, H. (1996). Effect of heat-moisture treatment on the structure and physicochemical properties of legume starches. *Food Research International, 29*, 731–750.

Hoover, R., & Vasanthan, T. (1994). The effect of annealing on the physiochemical properties of wheat, oat, potato and lentil starches. *Journal of Food Biochemistry,* 17, 303–325.

Hoover, R., Rorke, S. C., & Martin, A. M. (1991). Isolation and characterization of lima bean (*Phaseolus Lunatus*) starch. *Journal of Food Biochemistry, 15*, 117–136.

Hoover, R., Swamidas, G., & Vasanthan, T. (1993). Studies on the physicochemical properties of native, defatted and heat-moisture treated pigeon pea (*Cajanus Cajan L*) starch. *Carbohydrate research, 246*, 185–203.

Hoover, R., & Vasanthan, T. (1994). Effect of heat moisture treatment on the structure and physicochemical properties of cereal, legume and tuber starches. *Carbohydrate Research, 252*, 33–53.

Huang, J., Chen, Z., Xu, Y., Li, H., Liu, S., Yang, D., & Schols, H. A. (2014). Comparison of waxy and normal potato starch remaining granules after chemical surface gelatinization: Pasting behavior and surface morphology. *Carbohydrate Polymers, 102*, 1001-1007.

Huber, K., & BeMiller, J. (1997). Visualization of channels and cavities of corn and sorghum starch granules. *Cereal Chemistry, 74*, 537–541.

Imberty, A., & Perez, S. (1988). A revisit to the three-dimensional structure of B-type starch. *Biopolymers*, 27, 1205–1221.

Jane, J. (1993). Mechanism of starch gelatinization in neutral salt-solutions. *Starch – Stärke, 45*, 161–166.

Jane, J., & Robyt, J. F. (1984). Structure studies of amylose-V complexes and retro-graded amylose by action of alpha amylases, and a new method for preparing amylodextrins. *Carbohydrate Research, 132*, 105–118.

Jane, J., & Shen, J. J. (1993). Internal structure of the potato starch granule revealed by chemical gelatinization. *Carbohydrate Research, 247*, 279–290.

Jane, J., Chen, Y. Y., Lee, L. F., McPherson, A. E., Wong, K. S., Radosavljevic, M., & Kasemsuwan, T. (1999). Effects of amylopectin branch chain length and amylose content on the gelatinization and pasting properties of starch. *Cereal Chemistry*, *76*, 629–637.

Jane, J., Xu, A., Radosavljevic, M., & Seib, P. (1992). Location of amylose in normal starch granules. I. Susceptibility of amylose and amylopectin to cross-linking reagents. *Cereal Chemistry, 69*, 405–409.

Jane, J.-L., Wong, K.-S., & McPherson, E. A. (1997). Branch-structure difference in starches of A- and B-type X-ray patterns revealed by their Näegeli dextrins. *Carbohydrate Research 300*, 219–227.

Jane, J.-L. Structural features of starch granules II. In *Starch: Chemistry and Technology*, 3d ed.; Whistler, R.L., BeMiller, Eds.; Academic Press: Orlando, FL, 2009; pp 193–227.

Jenkins, P. J., & Donald, A. M. (1995). The influence of amylose on starch granule structure. *International Journal of Biological Macromolecules, 17,* 315.

Jung, Y., Lee, B., & Yoo, S. (2017). Physical structure and absorption properties of tailor-made porous starch granules produced by selected amylolytic enzymes. *Plos One, 12*, e0181372.

Kainuma, K. & French, D. (1971), Nägeli amylodextrin and its relationship to starch granule structure. I. Preparation and properties of amylodextrins from various starch types. *Biopolymers, 10*, 1673–1680.

Kasemsuwan, T., & Jane, J. (1994). Location of amylose in normal starch granules. II: Locations of phosphodiester cross-linking revealed by phosphorus-31 nuclear magnetic resonance. *Cereal Chemistry* 71, 282–287.

Katopo, H., Song, Y., & Jane, J. (2002). Effect and mechanism of ultrahigh hydrostatic pressure on the structure and properties of starches. *Carbohydrate Polymers*, *47*, 282–287

Kawabata, A., Takase, N., Miyoshi, T., Sawayama, S., Kimura, T., and Kudo, K. (1994). Microscopic observation and X-ray diffractometry of heat–moisture treated starch granules. *Starch – Stärke, 48*, 463–469.

Kawai, J., Fukami, K., & Yamamoto, K. (2007). Effects of treatment pressure, holding time, and starch content on gelatinization and retrogradation properties of potato starch-water mixtures treated with high hydrostatic pressure. *Carbohydrate Polymers*, 69, 590–596.

Kerr, R.W., Cleveland, F.C., & Katzbeck, W.J. (1951). The action of amyloglucosidase on amylose and amylopectin. *Journal of the American Chemical Society*, *73*, 3916–3921.

Khunae, P., Tran, T., & Sirivongpaisal, P. (2007). Effect of heat-moisture treatment on structural and thermal properties of rice starches differing in amylose content. *Starch – Stärke, 59*, 593–599.

Kim, H., Kim, B., & Baik, M. (2012). Application of ultra high pressure (UHP) in starch chemistry. *Critical Reviews in Food Science and Nutrition, 52*, 123–141.

Kim, H.-J., Lee, J., Kim, J.-Y., Lim, W.-J., & Lim S.-T. (2012). Characterization of Nanoparticles Prepared by Acid Hydrolysis of Various Starches. *Starch – Stärke*, *64*, 367–373.

Koch, K., & Jane, J. (2000). Morphological changes of granules of different starches by surface gelatinization with calcium chloride. *Cereal Chemistry, 77*, 115–120.

Kong, B., Kim, J., Kim, M., & Kim, J. (2003). Porcine pancreatic alpha-amylase hydrolysis of native starch granules as a function of granule surface area. *Biotechnology Progress, 19*, 1162–1166.

Kuakpetoon, D., & Wang, Y. (2007). Internal structure and physicochemical properties of corn starches as revealed by chemical surface gelatinization. *Carbohydrate Research, 342*, 2253–2263.

Lacerda, L. D., Leite, D. C., Soares, R. M. D., & da Silveira, N. P. (2018). Effects of α-amylase, amyloglucosidase, and their mixture on hierarchical porosity of rice starch. *Starch – Stärke, 70*, 1800008.

Le Corre, D., Bras, J., & Dufresne, A. (2010). Starch nanoparticles: A review. *Biomacromolecules, 11*, 1139–1153.

Leloup, V. M., Colonna, P. & Ring, S. G. (1991). Alpha-amylase adsorption on starch crystallites. *Biotechnology and Bioengineering, 38*, 127–134.

Lin, H., Lin, J., Chang, Y., Jane, J., Sheu, M., & Lu, T. (2006). Heterogeneity of lotus rhizome starch granules as revealed by α-amylase degradation. *Carbohydrate Polymers, 66*, 528–536.

Lintner, C. J. (1886). Studien über Diastase. *Journal Für Praktische Chemie, 34*, 378–394.

Liu, Y., Selomulyo, V. O., & Zhou, W. (2008). Effect of high pressure on some physicochemical properties of several native starches. *Journal of Food Engineering, 88*, 126–136.

Lorenz, K., & Kulp, K. (1983). Physicochemical properties of defatted heat–moisture treated starches. *Starch – Stärke, 35*, 123–129.

McCleary, B. V., & Monaghan, D. A. (2002). Measurement of resistant starch. *Journal of AOAC International, 85*, 665–675.

McPherson, A. E., & Jane, J. (1999). Comparison of waxy potato with other root and tuber starches. *Carbohydrate Polymers, 40*, 57–70.

Meagher, M. M., Nikolov, Z. L., & Reilly, P. J. (1989). Subsite mapping of *Aspergillus niger* glucoamylases I and II with malto- and isomaltooligosaccharides. *Biotechnology and Bioengineering, 34*, 681–688.

Mercier, C., Charbonnière Et, R., & Guilbot, A. (1968). Influence of pressure treatment on granular structure and susceptibility to enzymatic amylolysis of various starches. *Starch – Stärke, 20*, 6–11.

Miao, M., Jiang, B., Zhang, T., Jin, Z., & Mu, W. (2011). Impact of mild acid hydrolysis on structure and digestion properties of waxy maize starch. *Food Chemistry, 126*, 506–513.

Morrison, W.; Karkalas, J. Starch. In *Methods in Plant Biochemistry*; Dey, P.M., Ed; Academic Press: London, Vol. 2, 1990; pp 323–352.

Mussulman, W., & Wagoner, J. (1968). Electron microscopy of unmodified and acid-modified corn starches. *Cereal Chemistry, 45*, 162–162.

Nägeli, W. (1874). Beiträge zur näheren Kenntniss der Stärkegruppe. *Justus Liebig's Annalen Der Chemie, 173*, 218–227.

O'Brien, S., & Wang, Y. (2008). Susceptibility of annealed starches to hydrolysis by α-amylase and glucoamylase. *Carbohydrate Polymers, 72*, 597–607.

Pan, D., & Jane, J. (2000). Internal structure of normal maize starch granules revealed by chemical surface gelatinization. *Biomacromolecules, 1*, 126–132.

Payan, F., Haser, R., Pierrot, M., Frey, M., Astier, J. P., Abadie, B., Duee, E., & Buisson, G. (1980). 3-dimensional structure of alpha-amylase from porcine pancreas at 5-A° resolution - active-site location. *Acta Crystallographica*, 36, 416–421.

Pei-Ling, L., Qing, Z., Qun, S., Xiao-Song, H., & Ji-Hong, W. (2012). Effect of high hydrostatic pressure on modified noncrystalline granular starch of starches with different granular type and amylase content. *LWT - Food Science and Technology, 47*, 450–458.

Pérez, S. and Bertoft, E. (2010), The molecular structures of starch components and their contribution to the architecture of starch granules: A comprehensive review. *Starch – Stärke, 62*, 389–420.

Perry, P. A., & Donald, A. M. (2000). The effects of low temperatures on starch granule structure. *Polymer, 41*, 6361–6373.

Planchot, V., & Colonna, P. (1995). Purification and characterization of extracellular alpha-amylase from aspergillus fumigatus. *Carbohydrate Research, 272*, 97–109.

Planchot, V., Colonna, P., & Buleon, A. (1997). Enzymatic hydrolysis of α-glucan crystallites. *Carbohydrate Research, 298*, 319–326.

Planchot, V., Colonna, P., Gallant, D. J., & Bouchet, B. (1995). Extensive degradation of native starch granules by alpha-amylase from Aspergillus fumigatus. *Journal of Cereal Science*, 21, 163–171.

Qi, X., & Tester, R. F. (2019). Starch granules as active guest molecules or microorganism delivery systems. *Food Chemistry, 271*, 182–186.

Ratnayake, W. S., Hoover, R., Shahidi, F., Perera, C., & Jane, J. (2001). Composition, molecular structure, and physicochemical properties of starches from four field pea (*Pisum sativum L.*) cultivars. *Food Chemistry, 74*, 189–202.

Robyt, J. F. Enzymes and their action on starch.In *Starch chemistry and technology (3rd Ed.).* BeMiller, J. N. & Whistler R. L. Eds.; Academic press: New York, NY, 2009. pp. 237–292.

Robyt, J., & French, D. (1963). Action pattern and specificity of an amylase from Bacillus subtilis. *Archives of Biochemistry and Biophysics, 100*, 451–467.

Robyt, J., & French, D. (1967). Multiple attack hypothesis of α-amylase action: action of porcine pancreatic, human salivary, and *Aspergillus oryzae* α-amylases. *Archives of Biochemistry and Biophysics, 122*, 8–16.

Rubens, P., Snauwaert, J., Heremans, K., & Stute, R. (1999). In situ observation of pressure-induced gelation of starches studied with FTIR in the diamond anvil cell. *Carbohydrate Polymers, 39*, 231–235.

Rubens, P., & Heremans, K. (2000). Pressure-temperature gelatinisation phase diagram of starch: An in situ fourier transform infrared study. *Biopolymer, 54*, 524–530.

Sarikaya, E., Higasa, T., Adachi, M., & Mikami, B. (2000). Comparison of degradation abilities of alpha- and beta-amylases on raw starch granules. *Process Biochemistry, 35*, 711–715.

Sarko, A., & Wu, H. (1978). Crystal-structures of A-polymorphs, B-polymorphs and C-polymorphs of amylose and starch. *Starch – Stärke, 30*, 73–77.

Selmi, B., Marion, D., Perrier Cornet, J. M., Douzals, J. P., & Gervais, P. (2000). Amyloglucosidase hydrolysis of high-pressure and thermally gelatinised corn and wheat starches. *Journal of Agriculture and Food Chemistry*, *48*, 2629–2633.

Sevenou, O., Hill, S. E., & Farhat, I. A. (2002). Organisation of the external region of the starch granule as determined by infrared spectroscopy. *International Journal of Biological Macromolecules*, *31*,79–85.

Shen, X., Shang, W., Strappe, P., Chen, L., Li, X., Zhou, Z., & Blanchard, C. (2018). Manipulation of the internal structure of high amylose maize starch by high pressure treatment and its diverse influence on digestion. *Food Hydrocolloids, 77*, 40–48.

Shrestha, A., Blazek, J., Flanagan, B., Dhital, S., Larroque, O., Morell, M., Gilbert, E., & Gidley, M. (2012). Molecular mesoscopic and microscopic structure evolution during amylase digestion of maize starch granules. *Carbohydrate Polymers*, *90*, 23–33.

Shi, M., Gao, Q., & Liu, Y. (2018). Corn, potato, and wrinkled pea starches with heat–moisture treatment: Structure and digestibility. *Cereal Chemistry, 95*, 603–614.

Srichuwong, S., Isono, N., Mishsima, T., & Hisamatsu, M. (2005). Structure of lintnerized starch is related to X-Ray diffraction pattern and susceptibility to acid and enzyme hydrolysis of starch granules. *International Journal of Biological Macromolecules, 37*, 115–121.

Srichuwong, S., Sunnarti, C. T., Mishima, T., Isono, N., & Hisamatsu, M. (2005). Starches from different botanical sources I: contribution of amylopectin fine structure to thermal properties and enzyme digestibility. *Carbohydrate Polymers*, *60*, 529–538.

Stolt, M., Oinonen, S., & Autio, K. (2001). Effect of high pressure on the physical properties of barley starch. *Innovative Food Science and Emerging Technology*, *1*, 167–175.

Stute, R. (1992). Hydrothermal modification of starch: the difference between annealing and heat–moisture treatment. *Starch – Stärke, 44*, 205–214.

Sujka, M., Pankiewicz, U., Kowalski, R., Nowosad, K., & Noszczyk-Nowak, A. (2018). Porous starch and its application in drug delivery systems. *Polimery w Medycynie*, *48*, 25–29.

Tahir, R., Ellis, P. R., & Butterworth, P. J. (2010). The relation of physical properties of native starch granules to the kinetics of amylolysis catalysed by porcine pancreatic α-amylase. *Carbohydrate Polymers, 81*, 57–62.

Takahashi, T., Kawauchi, S., Suzuki, K., & Nakao, E. (1994). Bindability and digestibility of high-pressure-treated starch with glucoamylases from Rhizopus sp.1. *The Journal of Biochemistry, 116*, 1251–1256.

Tatge, H., Marshall, J., Martin, C., Edwards, E.A., &Smith, A.M. (1999). Evidence that amylose synthesis occurs within the matrix of the starch granule in potato tubers. *Plant, Cell & Environment, 22*, 543–550.

Teng, A., Witt, T., Wang, K., Li, M., Hasjim, J. (2016). Molecular rearrangement of waxy and normal maize starch granules during *in vitro* digestion. *Carbohydrate Polymers*, *139*, 10–19,

Tester, R.; Karkalas, J., & Qi, X. (2004) Starch-composition, fine structure and architecture. *Cereal Science,* 4, 39, 151–165.

Tomasik, P., & Zaranyika, M. F. Nonconventional methods of modification of starch. In *Advances in carbohydrate chemistry and biochemistry*; D. Horton, Ed.; Academic Press: New York, NY, 1995; pp. 296–298.

Ulbrich, M., Natan, C., & Flöter, E. (2014). Acid Modification of Wheat, Potato, and Pea Starch Applying Gentle Conditions—Impacts on Starch Properties. *Starch – Stärke, 66*, 903–913.

Vandeputte, G. E., & Delcour, J. A. (2004). From sucrose to starch granule to starch physical behaviour: A focus on rice starch. *Carbohydrate Polymers, 58*, 245–266.

Vermeylen, R., Goderis, B., & Delcour, J.A. (2006). An X-ray study of hydrothermally treated potato starch. *Carbohydrate Polymers*, *64*, 364– 375.

Vieira, F.C., & Sarmento, S.B.S. (2008). Heat-moisture treatment and enzymatic digestibility of Peruvian carrot, sweet potato and ginger starches. *Starch – Stärke, 60*, 223–232.

Warren, F. J., Royall, P. G., Gaisford, S., Butterworth, P. J., & Ellis, P. R. (2011). Binding interactions of α-amylase with starch granules: The influence of supramolecular structure and surface area. *Carbohydrate Polymers, 86*, 1038–1047.

Witt, T., Gidley, M., & Gilbert, R. (2010). Starch digestion mechanistic information from the time evolution of molecular size distributions. *Journal of Agricultural and Food Chemistry, 58*, 8444–8452.

Xie, S., Liu, Q., & Cui, S. Starch modifications and applications. In *Food Carbohydrates: Chemistry, Physical Properties and Applications*; Cui, S., Ed; CRC Press: Boca Raton, FL, 2005; pp 357–406.

Xie, Y., Li, M., Chen, H., & Zhang, B. (2019). Effects of the combination of repeated heat-moisture treatment and compound enzymes hydrolysis on the structural and physicochemical properties of porous wheat starch. *Food Chemistry, 274*, 351–359.

Yamada, T., Hisamatsu, M., Teranishi, K., Katsuro, K., Hasegawa, N., & Hayashi, M. (1995). Components of the porous maize starch granule prepared by amylase treatment. *Starch – Stärke, 47*, 358–36.

Zhang, B., Cui, D., Liu, M., Gong, H., Huang, Y., & Han, F. (2012). Corn porous starch: Preparation, characterization and adsorption property. *International Journal of Biological Macromolecules, 50*, 250–256.

Zhang, G., Venkatachalam, M., & Hamaker, B. R. (2006). Structural basis for the slow digestion property of native cereal starches. *Biomacromolecules, 7*, 3259–3266.

Zhao, A.-Q., Yu, L., Yang, M., Wang, C.-J., Wang, M.-M., & Bai, X. (2018). Effects of the combination of freeze-thawing and enzymatic hydrolysis on the microstructure and physicochemical properties of porous corn starch. *Food Hydrocolloids, 83*, 465–472.

Zhao, J., Madson, M., & Whistler, R. (1996). Cavities in porous corn starch provides a large storage space. *Cereal Chemistry, 73*, 379–380.

Zobel, H.F. (1988). Starch crystal transformations and their industrial importance. *Starch – Stärke, 40*, 1–7.

Table 2.1. Examples of methods used to prepare granular porous starch and properties evaluated*

Starch botanical source	Method	Properties evaluated	Reference
Common corn Waxy corn	Hydrolysis with GM at 40°C	Crystallinity; morphology; thermal properties	Yamada et al. (1995)
Common corn	Hydrolysis with GM at 60°C	Morphology; peppermint oil adsorption	Zhao et al. (1996)
Common corn	Hydrolysis with a combination of AM and GM with varying conditions of time temperature, and enzyme: starch ratio	Adsorption capacity; morphology; thermal properties; crystallinity	Zhang et al. (2012)
Common corn	Hydrolysis with GM at 50°C up to 8 h	Water and soybean oil adsorption; morphology	Chen and Zhang (2012)
Common corn	Hydrolysis with GM or AM at 50°C for 24 h.	Morphology; hydration properties; thermal properties; pasting properties	Dura et al. (2014)
Common corn	Hydrolysis with GM, and AM, at 50°C for 24 h at various enzymes concentration	Water and sunflower oil adsorption; morphology; viscosity; thermal properties	Benavent-Gil and Rosell (2017a)
Potato Wheat Cassava	Hydrolysis with GM and AM at 50°C for 24 h	Water and sunflower oil adsorption; morphology; viscosity; thermal properties	Benavent-Gil and Rosell (2017b)
Rice	Hydrolysis with GM, AM, and a combination of both enzymes at 50°C for up to 12 h	Morphology; methyl violet or methylene blue adsorption; particle size; thermal properties	Lacerda et al. (2018)
Wheat	Repeated heat-moisture treatment followed by hydrolysis with a mixture of GM and AM 50°C for 8 h	Water, sunflower oil, and methylene blue adsorption; morphology; solubility and swelling power thermal properties	Xie et al. (2019)

*Enzymes abbreviated names: GM (glucoamylase) and AM (α-amyalse).

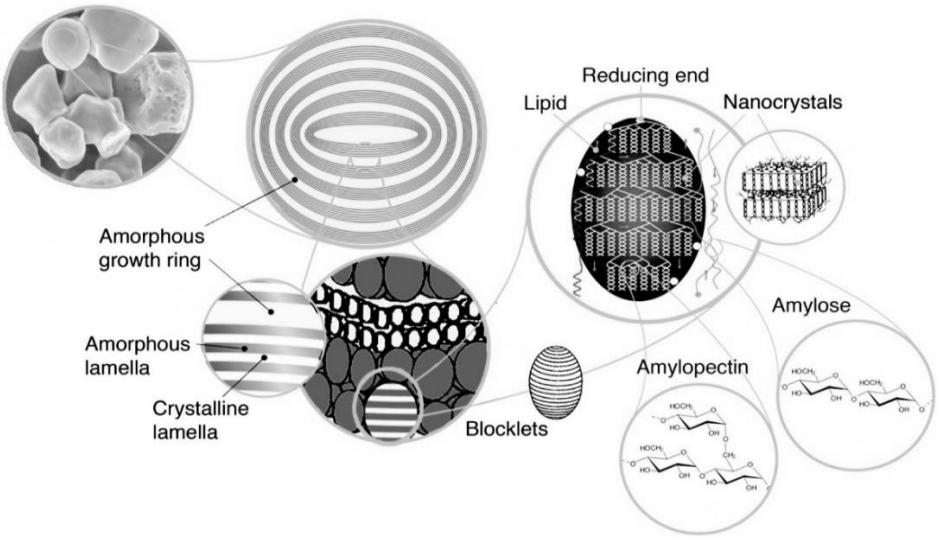

Figure 2.1. Starch granule levels of organizations (Le Corre, Bras, and Dufresne, 2010).

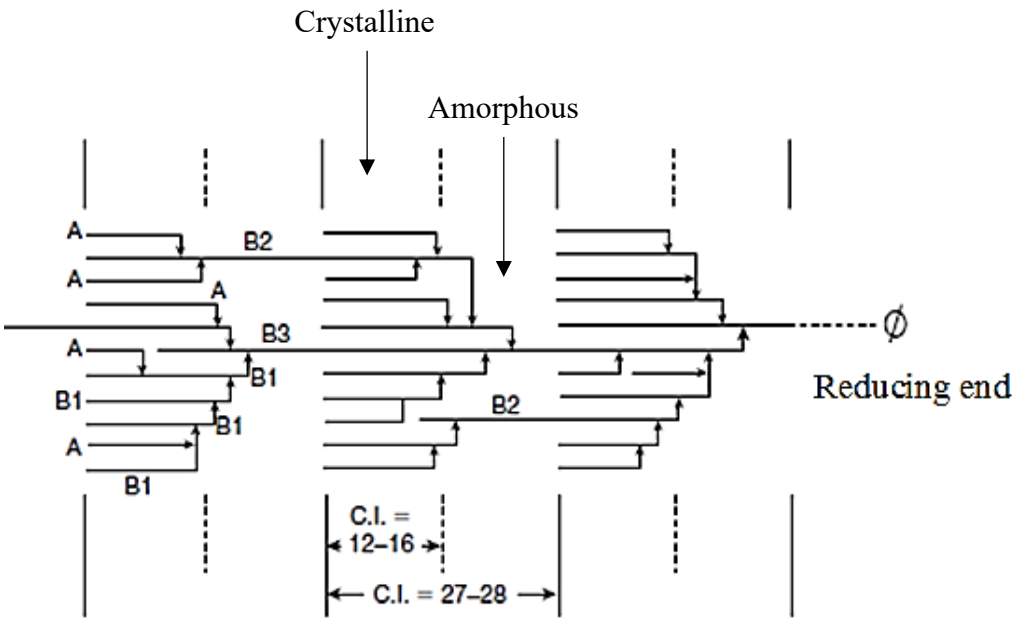

Figure 2.2. Amylopectin cluster structure (Hizukuri, 1986)

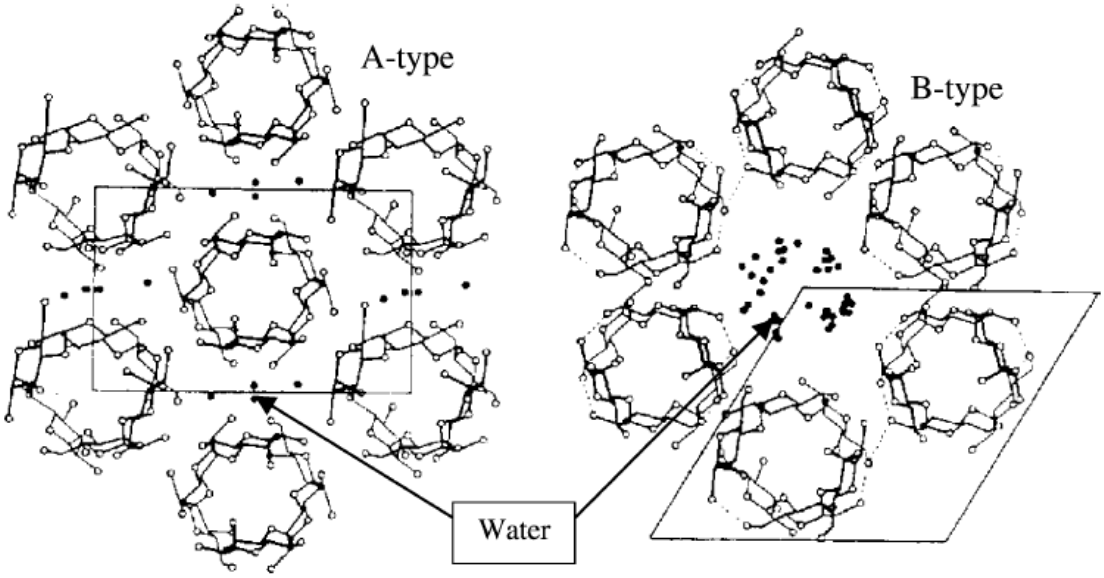

Figure 2.3. A- and B-type starch polymorphs (Wu and Sarko 1978).

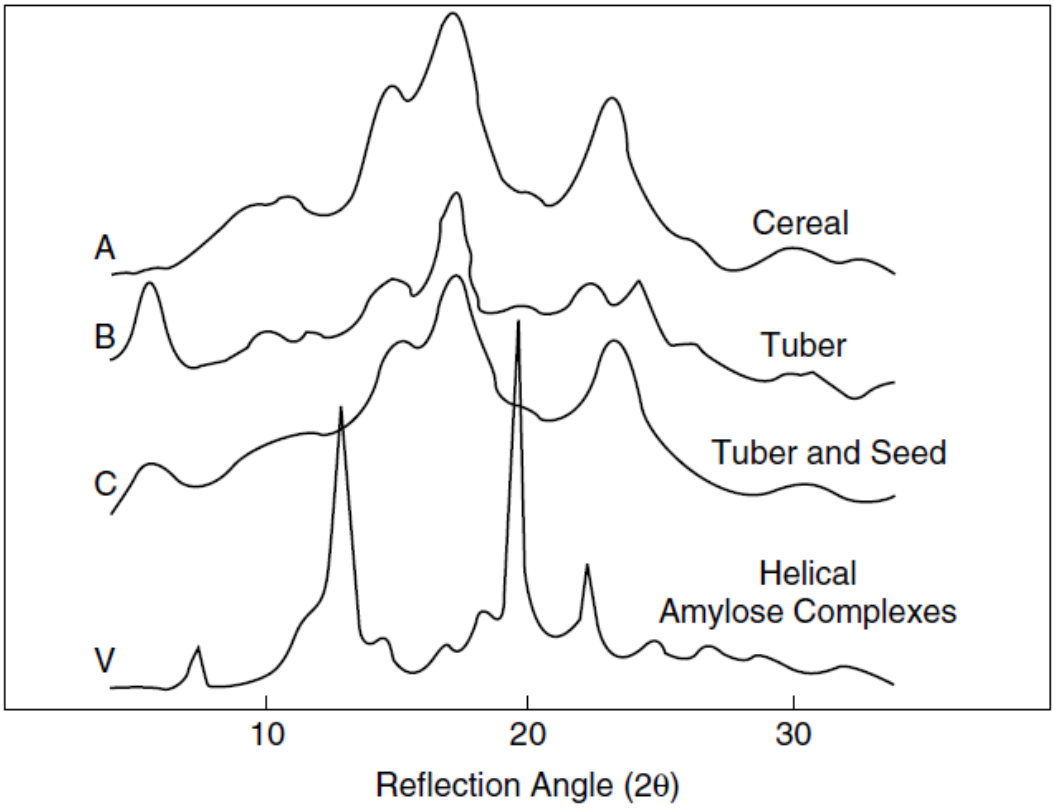

Figure 2.4. X-ray diffraction patterns of A-, B-, C-, and V-type starches (Zobel, 1988)

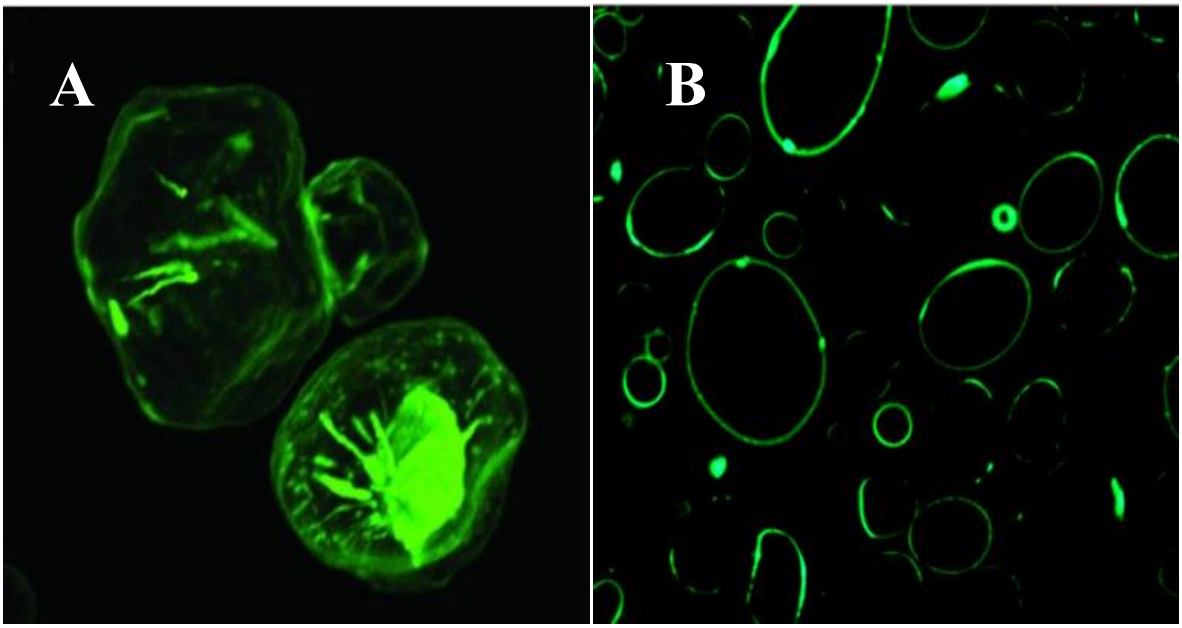

Figure 2.5. Confocal laser scanning microscopy photographs of A) common corn starch displaying pores and channels and B) potato starch (Kim, Kim, and Baik 2012; Jung, Lee, and Yoo, 2017).

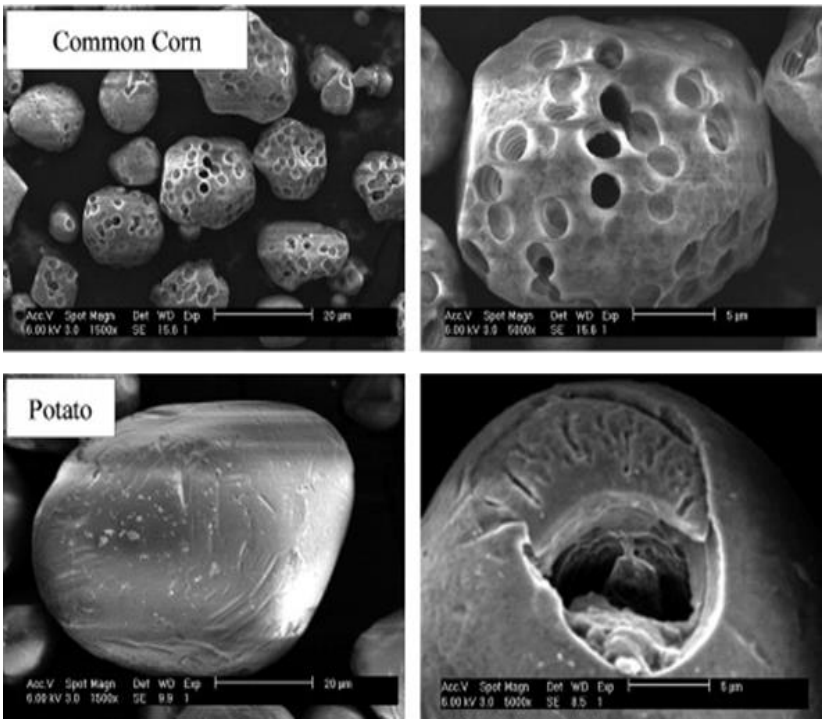

Figure 2.6. Scanning electron microscopy photographs (SEM) of common corn starch and potato starch after α-amylase digestion (O'Brien and Wang, 2002).

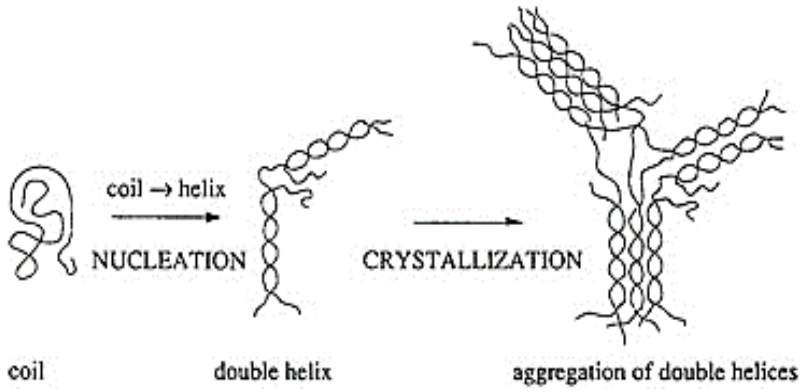

Figure 2.7. Transition from semicrystalline to amorphous state and crystallization (Colonna, Leloup, and Buleon 1992).

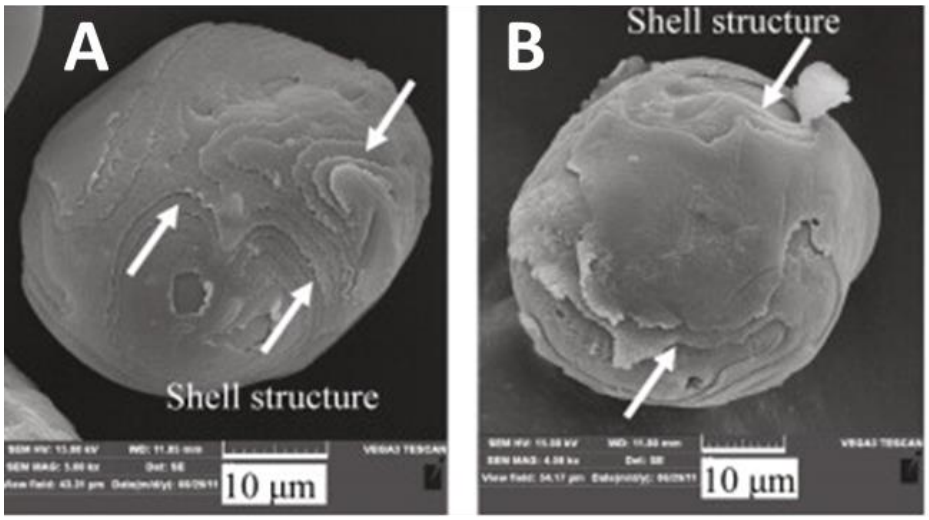

Figure 2.8. SEM micrographs of surface gelatinized waxy potato (A) and potato (B) starches (Huang et al., 2014).

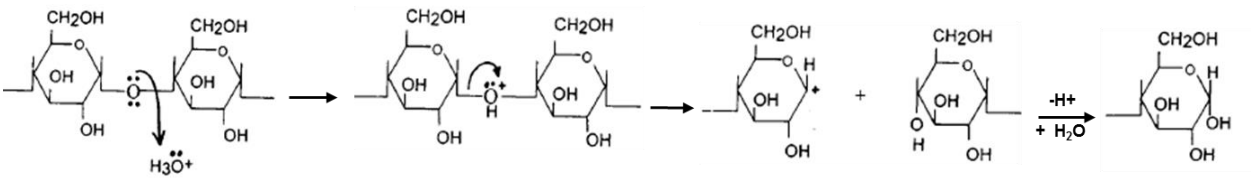

Figure 2.9. Mechanism of starch acid hydrolysis (Hoover, 2000).

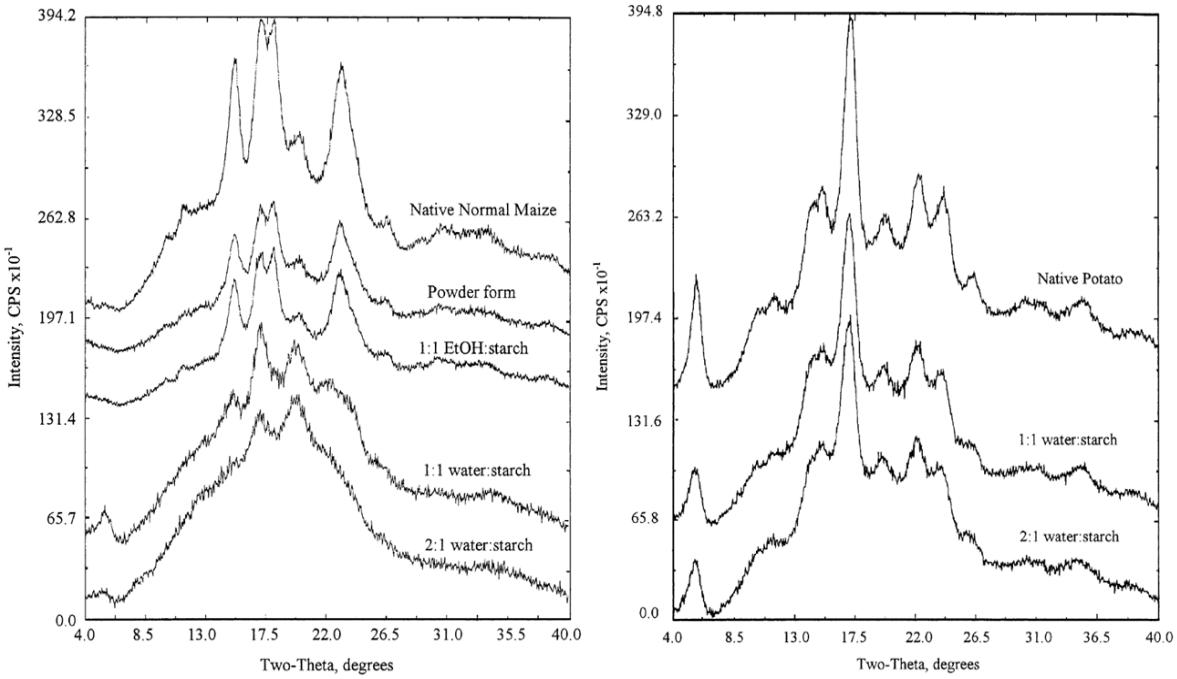

Figure 2.10. X-ray diffraction pattern of common corn and potato starch HHP treated at 690 MPa (Katopo, Song, and Jane, 2002).

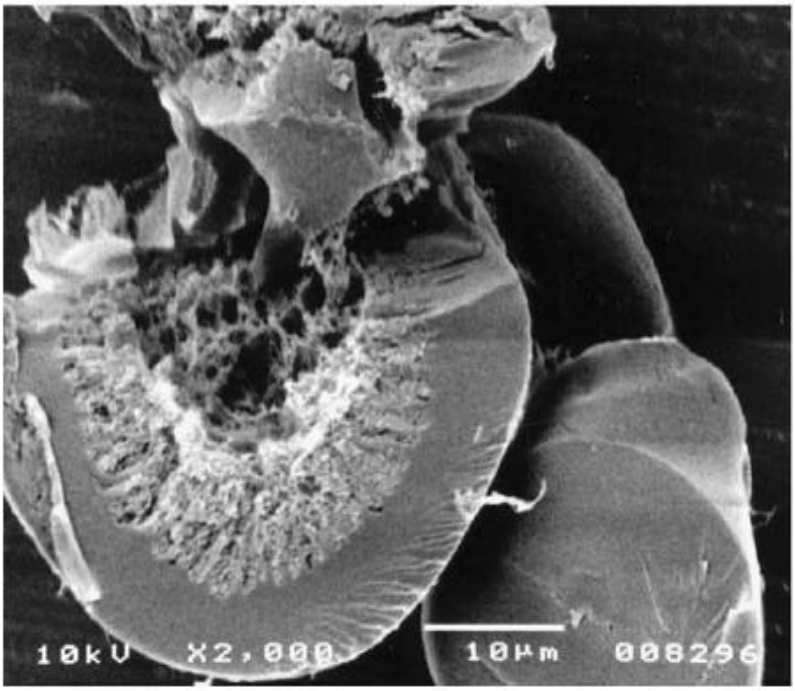

Figure 2.11. SEM micrograhs of potato starch granules tretated at 600 MPa for 3 min (Blaszczak, Valverde, and Fornal, 2005).

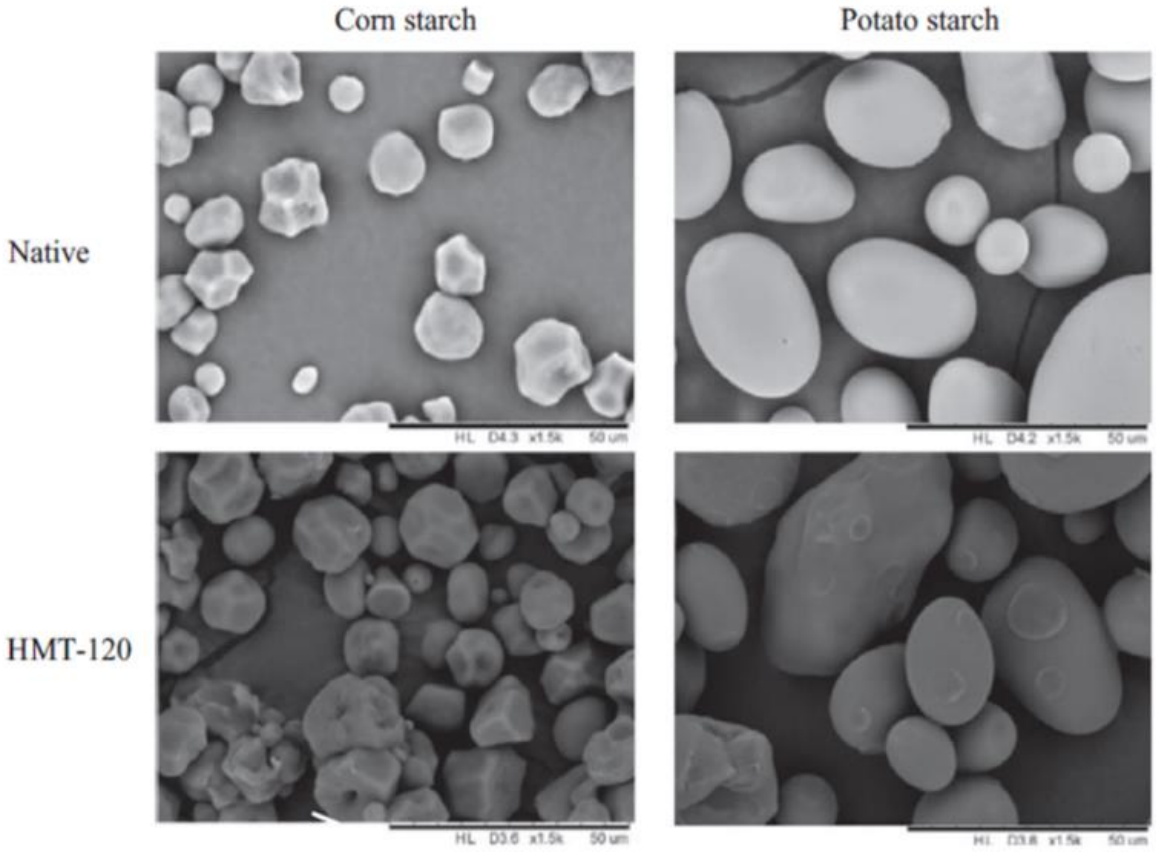

Figure 2.12. SEM micrograhs of native and HMT (120°C) corn and potato starches (Shi, Gao, and Liu, 2018).

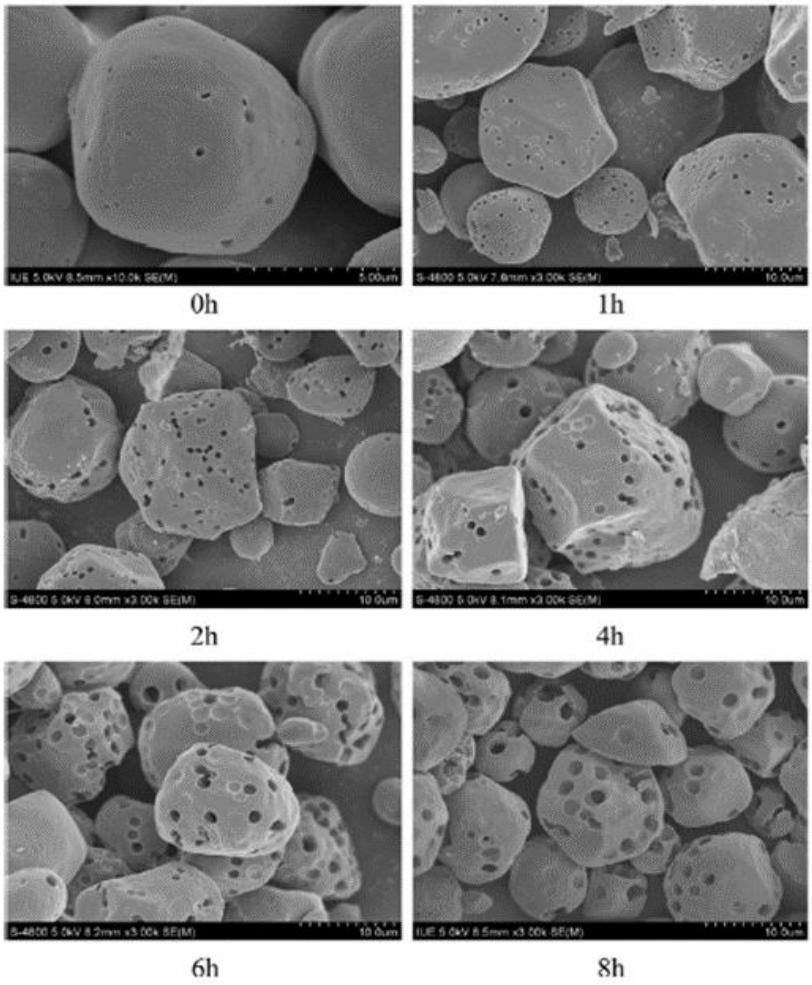

Figure 2.13. SEM micrograhs of common corn stacrh digested by glucoamylase for 0, 1, 2, 4, 6, and 8 h. (Chen and Zhang, 2012).

CHAPTER 3

ENHANCING THE FORMATION OF POROUS POTATO STARCH BY COMBINING α-AMYLASE OR GLUCOAMYLASE DIGESTION WITH ACID HYDROLYSIS

3.1 ABSTRACT

Granular porous starch has been prepared from A-type starch, but not from B-type starch, due, in part, to the smooth, dense surface of B-type starch. This study prepared and characterized acid-hydrolyzed common corn (A-type) and potato (B-type) starches, followed by digestion with α-amylase or glucoamylase. The results show that, compared to corn starch, potato starch was hydrolyzed faster by acid, whereas the degree of enzyme digestion varied with the starches and enzymes. The acid hydrolyzing conditions destabilized the crystalline lamellae and consequently increased the degree of binding and digestion in both enzymes, which resulted in the formation of the porous structure in the potato starch. A more defined porous structure was observed in the potato starch after the combination of extended acid hydrolysis and enzyme digestion. B-type porous starch could be a better colonic delivery system compared to A-type porous starch due to its more resistance to enzyme digestion.

Keywords: *Acid hydrolysis, α-amylase, glucoamylase, porous starch.*

3.2 INTRODUCTION

Granular porous starches have attracted much attention due to their adsorption and delivery capabilities (Benavent-Gil and Rosell, 2017). In general, porous starch is prepared by amylases digestion of A-type starches, such as corn, rice, and wheat, but not from B-type starches, such as potato and high amylose maize. A-type starches display naturally present surface pores and channels (Fannon, Hauber, and BeMiller, 1992; Fannon, Shull, and BeMiller, 1993; Huber and BeMiller, 1997), which have been suggested to facilitate diffusion, binding, and mobility of enzymes; thus, increasing starch digestibility and the formation of a porous structure capable of absorbing fluids (Zhao, Madson, and Whistler, 1996; Yao, and Yao, 2002; Bazin and Barresi, 2007). Enzymatic digestion of B-type starches, such as potato starch, is significantly slower and does not produce a defined porous structure, which is proposed to be due to the lack of channels and surface pores, a smaller bulk surface area, and/or the prevalence of densely packed blocklets near the surface that prevent the binding and subsequent digestion of glucan chains (Gallant, Bouchet, and Buleon, 1992; Dhital, Shrestha, and Gidley, 2010). Dhital, Warren, Zhang, and Gidley (2014) studied the binding of α-amylase labeled with fluorescein iso-thiocyanate (FITC) or tetramethylrhodamine isothiocyanate (TRITC) to potato and corn starches. They found that the binding of labeled α-amylase was more homogeneous and preferentially bound to the naturally present pores and channels of A-type starches but was concentrated at the granule periphery of B-type starch granules, and concluded that the availability of more disorganized binding sites determined the specificity of α-amylase catalytic location.

Besides amylases, acids are also capable of hydrolyzing starch. The differences in susceptibility to acid hydrolysis among starches have been partly ascribed to their differences in the distribution of α-(1→6) glucosidic linkages between the amorphous and crystalline domains

(Jane, Wong, and McPherson, 1997) and the extent of starch chain interactions within the amorphous and crystalline domains of the granule (Hoover, Swamidas, and Vasanthan,1993). By characterizing Naegeli dextrins and debranched Naegeli dextrins of A-type and B-type starches, Jane, Wong, and McPherson (1997) concluded that the A-type starches had branch points distributed in both amorphous and crystalline regions, whereas the B-type starch had most branch points clustered in the amorphous region. Therefore, the branch linkages present in the crystalline region may be protected during the acid hydrolysis, but those present in the amorphous region were more susceptible to the acid hydrolysis. Hoover, Swamidas, and Vasanthan (1993) suggested that the extent of acid hydrolysis is affected by the interactions of starch chains in both the amorphous and crystalline lamellae. This suggestion arose after they compared a number of separate studies that the extent of acid hydrolysis of different legume starches (Biliaderis, Grant, Vose, 1981; Hoover, Rorke, Martin, 1991) did not correlate with the amylose contents ranging from 28.5% to 64%.

Srichuwong, Isono, Mishsima, and Hisamatsu (2005) studied the α-amylase digestion of the residues of A-, B-, and C-type starches after they, along with their non-acid treated counterparts, were hydrolyzed by 2.2 M HCl at 35°C for 12 days; they found that the susceptibility to α-amylase digestion followed the order A- > C- > B-type starches, and α-amylolysis was enhanced by the acid treatment. They hypothesized that the acid hydrolyzed the α-(1→6) branching points and intercluster chains of the amorphous lamellae, thus increasing the access of α-amylase to the internal structures of the crystallites. Furthermore, they hypothesized the resistance of both acid residues and native B-type granules to α-amylolysis was related to the greater proportion of long chains and the clustered distribution of branching points in the amorphous lamellae of B-type crystallites. A similar trend was reported by Zhang,

Venkatachalam, and Hamaker (2006) using a combination of α-amylase and glucoamylase on acid-hydrolyzed common corn (60%, 70%, and 85%) and potato (82%) starches. They observed increased digestion of all acid-hydrolyzed starches, with potato starch displaying an increase of ~44.0 percentage points.

Both Srichuwong, Isono, Mishsima, and Hisamatsu (2005) and Zhang, Venkatachalam, and Hamaker (2006) targeted a high degree of acid hydrolysis (>50%) to obtain crystalline residues but did not emphasize the formation of a porous starch structure. Because of its large granule size and greater resistance to amylases, porous potato starch offers advantages over other starches by better protecting sensitive bioactive components from breakdown in the digestive system, which aids in their targeted colonic delivery. Thus, the objective of this study was to investigate the effect of controlled acid hydrolysis on the formation of a porous structure in corn and potato starches in combination with α-amylase or glucoamylase digestion. The changes in the fine structure of both starches were also characterized to illustrate their structural differences responsible for their differences in enzyme susceptibility.

3.3 MATERIALS AND METHODS

Materials

Common corn and potato starches were donated by Ingredion (Bridgewater, NJ). Alpha-amylase from *B. licheniformis* (specific activity 55 U/mg protein; EC number 3.2.1.1) and glucoamylase from *A. niger* (specific activity 36 U/mg protein; EC number 3.2.1.3) were purchased from Megazyme Ltd. (Wicklow, Ireland) and used without further dilution. All chemicals and reagents were of analytical grade.

Acid hydrolysis

Starches were hydrolyzed to different levels according to the method described by Kim, Lee, Kim, Lim, and Lim (2012) with modifications. Common corn starch (15 g, db) was dispersed in 100 mL of 3.16 M H_2SO_4, the mixture was incubated at 50°C with constant shaking (120 strokes/min), and samples were taken regularly over a period of 120 min. The sample was vacuum filtered through a Whatman No. 2 filter paper, and the recovered starch residue was washed with 4-fold volumes of deionized (DI) water after adjusting the pH to 7 with 6 M NaOH and then dried at 40°C for 48 h. The degree of hydrolysis was determined as the percentage of total solubilized carbohydrates in the filtrate as measured by the phenol-sulfuric method (Dubois, Gilles, Hamilton, Rebers, and Smith, 1956) based on the initial dry weight of the starch. The same procedure was applied to the potato starch. Acid-treated common corn and potato starch with 5% and 10% hydrolysis levels were obtained and subjected to digestion by α-amylase and glucoamylase.

Enzymatic digestion

Starches were enzymatically digested following the method of O'Brien and Wang (2008) with modifications. A slurry of 2.5 g (db) of native or acid-treated common corn or potato starch and 10 mL buffer was incubated at 50°C with constant mixing at 400 rpm. The digestion by α-amylase was carried out in 20 mM phosphate buffer at pH 6.9, while 20 mM acetate buffer at pH 4.5 was used for glucoamylase digestion. Fifty U enzyme/g dry starch was added to the slurry, aliquots were taken at 1, 5, 10, and 24 h and centrifuged at 1520 ×g for 10 min, and the supernatant was used to measure the digestion degree (%) by following the phenol-sulfuric method (Dubois, Gilles, Hamilton, Rebers, and Smith, 1956). The recovered starch was washed

three times with DI water, centrifuged at 1520 ×g for 10 min, dried at 40°C for 48 h, and ground using a mortar and pestle and sieved through a 250-μm screen.

Scanning electron microscopy

Scanning electron microscopy was utilized to reveal morphology changes on starch granules. The granules of native, acid-treated, and acid-enzyme treated starches were mounted onto a stub with double-backed tape prior to coating with gold, and their micrographs were taken with an FEI Nova Nanolab 200 Dual-Beam (Hillsboro, OR) with an accelerating voltage of 30 kV.

Wide angle X-ray diffraction pattern

Crystalline structure, as revealed by a wide-angle powder X-ray diffraction pattern, was determined with a Philips PW 1830 MPD diffractometer (Almelo, the Netherlands) after starch samples were equilibrated in a 100% RH chamber for 18 h. The X-ray generator was set at 45 kV and the current tube at 40 mA at the scanning 2θ angle from 5° to 35° with a step size of 0.02° at 1 s per step. The data was collected using X'Pert HighScore® software, and the relative crystallinity (%) was calculated as the ratio of the sum of each individual peak area divided by the total area.

Gelatinization properties

Gelatinization properties were measured using a differential scanning calorimeter (DSC, model Diamond, Perkin-Elmer, Norwalk, CT). Starch (8.0 mg, db) was weighed in a stainless-steel pan and added with 16 μL of DI water. The pan was hermetically sealed, equilibrated for 1 h at room temperature, and scanned from 25 to 120°C at a heating rate of 10°C/min. The

gelatinization enthalpy (ΔH), and the onset (T_o), peak (T_p), and end (T_e) temperatures were registered. The gelatinization range was calculated as the difference between T_e and T_o.

Starch molecular-size distribution

High-performance size exclusion chromatography (HPSEC) was used to characterize the molecular-size distribution of starches following the method of Arijaje, Wang, Shin, Shah, and Proctor (2014). Twenty mg of starch was dissolved in 5 mL of 90% dimethyl sulfoxide (DMSO), boiled for 1 h, stirred overnight at room temperature, and centrifuged at 9,300 ×g for 10 min prior to injection into an HPSEC system (Waters Corp., Milford, MA). The HPSEC system consisted of an inline degasser, a model 515 HPLC pump with a 200-μL injector valve (model 7725i, Rheodyne, Cotati, CA), a model 2414 refractive index detector, a guard column (OHpak SB-G, 6.0 × 50 mm i.d. × length), and two Shodex columns (OHpak SB-804 and KB-802, 8.0 × 300 mm i.d. × length). The flow rate was set at 0.5 mL/min with a mobile phase of 0.1 M sodium nitrate with 0.02% sodium azide. The columns were kept at 55°C and the detector at 40°C. The data was collected with Empower Pro2 software (Waters Corp., Milford, MA), and the molecular-size distribution was calculated by comparing the retention times against dextran standards of molecular weight 180.16, 828.72, 1,153, 5,200, 148,000, 872,300, and 1,100,000 g/mol (Waters Corp., Milford, MA), and 1,100,000 g/mol (Sigma-Aldrich, St. Louis, MO) retention times.

Statistical analysis

All of the experiments were replicated, and each analysis was done in duplicate. The data was analyzed using JMP Pro14 Software (SAS Institute Inc., Cary, NC, USA), and the means compared using Student's t least significant differences (LSD) test.

3.4 RESULTS AND DISCUSSION

3.4.1 Acid Hydrolysis

The acid hydrolysis profiles of common corn and potato starches over 120 min are presented in Figure 3.1. Acid hydrolysis has been reported to take place in two distinct phases, a fast hydrolysis of the amorphous lamellae and a second phase of slow hydrolysis of the crystalline lamellae (Kim, Lee, Kim, Lim, and Lim, 2012). Both common corn and potato starches exhibited rapid hydrolysis when subjected to 3.16 M H_2SO_4 at 50°C up to 120 min. Potato starch was hydrolyzed faster, reaching 5% and 10% hydrolysis after 15 and 45 min, respectively; whereas common corn starch reached 5% and 10% hydrolysis after 52 and 84 min, respectively. Under the present high acid concentration at a high temperature of 50°C, the differences in the degree of hydrolysis between the two starches widened with time. Jenkins and Donald combined small-angle X-ray scattering (SAXS) and wide-angle X-ray scattering (WAXS) and showed that the amorphous background was preferentially hydrolyzed at the early stages of acid hydrolysis (Jenkins and Donald, 1997). They concluded that the removal of the amorphous background led to the destabilization of the crystalline lamellae. It is possible that in the present study, the amorphous background of potato starch expanded more rapidly relative to common corn starch due its inherent greater water and phosphate contents, thus increasing the extent of acid hydrolysis. Bertoft (2004) observed a similar hydrolysis profile when waxy maize

and waxy potato starches were treated with 2.2 M HCl at different temperatures (22, 29, and 35°C), and suggested that at low levels of hydrolysis waxy potato starch was hydrolyzed faster than waxy maize starch due to differences in their amorphous structures.

There are conflicting reports regarding the structural basis of the susceptibility of different starches to acid hydrolysis. Singh and Ali (2008) found A-type starches more susceptible to acid hydrolysis than B-type starches when treated with the same concentrations of HCl and H_2SO_4 at 50°C. They suggested that the greater susceptibility of A-type starches to acid is due to the smaller size of A-type granules that comprise a larger surface area, and thus greater hydrolysis was attained. They also observed that the degree of hydrolysis was greater when HCl was used and attributed this to the greater dissociation constant of HCl as compared to the dibasic H_2SO_4. Recently, however, after treating waxy corn (A-type) and high amylose (80%) corn (B-type) starch with 2 M HCl at 20°C for 12 days, Chen, Xie, Zhao, Qiao, Liu (2017) concluded that the many pores and channels on the granule surface structure of waxy corn starch was responsible for its greater acid susceptibility.

In contrast, Jane, Wong, and McPherson (1997) treated common corn and potato starches with 15% (v/v) H_2SO_4 at 25°C and 38°C and observed that at 25°C the hydrolysis rate of potato starch was slightly lower than that of common corn starch, but at 38°C the hydrolysis rate of potato starch became significantly greater than that of common corn starch. Nakazawa and Wang (2003) and Kim, Lee, Kim, Lim, and Lim (2012) applied similar conditions using 15.3% H_2SO_4 at 38°C and 3.16 M H_2SO_4 at 40°C, respectively, and reported potato starch had a greater susceptibility to acid hydrolysis compared with common corn starch. Jane, Wong, and McPherson (1997) and Kim, Lee, Kim, Lim, and Lim (2012) attributed the greater hydrolysis rate of potato starch to its larger granule size and high phosphate content, which promote

swelling and consequently, increases the acid access to both amorphous and crystalline lamellae of the granule. Therefore, the high temperature (50°C) used in the present study may initiate a destabilizing effect on potato starch because of its greater swelling noted by Jane, Wong, and McPherson (1997) and Kim, Lee, Kim, Lim, and Lim (2012). Furthermore, the less compact structure and greater water content of potato starch compared with the more compact structure of common corn starch also presented more hydrolyzing sites for acid (Jane, 2006); hence, the degree of hydrolysis in the potato starch was greater.

3.4.2 Characterization of acid-hydrolyzed starches

The gelatinization properties of the native (0%) and acid-hydrolyzed (5% and 10%) starches, as determined by differential scanning calorimetry (DSC), are presented in Table 3.1. Under the conditions used in this study, the onset (T_o) temperature decreased, but the peak (T_p) and end (T_e) temperatures and the gelatinization range (T_e–T_o) of common corn starch increased with increasing acid hydrolysis. Potato starches exhibited a similar trend except the T_o increased with increasing acid hydrolysis.

The decrease in T_o and enthalpy of the acid-treated corn starches was different from most other studies showing increased acid hydrolysis associated with increased T_o, enthalpy, and relative crystallinity (Miao, Jiang, Zhang, Jin, and Mu, 2011; Palma-Rodriguez et al., 2012; Ulbrich, Natan, and Flöter, 2014). The increased T_p and T_e but decreased T_o for acid-hydrolyzed corn starches in the present study suggest that the molecular architecture of the amorphous and crystalline lamellae was disrupted, but not destroyed, under the severe acid hydrolysis condition used, thus becoming a broader range of crystalline structure. On the other hand, the increase in T_o of acid-hydrolyzed potato starches suggests that the amorphous lamellae in potato starch was

hydrolyzed more rapidly than in common corn starch. Kim, Lee, Kim, Lim, and Lim (2012) and Utrilla-Coello et al. (2014) reported decreased T_o for acid-hydrolyzed common corn starch at the initial stages of hydrolysis and attributed the decrease to the separation of the amorphous and the crystalline lamellae, and the hydrolysis of amylose chains.

Jenkins and Donald (1995) showed that the presence of intertwined amylose in the granule disrupted the perfect crystalline order within the amylopectin crystallites by pulling out short chains toward the background, but also contributed to the density of the amorphous lamellae. Additionally, the amylopectin side chains located at the edge of the semi-crystalline regions were suggested to form bonds in the growth rings, thus imposing stress in the amylopectin crystallites during gelatinization (Jenkins and Donald, 1998). It is speculated that in the present study the increase in the gelatinization range (T_e–T_o) for both starches was the product of the hydrolysis of the amylose and amylopectin side chains that were located towards the amorphous background and the edge of the semi-crystalline regions, thus contributing to reduced swelling of the remaining amorphous background and consequently, the melting of crystallites at a broader temperature range with increasing acid hydrolysis. Both starches displayed decreased gelatinization enthalpy with increasing acid hydrolysis as a result of decreased crystalline structure, with corn starches displaying a greater decrease with respect to potato starches. The greater decrease in enthalpy in corn starches corroborates its decrease in T_o and supports the proposed disruption of its crystalline lamellae during the present acid hydrolysis conditions.

The X-ray diffraction patterns and relative crystallinity (RC) values of native (0%) and acid-hydrolyzed (5% and 10%) starches are presented in Figure 3.2. The main peaks of corn starches at 15°, 17°, 18°, and 23° became sharper with increased hydrolysis and the RC increased

from 41.1% to 43.4% and 44.9% after 5% and 10% hydrolysis (Figure 3.2A). In contrast, the main peaks of potato starches at 5.5°, 14°, 17°, 22°, and 24° decreased slightly, and the RC decreased after 5% hydrolysis (40.3%) and then increased after further hydrolysis of 10% (43.8% RC) (Figure 3.2B). The progressive increase in starch RC during acid hydrolysis is associated with the preferential hydrolysis of the amorphous background and amorphous lamellae (Jenkins, 1998), which however, does not necessarily lead to a corresponding increase in gelatinization enthalpy (Table 3.1). Starch gelatinization involves the melting of crystallites, and therefore, low gelatinization enthalpies are an indication of less densely packed crystalline units (Blazek and Gilbert, 2010). It has also been suggested that the amorphous lamellae restrict the swelling and water access to the crystallites during gelatinization. Thus, the energy required to melt the crystallites decreases when the amorphous lamellae are preferentially removed by acid (Muhr, Blanshard, and Bates, 1984). The decrease in RC of 5% acid-hydrolyzed potato starch implies a simultaneous hydrolysis of both crystalline and amorphous lamellae, which is supported by the observed decreased gelatinization enthalpy (Table 3.1). The results suggest that during the acid hydrolysis of starch, the crystalline lamellae was also hydrolyzed but at a slower rate than the amorphous lamellae. In addition, we suspect that due to the observed increase in RC at 10% hydrolysis and due to the smaller decrease in gelatinization enthalpy compared with corn starch, some rearrangement of crystallites in potato starch could occur during acid hydrolysis.

Native common corn starch displayed the typical polygonal shape (Figure 3.3A), and potato starch appeared oval with a smooth surface (Figure 3.3B) under scanning electron microscopy. After the acid treatment, no significant change was observed on the surface of common corn starch (Figures 3.3C and 3.3E). In contrast, the surface of the potato starch granules became rough, and this change was more evident as the level of acid hydrolysis

increased (Figure 3.3D and 3.3F). The roughness on the surface of acid-treated potato starches appeared as surface peeling, and its distribution varied with granule size, both agreeing with Jayakody and Hoover (2002). The naturally present pores and channels in corn starch facilitated the acid hydrolysis of the granules from the inside (Chen, Xie, Zhao, Qiao, and Liu, 2017); therefore, surface roughness was not observed. However, the relatively compact surface of potato starch granules (Oates, 1997) only permitted the exo-erosion of the granules, resulting in more visible surface roughness. The distribution of loosely packed areas could account for the differences in the roughness, with a more homogenous distribution in the larger potato starch granules but more concentrated in one end in the smaller potato starch granules (Lin et al., 1993). Furthermore, Jane and Shen (1993) demonstrated that a greater proportion of amylose was located at the periphery of starch granules. Because larger potato starch granules comprise more amylose (Dhital, Shrestha, Hasjim, and Gidley, 2011), a greater amount of amylose may be hydrolyzed at the periphery, thus producing more rough areas in larger granules.

The molecular-size distribution of native and debranched common corn and potato starch after different degrees of acid hydrolysis are shown in Figure 3.4, and the numbers represent the peak degree of polymerization (DP) of the fractions. The molecular-size distribution profile of native starches consisted of three fractions: amylopectin, intermediate materials, and amylose with their peak DP 50612, 14403, and 2531 for common corn starch, respectively, and 34346, 15174, and 3026 for potato starch, respectively. After the acid treatment, both the amylopectin and intermediate material fractions of common corn starch disappeared, and the remaining fraction displayed a unimodal distribution with an average DP of 670 and 299 for the 5% and 10% hydrolysis, respectively. For potato starch, the amylopectin fraction diminished after 5% hydrolysis and the intermediate material fraction was absent after 10% hydrolysis. The

remaining fraction of 10% acid-hydrolyzed potato starch displayed a bimodal distribution. The bimodal distribution of potato starch suggests an uneven hydrolysis pattern of potato starch compared with a more even hydrolysis pattern of common corn starch, presumably, due to their differences in granule surface structure and/or structural arrangement in the amorphous lamellae. For example, potato starch granules are more ordered on their periphery regions (Sevenous, Hill, Farhat, and Mitchell, 2002), and branch points are clustered mostly in the amorphous lamellae (Jane, Wong, and McPherson, 1997) compared with the less ordered periphery regions and the more evenly distributed branch points in both amorphous and crystalline lamellae in common corn starch.

The debranched starch also comprised three fractions, including amylose, and long and short amylopectin chains. As the acid hydrolysis progressed, the amylose fraction of both the potato and the corn starch decreased considerably. With increased acid hydrolysis, the peak DP of the short amylopectin chain fraction decreased from 58 to 47 and 46 for the native (0%), 5%, and 10% acid-hydrolyzed corn starches, respectively. Similarly, the peak DP of the short amylopectin chain fraction decreased from 66 to 51 and 53 for the native (0%), 5%, and 10% acid-hydrolyzed potato starches, respectively. The proportion of the long amylopectin chain fractions was consistently smaller than that of the short amylopectin chain fractions for corn starches. In contrast, the proportions of the long and the short amylopectin chain fractions were comparable for potato starch, but the proportion of the long amylopectin chain fractions decreased with increasing acid hydrolysis. Komiya and Nara (1986) observed a similar distribution of short and long amylopectin chains in acid-hydrolyzed potato starch (1 N H_2SO_4 at 45°C for 6 days) and suggested that it was the product of a slight deterioration of the crystalline lamellae that occurred from the acid hydrolysis. The present results support the hypothesis that

acid initially attacks the amorphous region since amylose was degraded to a greater extent than amylopectin (Wang and Wang, 2001), and since there were differences between the amorphous background and amorphous lamellae in the common corn starch and the potato starch.

3.4.3 Enzyme digestion of native and acid-hydrolyzed starches

Both endo-acting α-amylase and exo-acting glucoamylase were used in this study to elucidate the acid treatment effects on their digestion of common corn versus potato starch. The degree of digestion (%) significantly increased after the acid treatment and varied with the starches and enzymes (Table 3.2). Compared to their native counterparts (0%), the digestion of 5% and 10% acid-hydrolyzed corn starch increased by 4.7 and 11.3 percentage points, respectively, after just 1 h of α-amylase digestion, and after 24 h, it increased by 12.2 and 29.4 percentage points, respectively; the α-amylolysis of potato starch increased by 4.2 and 9.1 percentage points for 5% and 10% acid-hydrolysis, respectively, after 24 h.

The digestion of native starch granules involves the diffusion of enzymes onto the starch granule surface, followed by adsorption, and subsequent hydrolysis of glucan chains (Colonna, Leloup, and Buleon, 1992). This reaction is heterogeneous and affected by starch granule morphology, different levels of starch granular organization, and the mode and concentration of amylase used (O'Brien and Wang, 2008; Kimura and Robyt, 1996; Yook and Robyt, 2002). Alpha-amylase from *B. licheniformis* and glucoamylase from *A. niger* have large binding sites of eight and seven D-glucosyl units, respectively (Robyt and French, 1967; Kandra, Gyémánt, Remenyik, Hovánszki, and Lipták, 2003; Zhang, Dhital, and Gidley, 2013). The increased α-amylolysis of acid-treated starches indicates that acid not only hydrolyzed the amorphous lamellae, but also exposed the crystalline structure that became more available to α-amylase,

supporting the reduced gelatinization enthalpy results (Table 3.1). The increased binding sites combined with the naturally present pores and channels would accelerate the digestion of acid-hydrolyzed corn starch. The lower susceptibility of potato starch to α-amylase digestion has been attributed to the clustering of branching points within the amorphous lamellae, which results in a greater density, and its greater proportion of long amylopectin chains that form more organized crystallites (Jane, Wong, and, McPherson, 1997). The decreased disruption of the crystalline lamellae in potato starch compared to corn starch, as shown in the gelatinization results (Table 3.1), may explain its lower susceptibility to α-amylase digestion. Therefore, the difference in the degree of digestion between common corn starch and potato starch could be linked to their inherent differences in the distribution of the amorphous lamellae and the crystalline structure of the granules.

A similar trend was observed in the degree of digestion by glucoamylase for both starches, but the increase was less compared with that of α-amylase, except that 5% and 10% acid-hydrolyzed potato starches after 24 h showed significantly increased glucoamylolysis of 11.0 and 16.2 percentage points, respectively. Zhang, Dhital, and Gidley (2013) suggested that the activity of glucoamylase is restricted to the available non-reducing ends of starch chains; therefore, its digestion rates tend to be lower compared with that of α-amylase. Lineback (1984) hypothesized that glucoamylase can begin its catalytic activity on the starch granule surface where disorganized branches of amylopectin with exposed non-reducing ends are available; hence, the activity of the enzyme is carried out preferentially in longer chains that have an affinity for the large binding site of glucoamylase. The glucoamylolysis of corn starch was faster than that of potato starch up until 10 h and then decreased at 24 h, which is consistent with a reaction of pseudo first-order behavior (Zhang, Dhital, and Gidley, 2013) and implies that the

substrate initially was readily available but became scarce due to a rapid reduction in the DP of the available chains. The increase in glucoamylolysis was less for the 5% and 10% acid-hydrolyzed potato starches during the first 10 h, suggesting that some densely packed areas in the amorphous lamellae were still present and restrict the enzyme binding. The greatly increased digestion after 24 h implies that the densely packed crystallites were unwound and became more accessible after glucoamylase diffused throughout the remaining structures in an attack from the end of the starch chains.

3.4.4 Characterization of enzyme-digested acid-hydrolyzed starches

The relative crystallinity (RC) values of enzyme-digested starches are summarized in Table 3.3. After 24 h of enzymatic digestion, the RC of most starches decreased, and the reduction varied with enzymes and acid levels. The greatest decrease in RC was observed for the native (0%) starches after 24 h of digestion by both enzymes, with ~14.0 and ~8.0 percentage points for potato and common corn starches, respectively. Aggarwal and Dollimore (1998) reported a similar trend for native common corn and other A-type starches digested with glucoamylase, but they did not observe significant changes in the RC of native potato starch, which could be attributed to the different digestion conditions used. In the present study, the acid treatment changed the hydrolysis pattern of both α-amylase and glucoamylase, which consequently, had a profound impact on the granule surface structure of the potato starch, resulting in the formation of pores. The porous structure was observed in both of the acid-treated corn and potato starch even after just 1 h of digestion by α-amylase or glucoamylase.

After 24 h of digestion, the extensive collapse and breakage of both corn and potato starch granules was observed by SEM, particularly by α-amylase. Therefore, the micrographs of

treated starches after 10 h of enzymatic digestion are presented (Figure 3.5 and Figure 3.6) to illustrate the porous structure in detail. As observed in previous reports, native common corn starch, digested by α-amylase (Figure 3.5A) or glucoamylase (Figure 3.5G) for 10 h, displayed enlarged pores with a uniform distribution among the granules (Kimura and Robyt, 1995; Shrestha et al., 2012). Alpha-amylase digestion produced corn starch granules with pores whose diameter increased with increased digestion time and appeared to correlate with the acid hydrolysis levels. The rate of digestion by α-amylase of the native and acid-treated corn starch was significantly greater than that of glucoamylase (Table 3.2), and their micrographs (Figure 3.5A-C vs. 3.5G-I) confirm the difference in the activity between the two enzymes. The glucoamylolysis also resulted in corn starch granules with a porous structure.

The attack of α-amylase on the native potato starch granule was more concentrated around the end periphery and the vertical axis, thus resulting in a single enlarged opening (Figure 3.5D). Some granules displayed breakage and surface pitting, and other granules remained intact. A similar action pattern was observed for the glucoamylolysis of the native potato starch granules, but there was no observable formation of pores on the surface (Figure 3.5J). Acid-treated potato starch, when digested by α-amylase, resulted in a porous structure (Figure 3.5E-F) that became more defined as acid hydrolysis increased. Moreover, the distribution of the pores was not uniform throughout the potato starch granule as opposed to the more evenly distributed porous structure in the corn starch. Similarly, the glucoamylolysis of the 5% and 10% acid-hydrolyzed potato starch also produced granules with pores, but the pores appeared to be smaller and more evenly distributed (Figure 3.5K-L). The localized porous structure of the α-amylase-treated potato starch versus the more homogeneous porous structure of the glucoamylase-treated potato starch could be related to the inherent difference in the binding site of each enzyme. The

present study suggests that acid destabilized the areas of the granules that were tightly packed, thus facilitating the initial absorption and diffusion of both enzymes through the granule surface.

3.5 CONCLUSIONS

Potato starch granules were more susceptible to acid hydrolysis at a high acid concentration and high temperature. Under the conditions applied, the acid hydrolysis destabilized the crystalline lamellae in both common corn and potato starch, and the destabilization enhanced the digestion of both starches by α-amylase or glucoamylase. The extent of enzymatic digestion varied with the starch and enzyme. The combination of acid hydrolysis followed by digestion with α-amylase or glucoamylase resulted in the formation of a porous structure in potato starch, which has been not reported in previously published literature. The porous structure in potato starch became more defined with a greater hydrolysis level, and its distribution was dependent on the action mode of each enzyme. It is suggested that the acid hydrolysis of potato starch allows the removal of peripheral amylose chains, which destabilized the tightly packed crystalline lamellae that are composed of long amylopectin chains. Therefore, the observed porous structure in potato starch is proposed to be a product of increased binding of the enzymes after acid hydrolysis destabilized the tightly packed areas. The increased susceptibility to enzymatic digestion and the formation of the porous structure in potato starch could help the development of B-type porous starch delivery systems for the colonic delivery of bioactive components. This delivery system would have significant advantages over the currently utilized porous A-type starch delivery systems due to the greater resistance of B-type starches to enzyme digestion in the upper digestive tract.

3.6 REFERENCES

Aggarwal, P., Dollimore, D. A. (1998). Thermal analysis investigation of partially hydrolyzed starch. *Thermochimica Acta, 319*, 17–25.

Arijaje, E., Wang, Y.-J., Shin, S., Shah, U., & Proctor, A. (2014). Effects of chemical and enzymatic modifications on starch-stearic acid complex formation. *Journal of Agricultural & Food Chemistry, 62*, 2963–2972.

Bazin, H., & Barresi, F. (2007). Method for preparing a fluid absorber. US Patent US7226760B2. June 5, 2007.

Benavent-Gil, Y., & Rosell, C. (2017). Comparison of porous starches obtained from different enzyme types and levels. *Carbohydrate Polymers,157*, 533–540.

Bertoft, E. (2004). Lintnerization of two amylose-free starches of A- and B-crystalline types, respectively. *Starch – Stärke, 56*, 167–180.

Biliaderis, C. G., Grant, D. R., & Vose, J. R. (1981). Structural characterization of legume starches. II. Studies on acid-treated starches. *Cereal Chemistry, 58*, 502–507.

Blazek, J., & Gilbert, E. P. (2010). Effect of enzymatic hydrolysis on native starch granule structure. *Biomacromolecules, 11*, 3275–3289.

Chen, P., Xie, F., Zhao, L., Qiao, Q., Liu, X. (2017). Effect of acid hydrolysis on the multi-scale structure change of starch with different amylose content. *Food Hydrocolloids, 69*, 359–368.

Colonna, P., Leloup, V., & Buleon, A. (1992). Limiting factors of starch hydrolysis. *European Journal of Clinical Nutrition, 46*, S17–S32.

Dhital, S., Shrestha, A. K., Hasjim, J., & Gidley, M. J. (2011). Physicochemical and structural properties of maize and potato starches as a function of granule size. *Journal of Agricultural & Food Chemistry, 59*, 1015–10161.

Dhital, S., Shrestha, A., & Gidley, M. (2010). Relationship between granule size and *in vitro* digestibility of maize and potato starches. *Carbohydrate Polymers, 82*, 480–488.

Dhital, S., Warren, F., Zhang, B., & Gidley, M. J. (2014). Amylase binding to starch granules under hydrolysing and non-hydrolysing conditions. *Carbohydrate. Polymers*, *113*, 97–107.

Dubois, M., Gilles, K., Hamilton, J., Rebers, P., & Smith, F. (1956). Colorimetric method for determination of sugars and related substances. *Analytical Chemistry*, *28*, 350–356.

Fannon, J., Hauber, R., & BeMiller, J. (1992). Surface pores of starch granules. *Cereal Chemistry*, *69*, 284–288.

Fannon, J., Shull, J., & BeMiller, J. (1993). Interior channels of starch granules. *Cereal Chemistry*, *70*, 611–613.

Gallant, D., Bouchet, B., Buleon, A., & Perez, S. (1992). Physical characteristics of starch granules and susceptibility to enzymatic degradation. *European Journal of Clinical Nutrition*, *46*, 3–16.

Hoover, R., Rorke, S. C., & Martin, A. M. (1991). Isolation and characterization of lima bean (*Phaseolus Lunatus*) starch. *Journal of Food Biochemistry*, *15*, 117–136.

Hoover, R., Swamidas, G., & Vasanthan, T. (1993). Studies on the physicochemical properties of native, defatted and heat-moisture treated pigeon pea (*Cajanus Cajan L*) starch. *Carbohydrate Research*, *246*, 185–203.

Huber, K., & BeMiller, J. (1997). Visualization of channels and cavities of corn and sorghum starch granules. *Cereal Chemistry*, *74*, 537–541.

Jane, J.-L. Current understanding on starch granule structures. *Journal of Applied Glycoscience*, *53*, 205–213.

Jane, J.-L., & Shen, J. J. (1993) Internal structure of the potato starch granule revealed by chemical gelatinization. *Carbohydrate Research*, *247*, 279–290.

Jane, J.-L., Wong, K.-S., & McPherson, A. (1997). Branch-structure difference in starches of A- and B-type X-ray patterns revealed by their Naegeli dextrins. *Carbohydrate Researh*, *300*, 219–227.

Jayakody, L., & Hoover, R. (2002). The Effect of lintnerization on cereal starch granules. *Food Research International, 35,* 665–680.

Jenkins, P. (1994). X-Ray and neutron scattering studies of starch granule structure. Ph.D. Thesis, University of Cambridge, U.K.

Jenkins, P. J., & Donald, A. M. (1995). The influence of amylose on starch granule structure. *International Journal of Biological Macromolecules, 17,* 315–321.

Jenkins, P. J., & Donald, A. M. (1997). The effect of acid hydrolysis on native starch granule structure. *Starch – Stärke, 49,* 262–267.

Jenkins, P. J., & Donald, A. M. (1998). Gelatinization of starch: A combined SAX/WAXS/DSC and SANS study. *Starch – Stärke, 308,* 133–147.

Kandra, L. (2003). α-Amylases of medical and industrial importance. *Journal of Molecular Structure: THEOCHEM, 666,* 487–498.

Kandra, L., Gyémánt, G., Remenyik, J., Hovánszki, G., & Lipták, A. (2002). Action pattern and subsite mapping of *Bacillus licheniformis* α-amylase (BLA) with modified maltooligosaccharide substrates. *FEBS Letters, 518,* 79–82.

Kim, H.-J., Lee, J., Kim, J.-Y., Lim, W.-J., & Lim S.-T. (2012). Characterization of nanoparticles prepared by acid hydrolysis of various starches. *Starch – Stärke, 64,* 367–373.

Kimura, A., & Robyt, J. F. (1995). Reaction of enzymes with starch granules: Kinetics and products of the reaction with glucoamylase. *Carbohydrate Research, 277,* 87–107.

Kimura, A., & Robyt, J. F. (1996). Reaction of enzymes with starch granules: Enhanced reaction of glucoamylase with gelatinized starch granules. *Carbohydrate Research, 288,* 233–240.

Komiya, T., & Nara, S. (1986). Changes in crystallinity and gelatinization phenomena of potato starch by acid treatment. *Starch – Stärke, 38,* 9–13.

Lin, H.-M, Chang, Y.-H, Lin, J.-H., Jane, J.-L, Sheu, M.-J, & Lu, T.-J. (1993). Heterogeneity of lotus rhizome starch granules as revealed by α-amylase degradation. *Carbohydrate Polymers, 66,* 528–536.

Lineback. D.R. (1984). The starch granule organization and properties. *Bakers Digest, 58,* 16–21.

Miao, M., Jiang, B., Zhang, T., Jin, Z., & Mu, W. (2011). Impact of mild acid hydrolysis on structure and digestion properties of waxy maize starch. *Food Chemistry, 126,* 506–513.

Muhr, A. H., Blanshard, J.M. V., & Bates, D. R. (1984). The effect of lintnerisation on wheat and potato starch granules. *Carbohydrate Polymers, 4,* 399–425.

Nakazawa, Y., & Wang, Y. (2003). Acid hydrolysis of native and annealed starches and branch-structure of their Naegeli dextrins. *Carbohydrate Research, 338,* 2871–2882.

O'Brien, S., & Wang, Y.-J. (2008). Susceptibility of annealed starches to hydrolysis by α-amylase and glucoamylase. *Carbohydrate Polymers, 72,* 597–607.

Oates, C. G. (1997). Towards an understanding of starch granule structure and hydrolysis. *Food Science & Technology, 8,* 375–382.

Palma-Rodriguez, H. M., Agama-Acevedo, E., Mendez-Montealvo, G., Gonzalez-Soto, R. A., Vernon-Carter, E. J., & Bello-Pérez, L. A. (2012). Effect of acid treatment on the physicochemical and structural characteristics of starches from different botanical sources. *Starch – Stärke, 64,* 115–125.

Robyt, J. F., & French, D. (1967). Multiple attack hypothesis of α-amylase action: Action of porcine pancreatic, human salivary, and *Aspergillus Oryzae* α-amylase. *Archives of Biochemistry and Biophysics, 122,* 8–16.

Sevenous, O., Hill, S. E., Farhat, I. A., & Mitchell, J. R. (2002). Organisation of the external region of the starch granule as determined by infrared spectroscopy. *International Journal of Biological Macromolecules, 31,* 79-85.

Shrestha, A. K., Blazek, J., Flanagan, B. M., Dhital, S., Larroque, O., Morell, M. K., Gilbert, E., & Gidley, M. J. (2012). Molecular, mesoscopic and microscopic structure evolution during amylase digestion of maize starch granules. *Carbohydrate Polymers, 90,* 23–33.

Singh, V., & Ali, S. Z. (2008). Properties of starches modified by different acids. *International Journal of Food Properties, 11,* 495–507.

Srichuwong, S., Isono, N., Mishsima, T., & Hisamatsu, M. (2005). Structure of lintnerized starch is related to X-ray diffraction pattern and susceptibility to acid and enzyme hydrolysis of starch granules. *International Journal of Biological Macromolecules*, *37*, 115–121.

Ulbrich, M., Natan, C., & Flöter, E. (2014). Acid modification of wheat, potato, and pea starch applying gentle conditions—Impacts on starch properties. *Starch – Stärke*, *66*, 903–913.

Utrilla-Coello, R. G., Hernández-Jaimes, C., Carrillo-Navas, H., González, F., Rodríguez, E., Bello-Pérez, L. A., Vernon-Carter, E. J., Alvarez-Ramirez, J. (2014). Acid hydrolysis of native corn starch: Morphology, crystallinity, rheological and thermal properties. *Carbohydrate Polymers*, *103*, 596–602.

Wang, L., & Wang, Y.-J. (2001). Structures and physicochemical properties of acid-thinned corn, potato and rice starches. *Starch – Stärke*, *53*, 570–576.

Yao, W., & Yao, H. (2002). Adsorbent characteristic of porous starch. *Starch – Stärke*, *54*, 260–263.

Yook, C., & Robyt, J. F. (2002). Reactions of alpha amylases with starch granules in aqueous suspension giving products in solution and in a minimum amount of water giving products inside the granule. *Carbohydrate Research*, *337*, 1113–1117.

Zhang, B., Dhital, S., & Gidley, M. J. (2013). Synergistic and antagonistic effects of α-amylase and amyloglucosidase on starch digestion. *Biomacromolecules*, *14*, 1945–1954.

Zhang, G., Venkatachalam, M., & Hamaker, B. R. (2006). Structural basis for the slow digestion property of native cereal starches. *Biomacromolecules*, *7*, 3259–3266.

Zhao, J., Madson, M., & Whistler, R. (1996). Cavities in porous corn starch provides a large storage space. *Cereal Chemistry*, *73*, 379–380.

Zhu, Q., & Bertoft, E. (1996). Composition and structural analysis of alpha-dextrins from potato amylopectin. *Carbohydrate Research*, *288*, 155–174.

Table 3.1. Gelatinization properties of native (0%) and acid-treated (5% and 10%) common corn and potato starch.[a]

Starch	Gelatinization Temperature (°C)				Enthalpy (J/g)
	Onset	Peak	End	Range[b]	
Common corn					
0%	69.9 ± 0.1a	73.8 ± 0.3c	80.3 ± 0.0d	10.7 ± 0.0e	14.7 ± 0.1c
5%	67.6 ± 0.1c	78.9 ± 0.1a	91.3 ± 0.1b	23.7 ± 0.2b	9.4 ± 0.2d
10%	60.4 ± 0.0f	78.7 ± 0.6a	95.5 ± 0.4a	35.1 ± 0.3a	9.4 ± 0.3d
Potato					
0%	65.7 ± 0.1e	71.1 ± 0.2d	78.9 ± 0.2e	13.2 ± 0.1d	18.0 ± 0.1a
5%	66.0 ± 0.1d	71.2 ± 0.5d	78.7 ± 0.4e	12.8 ± 0.2d	14.7 ± 0.2c
10%	68.0 ± 0.1b	74.8 ± 0.1b	84.4 ± 0.2c	16.3 ± 0.0c	15.3 ± 0.0b

[a] Means of two replicates ± standard deviation followed by a common letter in the same column are not significantly different (*$p < 0.05$)

[b] (End-Onset) temperature.

Table 3.2. Degree of digestion (%) of native (0%) and acid hydrolyzed (5% and 10%) starches by α-amylase and glucoamylase.[a]

Starch	Duration (h)	α-Amylolysis			Glucoamylolysis		
		0%	5%	10%	0%	5%	10%
Common corn	1	12.0 ± 0.8c	16.7 ± 0.6b	23.3 ± 0.1a	5.4 ± 0.0d	10.1 ± 0.1c	15.0 ± 0.1b
	5	14.3 ± 0.7e	23.4 ± 1.7c	31.1 ± 1.7a	17.5 ± 0.2d	23.6 ± 0.1c	27.3 ± 0.3b
	10	27.5 ± 1.0e	43.0 ± 0.3b	50.6 ± 0.5a	25.9 ± 0.4e	31.7 ± 0.1d	35.6 ± 2.2c
	24	41.9 ± 2.5e	54.1 ± 0.7b	71.3 ± 1.5a	42.4 ± 0.5de	45.5 ± 0.2d	50.6 ± 1.2c
Potato	1	6.4 ± 0.2b	6.7 ± 0.2b	9.8 ± 0.2a	3.1 ± 0.2e	4.8 ± 0.0c	4.0 ± 0.1d
	5	12.9 ± 0.7c	19.8 ± 0.4b	21.2 ± 0.6a	13.2 ± 0.1c	13.4 ± 0.3c	19.4 ± 0.4b
	10	23.0 ± 0.2b	24.0 ± 0.8b	28.8 ± 1.9a	23.4 ± 0.1b	24.1 ± 0.2b	30.1 ± 0.5a
	24	31.6 ± 2.0e	35.8 ± 1.8de	40.7 ± 2.9c	38.6 ± 0.5cd	49.6 ± 1.0b	54.8 ± 2.0a

[a] Mean of two replicates ± standard deviation followed by a common letter in the same row are not significantly different (*$p <$ 0.05)

Table 3.3. Relative crystallinity (%) of native (0%) and acid-treated (5% and 10%) starches after digestion by α-amylase and glucoamylase.[a]

Starch	Duration (h)	α-Amylolysis			Glucoamylolysis		
		0%	5%	10%	0%	5%	10%
Common corn	0	41.1 ± 0.1c	43.4 ± 0.2b	44.9 ± 0.0a	41.1 ± 0.1c	43.4 ± 0.2b	44.9 ± 0.0a
	1	43.1 ± 0.1a	38.8 ± 0.3c	44.9 ± 0.0a	44.0 ± 0.6a	43.2 ± 0.3a	40.6 ± 0.2b
	5	36.2 ± 0.1e	39.8 ± 0.0c	42.3 ± 1.6a	41.3 ± 0.1b	39.3 ±0.2d	40.1 ± 0.0c
	10	33.8 ± 0.0d	41.9 ± 0.2b	41.7 ± 0.1b	37.3 ± 1.0c	43.5 ± 0.0a	42.3 ± 0.1b
	24	33.2 ± 0.8d	34.9 ± 0.0c	41.0 ± 0.0b	33.3 ± 0.8d	41.6 ± 0.0ab	42.5 ± 0.2a
Potato	0	43.3 ± 0.8a	40.3 ± 0.8b	43.8 ± 0.9a	41.1 ± 0.1c	43.4 ± 0.2b	44.9 ± 0.0a
	1	40.3 ± 1.8b	35.3 ± 0.1d	43.6 ± 0.5a	37.8 ± 0.1c	37.2 ± 0.1cd	43.4 ± 0.3a
	5	38.1 ± 0.2c	37.6 ± 0.2c	40.4 ± 0.0b	33.6 ± 1.2d	37.7 ± 0.0c	42.8 ± 0.3a
	10	31.7 ± 0.0e	36.6 ± 0.7c	40.7 ± 0.4b	31.1 ± 0.4e	33.5 ± 0.5d	44.4 ± 1.1a
	24	29.6 ± 0.3d	32.1 ± 0.1c	43.4 ± 1.8a	29.7 ± 0.7d	33.4 ± 0.1c	40.3 ± 0.0b

[1]Mean of two replicates ± standard deviation followed by a common letter in the same row are not significantly different (*$p <$ 0.05)

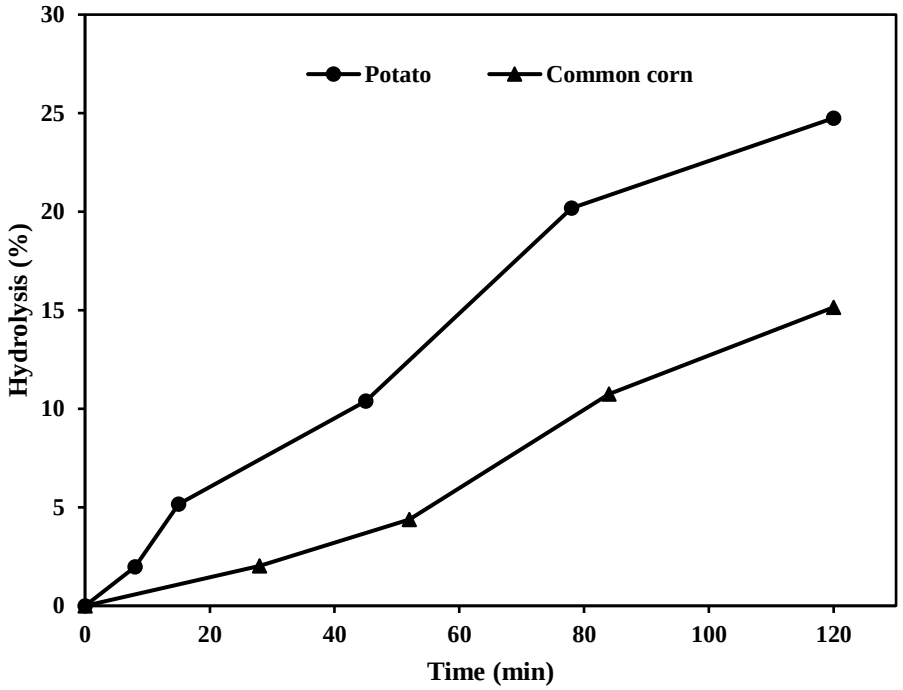

Figure 3.1. Acid hydrolysis profiles of native potato and common corn starch by 3.16 M H_2SO_4 at 50°C.

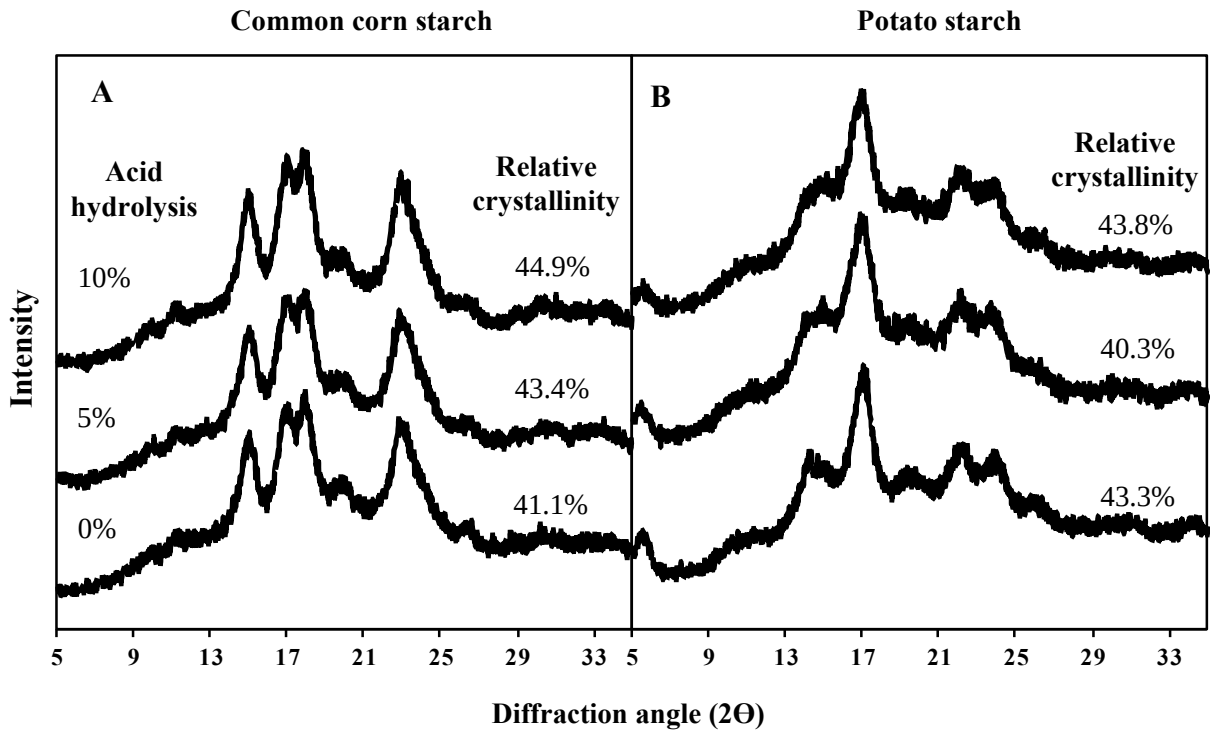

Figure. 3.2. X-ray diffractograms and relative crystallinity values of native (0%) and acid-treated (5% and 10%) common starch (A) and potato starch (B) before digestion by α-amylase and glucoamylase.

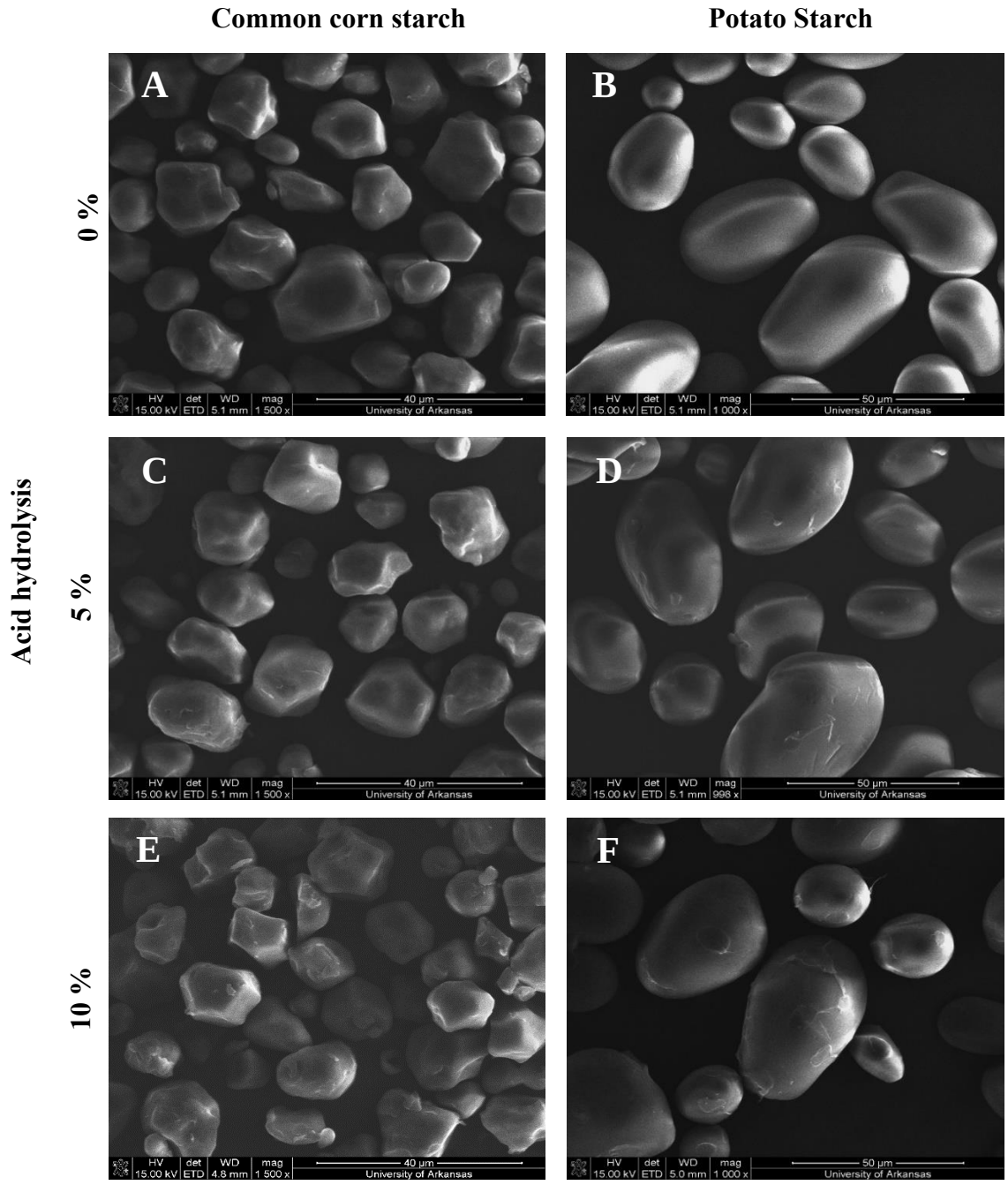

Figure 3.3. Scanning electron micrographs of native (0%) and acid-treated (5% and 10%) common corn (A, C, E) and potato starch (B, D, F).

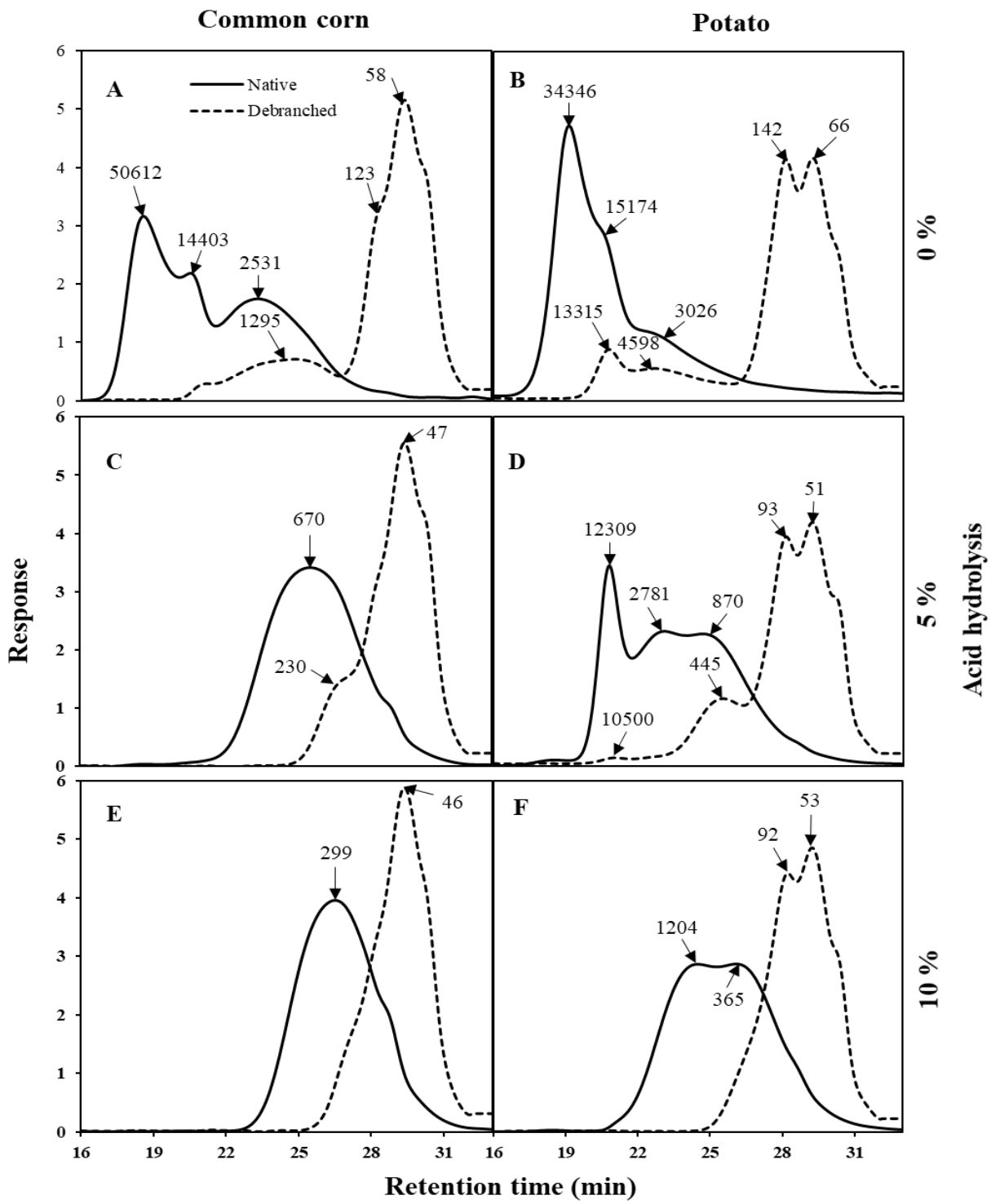

Figure 3.4. Normalized size-exclusion chromatograms of native and debranched common corn (A, C, E) and potato starches (B, D, F) after different degrees (0, 5, and 10%) of acid hydrolysis.

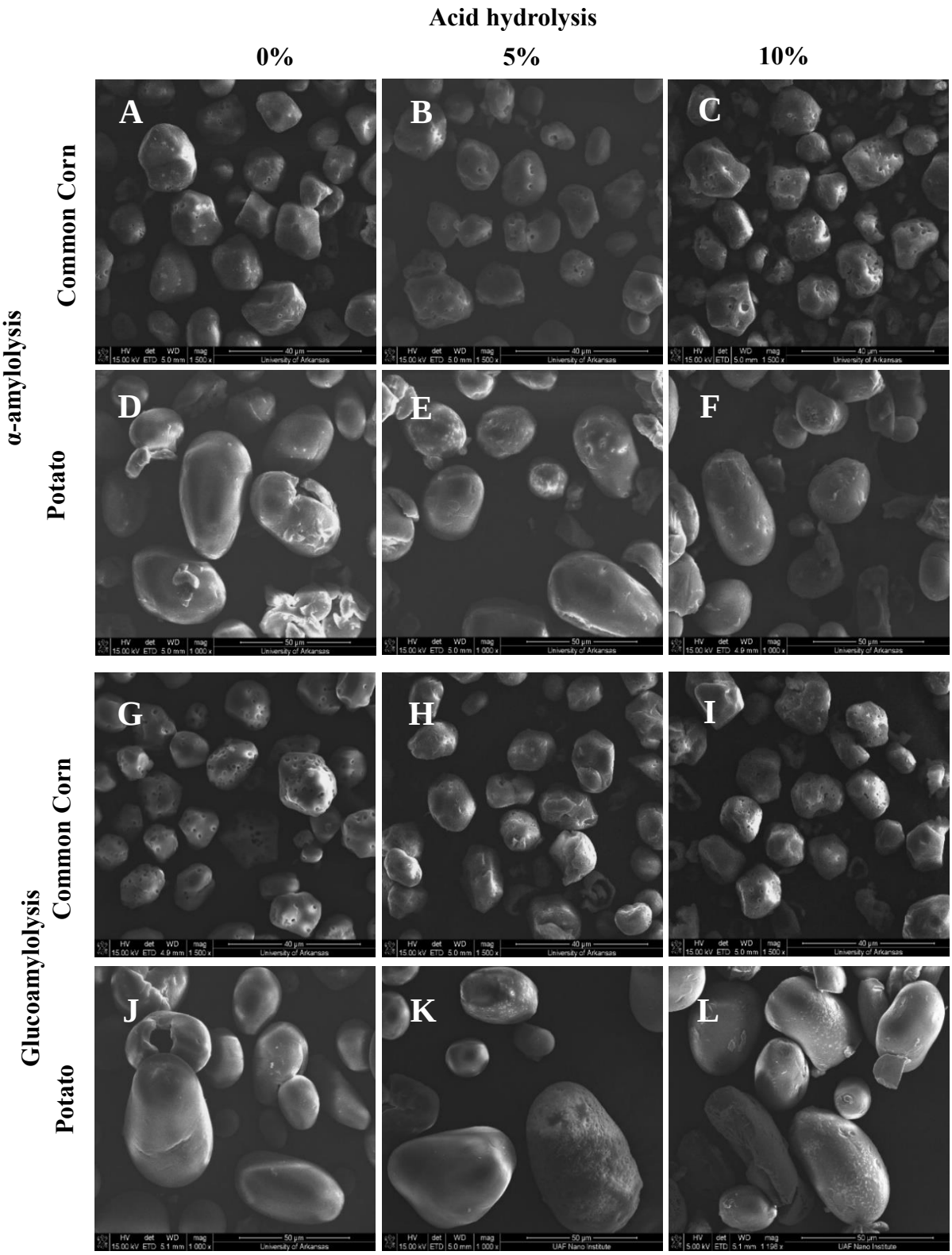

Figure 3.5. Scanning electron micrographs of native (0%) and acid-treated (5% and 10%) common corn and potato starch after 10 h of α-amylase (A-F) and glucoamylase (G-L) digestion.

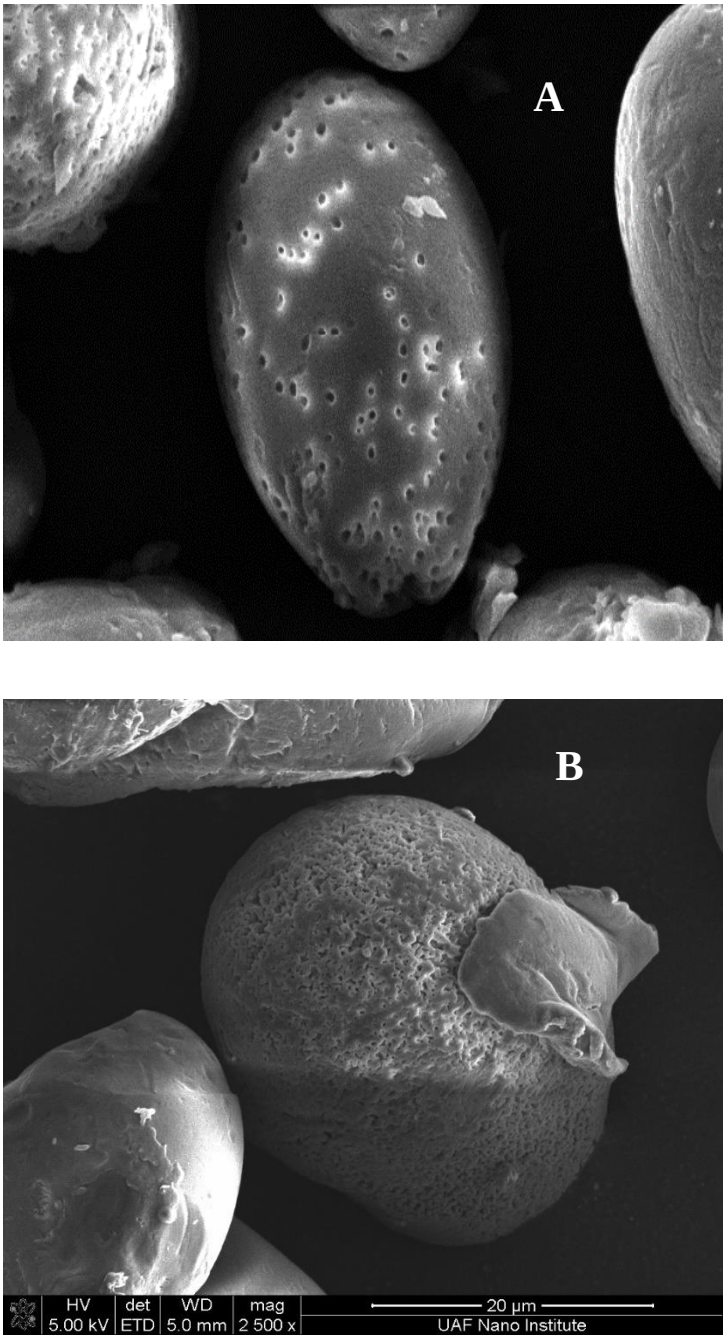

Figure 3.6. Scanning electron micrographs 10% acid hydrolyzed potato starch after 10 h of α-amylase (A) and glucoamylase (B) digestion at a magnification of ×2500 (10-20 µm).

CHAPTER 4

SURFACE REMOVAL ENHANCES THE FORMATION OF A POROUS STRUCTURE IN POTATO STARCH

4.1 ABSTRACT

Native potato starch exhibits limited susceptibility to enzyme digestion and does not form a porous structure. This study investigated the impact of granule surface on starch susceptibility to amylases. Two levels of surface removal via chemical gelatinization of common corn and potato starches were prepared and subjected to digestion by α-amylase or glucoamylase. The degree of digestion varied with the surface removal level and starch type. A porous structure was observed in potato starch after combining surface removal and digestion by amylases. However, the pores in the surface-removed potato starches were not as homogeneous or enlarged compared with corn starch. The removal of dense and tightly packed crystallites on the granule surface was proposed to enhance the degree of binding and hydrolytic activity of both amylases in potato starch. This study provides direct evidence that surface structure hinders amylase digestion and the formation of a porous structure in potato starch.

Keywords: *Surface gelatinization, α-amylase, glucoamylase, porous starch.*

4.2 INTRODUCTION

Porous starch, which is generated by the enzymatic digestion of native starches, is comprised of micropores that are significant due to their capability of retaining and protecting bioactive components through processing and storage (Han et al., 2020; Luo et al., 2013). The formation and distribution of pores are affected by the type of starch and enzyme. The rate of digestion of native starch granules and their susceptibility to amylases have been linked to granule features such as size, surface morphology, and crystalline organization. Overall, A-type starches, such as common corn starch, display greater susceptibility to enzyme digestion and form a well-defined and homogeneous porous structure after digestion (Quigley, Kelly, Doyle, and Fogarty, 1998). In contrast, B-type starches, such as potato starch, show lower digestion rates and do not yield a porous structure resulting in granules with an enlarged single opening or completely collapsed structure (O'Brien and Wang, 2008).

Dhital, Shrestha, and Gidley (2010) studied the relationship between granule size and *in vitro* digestibility of native common corn and potato starches by separating the granules into different size fractions through sedimentation. They observed that granule size did not significantly affect the rate of digestion for common corn starch, whereas extremely large potato starch granules displayed a lower digestion rate. The authors suggested that the digestion rate of starches is a function of the effective surface area. The presence of pores and channels in common corn starch increases the effective surface area, and therefore, its hydrolysis is consistently greater than that of potato starch regardless of the size. In contrast, the lack of pores and channels in potato starch reduces the effective surface area and restricts the activity of amylases.

Large blocklets (200-500 nm) stacked at the surface of potato starch have also been linked to its resistance to enzymatic digestion (Baldwin, Adler, Davies, and Melia, 1998; Gallant, Bouchet, and Buleon, 1992). Jane and Shen (1993) utilized chemical surface gelatinization via calcium chloride to study the distribution of amylose and amylopectin in potato starch and found amylose more concentrated at the periphery of the granules than towards the center. It was also observed that the molecular size of amylose was larger at the granule core than at the periphery, while a greater proportion of long B-chains of amylopectin was present at the center than at the periphery. These same observations were also found in common corn starch (Pan and Jane, 2000). More recently, Huang et al. (2014) applied chemical surface gelatinization via calcium chloride and observed that the remaining granules of waxy and normal potato starches differed in the distribution and the size of the blocklets. Based on scanning electron micrographs (SEM) and atomic force micrographs (AFM), both normal potato starch and waxy potato starch were comprised of large blocklets on the surface, but the blocklets in waxy potato starch were more homogeneously distributed and tightly packed.

In our previous study (Gonzalez and Wang, 2020), potato starch with a defined porous structure was produced by combining acid hydrolysis and amylase digestion. The severe acid hydrolysis conditions destabilized the crystallites to allow for increased amylase binding. Chemical surface gelatinization has been used to characterize the structure and the distribution of amylose and amylopectin on starch granule surfaces. However, there is no information regarding the susceptibility of surface-removed starches to digestion by amylases in order to form a porous structure. We hypothesized that the removal of the tightly packed granule surface through controlled chemical surface gelatinization may facilitate the binding and hydrolytic activity of amylases, and thus, result in the formation of porous potato starch. The objective of this study

was to investigate the effect of different levels of surface removal via chemical gelatinization to form porous common corn and potato starches after digestion by α-amylase or glucoamylase. The crystalline structure, morphology, and starch fine structure of the surface-removed granules were characterized to elucidate their impacts on enzyme digestibility.

4.3 MATERIALS AND METHODS

Materials

Common corn starch and potato starch were donated by Ingredion (Bridgewater, NJ). Alpha-amylase from *B. licheniformis* (specific activity 55 U/mg protein), glucoamylase from *A. niger* (specific activity 36 U/mg protein), and isoamylase from *Pseudomonas sp*. (specific activity 180 U/mg protein) were purchased from Megazyme Ltd. (Wicklow, Ireland) and used without further dilution. All chemicals and reagents were of analytical grade.

Gelatinization and removal of gelatinized starch surface

The native starches were surface gelatinized according to the method described by Kuakpetoon and Wang (2007) with the following modifications. Common corn starch (20 g, db) was suspended in 150 mL of 13 M LiCl and was constantly stirred, at room temperature, for different time periods to obtain approximately 9 or 16% of surface gelatinization. The reaction was stopped by the addition of 1200 mL of 4°C deionized (DI) water with vigorous mixing. The slurry was centrifuged at 3840 ×g for 15 min; the supernatant was discarded, and the remaining precipitate, containing the surface gelatinized starch, was washed twice with 1200 mL of 4°C DI water.

To remove the gelatinized starch fraction, the surface gelatinized starch was transferred to a 250-mL stainless steel blender (Waring, 51 BL31, Torrington, CT, USA) and added with 120 mL of 4°C DI water. The mixture was mechanically blended at 22,000 rpm for 3 min and then centrifuged at 3840 ×g for 15 min. The supernatant, containing the gelatinized fraction, was discarded, and blending and centrifugation were repeated four more times for the remaining fraction. The recovered precipitate was washed twice with 200 mL of ethanol, dried at 40°C for 18 h, ground using a mortar and pestle, and sieved through a 250-μm screen. The degree of surface gelatinization was expressed as the percentage of gelatinized starch removed according to the equation below, which was also used to express the surface removal level. This same procedure was applied to potato starch. Two levels (~9.0 and 16%) of surface-removed common corn and potato starches were prepared and subjected to digestion by α-amylase and glucoamylase.

$$\% \text{ Surface gelatinization} = \frac{[\text{Initial starch weight (db)} - \text{Remaining granules weight (db)}]}{\text{Initial starch weight (db)}} \times 100$$

Enzymatic digestion

Starches were digested by α-amylase and glucoamylase following the method of Gonzalez and Wang (2020). The digestion degree was measured by the phenol-sulfuric method (Dubois, Gilles, Hamilton, Rebers, and Smith, 1956) and expressed as percentage of hydrolyzed starch as shown in the equation below.

$$\text{Digestion degree (\%)} = \frac{\text{Total soluble carbohydrate (g)} \times 0.9}{\text{Starch weight (db)}} \times 100$$

Total soluble carbohydrate (mg/mL) is determined from a glucose standard curve and 0.9 is used to convert glucose to starch.

Starch characterization

The particle size (volume diameter, D50) was measured by a laser scattering particle size analyzer (LA-910, Horiba Ltd., Kyoto, Japan) at room temperature following the method of Qiu, Yang, and shi (2015). The morphology of native, surface-removed, and surface-removed enzyme-treated starches were elucidated with scanning electron microscopy (SEM) and confocal laser scanning microscopy (CLSM). Starches were sprinkled onto a stub with double-backed tape prior to coating with gold, and scanning electron micrographs were taken with an FEI Nova Nanolab 200 Dual-Beam (Hillsboro, OR) with an accelerating voltage of 30 kV.

The preparation of the starches for CLSM followed the method of Blennow et al. (2003) with modifications. A starch sample of 10 mg was suspended in a freshly prepared mixture of 15 μL of 20 mM 8-amino-1,3,6-pyrenetrisulfonic acid (APTS, dissolved in 15% acetic acid) and 15 μL of 1 M sodium cyanoborohydride. The mixture was incubated at 30°C for 18 h, washed 5 times with 1 mL of water, centrifuged at 9300 ×g for 3 min, and suspended in 50 μL of 50% glycerol. The APTS-stained samples were fixed on a glass slide using a mixture of 2% agar and 85% glycerol in water, and observed with CLSM (CS SP5 Leica Microsystems, Mannheim, Germany) equipped with an argon laser. The emission was set from 500 to 535 nm, and the excitation wavelength was set at 488 nm with 20% capacity.

The gelatinization properties were measured using a differential scanning calorimeter (DSC, model Diamond, Perkin-Elmer, Norwalk, CT), and the crystalline structure was

characterized by a wide-angle powder X-ray diffraction pattern according to the methods of Gonzalez and Wang (2020).

The molecular-size distribution of native and debranched surface-removed starches was characterized by high-performance size exclusion chromatography (HPSEC) according to Arijaje, Wang, Shin, Shah, and Proctor (2014). Starch (20 mg) was dissolved in 5 mL of 90% dimethyl sulfoxide (DMSO), boiled for 1 h, constantly stirred overnight at room temperature, and centrifuged at 9,300 ×g for 10 min. Debranched samples were prepared by dissolving 10 mg of starch in 3.2 mL of Millipore water, boiled for 30 min, and added with 0.4 mL of 0.1 M acetate buffer with a pH of 3.5. Ten µL of isoamylase were added, and the samples incubated at 45°C for 2 h with constant stirring. After neutralizing with 0.21 mL of 0.2 M NaOH, the samples were boiled for 15 min, cooled down to room temperature, mixed with 1.5 g of mixed bed exchange resin (IONAC® NM-60 H^+/OH^- form, type 1, beads 16-50 mesh) for exactly 1.0 min, and filtered through a 0.45-µm PTFE membrane filter.

Statistical analysis

All experiments were replicated, and each analysis was conducted in duplicate. The data were analyzed using JMP Pro14 Software (SAS Institute Inc., Cary, NC), and the means were compared using Tukey's honest significant difference (HSD) test.

4.4 RESULTS AND DISCUSSION

4.4.1 Surface gelatinization

The surface gelatinization (SG) profiles of common corn and potato starch by 13 M LiCl over 35 min are presented in Figure 4.1. The initial rate of SG was similar for both common corn

and potato starches, reaching ~9% in 5 min and ~10% in 15 min at room temperature. They differed in the degree of SG after 15 min, with common corn starch and potato starch reaching ~16% SG in 20 min and 35 min, respectively. Koch and Jane (2000) reported that the degree of SG followed the order of rice > common corn > wheat > barley > potato, and they attributed the lower SG of potato starch partly to its larger granule size. In the present study, starch granules were not separated by size before SG, and thus, the similar SG degree during the first 15 min was attributed to a similar susceptibility of small potato starch granules and common corn starch granules to SG.

4.4.2 Characterization of surface-removed starches

Particle size distribution

The particle size distribution profiles and the mean diameter of native and surface-removed common corn and potato starches are presented in Figure 4.2. The mean diameter of native common corn starch (16.7 μm) was smaller than that of potato starch (44.1 μm), whereas native potato starch showed a broader distribution, which was consistent with other reports (Dhital, Shrestha, and Gidley, 2010; Singh and Kaur, 2004). The mean diameter of common corn starch did not change considerably with 9% surface removal but increased significantly after 16% surface removal. In potato starch, the mean diameter increased (45.7 ± 0.0) at 9% surface removal, but then decreased (44.6 ± 0.3) after 16% surface removal. The observed increase in the mean diameter of potato starch at 9% surface removal suggests that smaller granules were more susceptible to surface gelatinization compared with larger granules, and a decrease in the small granules resulted in an increase in the fraction of granules with a greater diameter. Therefore, a

similar time for common corn and potato starches to reach 9% SG indicated the importance of granule size in determining surface gelatinization rate.

Gelatinization properties

The effect of surface removal on the onset (T_o), peak (T_p), end (T_e) temperatures, and the gelatinization range (T_e-T_o) varied with starch type and surface removal level (Table 4.1). The T_o, T_p, and T_e of both common corn and potato starches decreased after surface removal. For common corn starch, there were no significant differences in T_o and T_p between the two levels of surface removal, which is consistent with the findings of Kuakpetoon and Wang (2007). In contrast, potato starch showed higher T_o, T_p, and T_e at 16% surface removal than at 9%. Studies have shown that T_o is greatly influenced by the amylopectin chain length distribution and the glass transition temperature of the amorphous regions of the granule (Jane, Xu, Radosavuevic, and Seib, 1992; Shi and Seib, 1992). The observed lower T_o of 9% surface-removed potato starch with respect to 16% surface-removed potato starch suggests that the outermost 10% layer of potato starch was composed of a greater proportion of the crystalline structure that exerted a greater influence on the overall gelatinization properties (Huang et al., 2014; Sevenou, Hill, Farhat, and Mitchell, 2002). The removal of the outermost part of the granule resulted in a decrease in the glass transition temperature because the disruption of the densely organized chains increased the mobility of the remaining glucan chains. Jane and Shen (1993) showed that the interior of potato starch granules tended to be composed of longer B-chains of amylopectin and amylose of a greater molecular weight. Therefore, the increased T_o of the 16% surface-removed potato starch could be attributed to the remaining larger molecular weight amylose associated with the increased long B chains of amylopectin.

There was an increase in the gelatinization range for both starches after 16% surface removal, indicating the removal of some crystallites present at the outermost surface of both starch granules and the formation of more heterogenous crystalline structure. The gelatinization enthalpy was significantly decreased for both levels of surface removal in both starches, but potato starch differed in that there was no significant difference between the 9 and 16% levels of surface removal, while there was a significant decrease between the 9 and 16% surface-removed common corn starches (Table 4.1). After surface removal, the gelatinization enthalpy of common corn starch continuously decreased to a greater extent than that of potato starch, which implies a more stable double helical organization in potato starch, and may also explain the observed longer time for potato starch to achieve a similar degree of surface removal.

X-ray diffraction pattern

The X-ray diffraction pattern did not change regardless of the surface removal level, but the relative crystallinity decreased after surface removal, agreeing with the changes in their gelatinization properties (Table 4.1). The greater decrease in crystallinity of potato starch after 9% surface removal suggests that the periphery of potato starch granules is composed of a significantly greater proportion of crystallites compared with that of corn starch granules. The main peaks of corn starch increased in intensity with increasing SG, while those of potato starch decreased slightly (Supplemental Figure 4.1). The blocklets in the outer surface of potato starch were proposed to be smaller than those towards the interior of the granule, as well as to differ respect to their crystallites distribution (Huang, Wei, Li, Liu, and Yang, 2014). The decrease and then increase of crystallinity from 9% to 16% surface removal of potato starch supports the

proposed difference in the distribution and organization of crystalline blocklets within potato starch, and is similar to the changes observed for T_o.

The trend in the change of relative crystallinity differs from that of gelatinization enthalpy for both starches. According to Gao, Li, Bi, Mao, and Adhikari (2013), the gelatinization enthalpy reflects the loss of double helical order. In this study, the outermost 10% layer in potato starch is proposed to contain more crystallites, but those crystallites may not be entirely organized into double helices, which could account for the minor difference in the gelatinization enthalpy between the two levels of surface-removed potato starches. Our previous study (Gonzalez and Wang, 2020) also found no positive correlation between relative crystallinity and gelatinization enthalpy of acid hydrolyzed starches. Therefore, it is suggested that the relative crystallinity changes in the surface-removed starches reflect changes in the proportion of amorphous background towards the interior of the granule.

Molecular-size distribution

The molecular-size distribution of native starches was classified into three fractions: amylopectin, intermediate materials, and amylose with peak degrees of polymerization (DP) in glucose units of 49,573, 15,022, and 2,558, respectively for common corn starch, and 36,573, 15,022, and 3,431, respectively, for potato starch (Figure 4.3). Changes in the molecular-size distribution of the different fractions varied with starch type and surface removal level (Table 4.2). The proportion of the amylopectin fraction in common corn starch increased after surface removal, and the intermediate material and amylose fractions decreased, which agrees with Pan and Jane (2000). In contrast, the opposite trend was observed for surface-removed potato starch. The trend of a decreasing amylopectin fraction with increasing surface removal, as observed in

potato starch, supports the results of gelatinization enthalpy and crystallinity because amylopectin is responsible for the crystalline structure. Both surface-removed common corn and potato starches displayed a decrease in peak DP of the amylopectin and intermediate material fractions, while the peak DP of the amylose fraction increased slightly, which can be attributed to the removal of the larger DP amylopectin and intermediate material that eluted with amylose. The debranched starch profile was also classified into three fractions, including amylose, and long and short amylopectin chains. After debranching, corn starch displayed a similar or decreased proportion of long and short amylopectin chains, and an increased amylose fraction with increasing surface removal (Table 4.2). The debranched profile of surface-removed potato starches showed a similar or a slight increase in the fractions of long and short amylopectin chains, while the amylose fraction remained unchanged or decreased. The opposite trend in the debranched profiles between the two starches corroborates their differences in amylose and amylopectin fine structure. For corn starch, the peak DP of long and short amylopectin chains significantly decreased after surface removal, agreeing with the significant reduction in the gelatinization enthalpy between surface-removed corn starches. The peak DP of short and long amylopectin chains for surface-removed potato starch was slightly reduced, but there was no significant difference between the two levels of surface removal, agreeing with the greater stability of potato starch crystalline structure.

4.4.3 Enzyme digestion of native and surface-removed starches

The degree of digestion (%) generally increased or remained the same after surface removal treatment and varied with type of starch and enzyme (Table 4.3). Compared with their native counterparts (0%), the digestion degree by α-amylase for 9% and 16% surface-removed

corn starch increased by 4.3 and 7.5 percentage points, respectively, and by 4.0 and 20.6 percentage points for 9% and 16% surface-removed potato starches, respectively, after 24 h of α-amylase digestion.

The digestion of granular starch at subgelatinization temperatures begins with the diffusion of the enzyme on the granule surface, followed by adsorption, and final hydrolysis of starch chains. This reaction is not uniform but is greatly affected by the multi-scale starch structure and the enzyme type (Colonna, Leloup, and Buleon, 1992; Robyt and French, 1967; Yook and Robyt, 2002). The increased α-amylolysis of surface-removed starches suggests that the granule surface structure hinders the initial binding and diffusion of hydrolyzing enzymes, particularly for potato starch. This finding supports the results of the relative crystallinity from the X-ray diffraction pattern (Table 4.1), establishing that the outermost 10% layer in potato starch was highly organized. Jane, Wong, and McPherson (1997) suggested that a clustered distribution of the branching points provided potato starch with a dense amorphous lamella, which hinders its susceptibility to α-amylase since α-amylase is an endo-hydrolyzing enzyme with a binding size that requires at least eight D-glucosyl units (Oates, 1997). Therefore, it is suggested that a greater proportion of clustered branch points is present at the outermost layer, and once removed, the binding of α-amylase increases because chains with the appropriate length are exposed.

The glucoamylolysis of both levels of surface-removed common corn starch decreased by ~2.5 percentage points compared with that of the native counterpart after 24 h. In contrast, the glucoamylolysis of 9% and 16% surface-removed potato starches increased by 7.5 and 11.0 percentage points, respectively, after 24 h. The catalytic activity of glucoamylase is dependent on the availability of chains with non-reducing ends and a length of at least seven D-glucosyl units,

which corresponds to its binding size (Swanson, Emery, and Lim, 1977). Surface removal affected the fine structure of both starches as evidenced by the molecular-size distribution profiles; the greatly increased digestion of surface-removed potato starches suggests that the binding of glucoamylase with potato starch increased due to the disorganization of amylopectin branches and intertwined amylose, which exposed more chains with non-reducing ends that were not available initially. The observed slight decrease in the glucoamylolysis of surface-removed corn starches could be associated with the physical hindrance of the amylose and amylopectin glucan chains that became shorter, as evidenced by the significant peak DP decrease in Figure 4.3C- E, with respect to the size of the binding site (Kerr, Cleveland, and Katzbeck, 1951).

4.4.4 Morphology of enzyme-digested starches

The activity of α-amylase or glucoamylase in common corn and potato starches was evident as revealed by the erosion of the granule surface, even after 1 h of digestion, and all starches displayed extensive breakage after 24 h of digestion. Therefore, the micrographs of native and surface-removed common corn and potato starches after digestion by both amylases for 10 h are presented in Figure 4.4. Native common corn starch, when digested by α-amylase (Figure 4.4A) or glucoamylase (Figure 4.4G), for 10 h, displayed the typical homogeneously distributed enlarged pores. In contrast, α-amylolysis (Figure 4.4D) or glucoamylolysis (Figure 4.4J) of native potato starch granules resulted in some granules with a single enlarged opening toward one end of the granule and others with no apparent change on the surface, after 10 h of digestion (Figure 4.4D). These results agree with the morphology of enzyme digested native starches observed in previous studies (Gonzalez and Wang, 2020; Kimura and Robyt, 1995; Li et al., 2020).

The α-amylolysis of surface-removed common corn starches also resulted in granules with enlarged and uniformly distributed pores after 10 h of digestion (Figure 4.4B-C). The surface-removed potato starches displayed a porous structure after digestion by α-amylase for just 1 h (Figure 4.4E-F). The porous structure became more evident after the surface removal and with increasing digestion time but was not present in all potato starch granules. Compared with common corn starch, the pores in the surface-removed potato starches were smaller and not homogeneously distributed. The results confirm that the removal of the dense structures at the outermost 10% layer increased the binding α-amylase because the degree of α-amylase digestion of both starches increased after surface removal. The difference in the porous structure between the two starches is attributed to the lack of inherently present features in potato starch, such a pores and channels, which increase the accessible binding sites for α-amylase.

The gluocoamylolysis of surface-removed common corn starches produced a similar morphology to that of the α-amylase digested ones with uniformly distributed enlarged pores (Figure 4.4H-I). The glucoamylolysis of the 9% and 16% surface-removed potato starch also produced a porous structure, but the pores appeared to be larger, and some displayed a more localized distribution (Figure 4.4K-L) compared with their α-amylase-digested counterparts (Figure 4.4E-F). Lineback (1986) and more recently Baldwin et al. (20145) proposed that some immature amylose and amylopectin chains that radiate toward the edges of the granules are less tightly organized and present weak points susceptible to enzyme attack. It is proposed that the removal of the densely packed granule surface of potato starch exposed a greater proportion of these chains in the less organized parts of the granules for glucoamylase to act on.

Our previous study showed that acid-hydrolyzed potato starches also displayed a porous structure after α-amylase or glucoamylase digestion (Gonzalez and Wang, 2020). However, the

pores in the surface-removed potato starches were fewer and larger compared with more and smaller pores in the acid-hydrolyzed potato starches. Both acid hydrolysis and surface removal increased the digestion degree by both amylases and resulted in a porous structure in potato starch. Therefore, the contrasting pore distribution and size observed between Gonzalez and Wang (2020) and the present study supports the negative impact of dense surface structure on amylases. The chemical gelatinization removed the densely packed surface structure to expose weak points but did not create new binding sites. In contrast, the severe acid hydrolysis conditions disrupted the amorphous regions and created additional binding sites for glucoamylase.

The confocal-laser scanning micrographs (CLSM) confirmed the presence and widening of channels and pores in native and surface-removed common corn starches after 10 h of digestion for both amylases (Figure 4.5A-C, G-I). The CLSM of the digested native potato starches confirmed the preferential activity of both amylases toward one end of the granule, which is suggested to be the hilum (Baldwin et al., 2015) and the consequential formation of a hollow cavity (Figure 4.5D and J). The CLSM of 9% and 16% surface-removed potato starches after 10 h of α-amylase or glucoamylase digestion revealed that the observed porous structure did not result in deepened cavities compared with common corn starch. The increased fluorescence around the potato starch granule surface provides evidence for the increased binding of amylases after surface removal. These results support the hypothesis that surface structure hinders amylase digestion and the formation of a porous structure in potato starches.

4.5 CONCLUSIONS

Smaller potato starch granules were preferentially gelatinized than larger granules during chemical gelatinization. The overall digestion degree varied with starch and enzyme type, and surface removal level. The outermost 10% granule surface of potato starch was composed of a greater proportion of crystallites and clustered branching points compared with that of common corn starch. The destabilization of clustered branching points from chemical gelatinization enhanced the digestion of potato starch by both α-amylase and glucoamylase. The combination of surface removal and digestion by α-amylase and glucoamylase produced a porous structure in potato starch. The increased surface removal level promoted the formation of a more defined porous structure in potato starch, but the formation of pores and their distribution varied with the type of amylase. The results suggest that the removal of some crystallites and dense clustered branching points at the outermost 10% layer of potato starch granule exposed glucan chains that increased the initial binding of both amylases, and consequentially amylase digestion. The porous structure formed in the surface-removed potato starches after digestion by α-amylase and glucoamylase was not uniform and did not display enlarged channels compared with common starch because some remaining dense structures restricted the diffusion of both amylases towards the interior of the granule. The findings of this study confirmed that surface structure hinders and controls the digestion pattern of potato starch granules by amylases.

4.6 REFERENCES

Arijaje, E., Wang, Y.-J., Shin, S., Shah, U., & Proctor, A. (2014). Effects of chemical and enzymatic modifications on starch-stearic acid complex formation. *Journal of Agricultural and Food Chemistry, 62*, 2963–2972.

Baldwin, A. J., Egan, D. L., Warren, F. J., Barker, P. D., Dobson, C. M., Butterworth, P. J., & Ellis, P. R. (2015). Investigating the mechanisms of amylolysis of starch granules by solution-state NMR. *Biomacromolecules, 16*, 1614–1621.

Baldwin, P. M., Adler, J., Davies, M. C., & Melia, C. D. (1998). High resolution imaging of starch granule surfaces by atomic force microscopy. *Journal of Cereal Science, 27*, 255–265

Blennow, A., Hansen, M., Schulz, A., Jorgensen, K., Donald, A. M., & Sanderson, J. (2003). The molecular deposition of transgenically modified starch in the starch granule as imaged by functional microscopy. *Journal of Structural Biology, 143*, 229–241.

Colonna, P., Leloup, V., & Buleon, A. (1992). Limiting factors of starch hydrolysis. *European Journal of Clinical Nutrition. 46*, S17–S32.

Dhital, S., Shrestha, A. K., & Gidley, M. J. (2010). Relationship between granule size and in vitro digestibility of maize and potato starches. *Carbohydrate Polymers, 82*, 480–488.

Dubois, M., Gilles, K., Hamilton, J., Rebers, P., & Smith, F. (1956). Colorimetric method for determination of sugars and related substances. *Analytical Chemistry, 28*, 350–356.

Gallant, D., Bouchet, B., Buleon, A., & Perez, S. (1992). Physical characteristics of starch granules and susceptibility to enzymatic degradation. *European Journal of Clinical Nutrition, 46*, 3–16.

Gao, F., Li, D., Bi, C., Mao, Z., & Adhikari, B. (2013). Application of various drying methods to produce enzymatically hydrolyzed porous starch granules. *Drying Technology, 31*, 1627–1634.

Gonzalez, A., & Wang, Y.-J. (2020). Enhancing the formation of porous potato starch by combining α-amylase or glucoamylase digestion with acid hydrolysis. *Starch - Stärke,72*, 1900269.

Han, Z., Han, Y., Wang, J., Liu, Z., Buckow, R., & Cheng, J. (2020). Effects of pulsed electric field treatment on the preparation and physicochemical properties of porous corn starch derived from enzymolysis. *Journal of Food Processing and Preservation, 44*, e14353.

Huang, J., Chen, Z., Xu, Y., Li, H., Liu, S., Yang, D., & Schols, H. A. (2014). Comparison of waxy and normal potato starch remaining granules after chemical surface gelatinization: pasting behavior and surface morphology. *Carbohydrate Polymers, 102*, 1001–1007.

Huang, J., Wei, N., Li, H., Liu, S., & Yang, D. (2014). Outer shell, inner blocklets, and granule architecture of potato starch. *Carbohydrate Polymers, 103*, 355–358.

Jane, J., Xu, A., Radosavuevic, M., & Seib, P. A. (1992). Location of amylose in normal starch granules. I. Susceptibility of amylose and amylopectin to cross-linking reagents. *Cereal Chemistry, 69*, 405–409.

Jane, J., & Shen, J. J. (1993). Internal structure of the potato starch granule revealed by chemical gelatinization. *Carbohydrate Research, 247*, 279–290.

Jane, J.-L., Wong, K.-S., & McPherson, A. (1997). Branch-structure difference in starches of A- and B-type X-ray patterns revealed by their naegeli dextrins. *Carbohydrate Research, 300*, 219–227.

Kerr, R. W., Cleveland, F. C., & Katzbeck, W. J. (1951). The action of amylo-glucosidase on amylose and amylopectin. *Journal of the American Chemical Society, 73*, 3916–392.

Kimura, A., & Robyt, J. F. (1995). Reaction of enzymes with starch granules: kinetics and products of the reaction with glucoamylase. *Carbohydrate Research, 277*, 87–107.

Koch, K., & Jane, J. (2000). Morphological changes of granules of different starches by surface gelatinization with calcium chloride. *Cereal Chemistry, 77*, 115–120.

Kuakpetoon, D., & Wang, Y.-J. (2007). Internal structure and physicochemical properties of corn starches as revealed by chemical surface gelatinization. *Carbohydrate Research, 342*, 2253–2263.

Li, C., Gong, B., Hu, Y., Liu, X., Guan, X., & Zhang, B. (2020). Combined crystalline, lamellar and granular structural insights into in vitro digestion rate of native starches. *Food Hydrocolloids, 105*, 105823.

Lineback. D.R. (1986). Current concepts of starch structure and its impact on properties. *Journal of the Japanese Society of Starch Science, 33*, 80–88.

Luo, Z., Cheng, W., Chen, H., Fu, X., Peng, X., Luo, F., & Nie, L. (2013). Preparation and properties of enzyme-modified cassava starch–zinc complexes. *Journal of Agricultural and Food Chemistry, 61*, 4631–4638.

Oates, C. G. (1997). Towards an understanding of starch granule structure and hydrolysis. *Trends in Food Science & Technology, 8*, 375–382.

O'Brien, S., & Wang, Y.-J. (2008). Susceptibility of annealed starches to hydrolysis by α-amylase and glucoamylase. *Carbohydrate Polymers, 72*, 597–607.

Pan, D., & Jane, J. (2000). Internal structure of normal maize starch granules revealed by chemical surface gelatinization. *Biomacromolecules, 1*, 126–132.

Quigley, T. A., Kelly, C. T., Doyle, E. M., & Fogarty, W. M. (1998). Patterns of raw starch digestion by the glucoamylase of *Cladosporium gossypiicola* ATCC 38026. *Process Biochemistry*, 33, 677–681.

Qiu, D., Yang, L. and Shi, Y.‐C. (2015). Formation of vitamin E emulsion stabilized by octenylsuccinic starch: factors affecting particle size and oil load. *Journal of Food Science*, 80, C680–C686.

Robyt, J. F., & French, D. Multiple attack hypothesis of α-amylase action: action of porcine pancreatic, human salivary, and *Aspergillus Oryzae* α-amylase. (1967). *Archives of Biochemistry and Biophysics, 122*, 8–16.

Sevenou, O., Hill, S. E., Farhat, I. A., & Mitchell, J. R. (2002). Organisation of the external region of the starch granule as determined by infrared spectroscopy. *International Journal of Biological Macromolecules, 31*, 79–85.

Shi, Y., & Seib, P. A. (1992). The structure of four waxy starches related to gelatinization and retrogradation. *Carbohydrate Research, 227*, 131–145.

Singh, N., & Kaur, L. (2004). Morphological, thermal, rheological and retrogradation properties of potato starch fractions varying in granule size. *Journal of the Science of Food and Agriculture, 84*, 1241–1252.

Swanson, S. J., Emery, A., & Lim, H. C. (1977). Kinetics of maltose hydrolysis by glucoamylase. *Biotechnology and Bioengineering, 19*, 1715–1718.

Yook, C., & Robyt, J. F. (2002). Reactions of alpha amylases with starch granules in aqueous suspension giving products in solution and in a minimum amount of water giving products inside the granule. *Carbohydrate Research, 337*, 1113–1117.

Table 4.1. Gelatinization properties and relative crystallinity of native (0%) and surface-removed (9% and 16%) common corn and potato starch.[a]

Starch	Surface removal (%)	Gelatinization Temperature (°C)				Enthalpy (J/g)	Relative crystallinity (%)
		Onset	Peak	End	Range[b]		
Common corn	0	68.5 ± 0.0a	73.0 ± 0.1a	78.2 ± 0.1a	9.7 ± 0.0e	16.7 ± 0.3c	41.1 ± 0.3b
	9	66.4 ± 0.1b	70.7 ± 0.1b	76.9 ± 0.0c	10.4 ± 0.1de	14.2 ± 0.3d	36.5 ± 0.1d
	16	66.5 ± 0.0b	71.4 ± 0.3b	77.5 ± 0.5b	11.0 ± 0.4cd	12.8 ± 0.3e	37.4 ± 0.2c
Potato	0	64.2 ± 0.1c	68.5 ± 0.1c	76.2 ± 0.2d	12.0 ± 0.3b	19.3 ± 0.1a	44.9 ± 0.3a
	9	60.1 ± 0.3e	64.7± 0.1d	71.7 ± 0.4f	11.6 ± 0.2bc	17.2 ± 0.7b	31.1 ± 0.4f
	16	62.1 ± 0.3d	67.1 ± 0.1c	75.6 ± 0.2e	13.4 ± 0.5a	17.4 ± 0.1bc	35.6 ± 0.3e

[a] Mean of two replicates ± standard deviation followed by a common letter in the same column are not significantly different (*$p < 0.05$)

[b] (End-Onset) temperature.

Table 4.2. Molecular-size fraction distribution (%) of native (0%) and surface gelatinized (9% and 16%) starches.[a]

Starch	Surface removal (%)	Fraction Distribution (%)[a]					
		Native			Debranched		
		Amylopectin	Intermediate material	Amylose	Amylose	Amylopectin	
						Long chains	Short chains
Common corn	0	45.5 ± 0.2f	16.5 ± 0.5d	38.0 ± 0.7a	16.5 ± 0.2b	21.4 ± 0.2b	62.0 ± 0.1a
	9	53.3 ± 0.2c	11.1 ± 0.3f	35.7 ± 0.1b	18.5 ± 1.0a	19.5 ± 0.9c	62.0 + 0.1a
	16	47.9 ± 0.1e	13.8 ± 0.3e	38.4 ± 0.2a	18.6 ± 0.4a	20.4 ± 0.1bc	61.0 ± 0.5b
Potato starch	0	58.4 ± 0.2a	21.9 ± 0.4c	19.7 ± 0.6d	14.7 ± 0.7c	37.7 ± 0.3a	47.6 ± 0.5d
	9	55.7 ± 0.2b	23.3 ± 0.3b	20.8 ± 0.2d	13.9 ± 0.2cd	37.0 ± 0.4a	49.1 ± 0.6c
	16	48.8 ± 0.1d	25.7 ± 0.1a	25.5 ± 0.2c	13.3 ± 0.1d	38.4 ± 0.4a	48.3 ± 0.3cd

[a] Means of two replicates ± standard deviation followed by a common letter in the same column are not significantly different (*$p < 0.05$).

Table 4.3. Degree of digestion (%) of native (0%) and surface gelatinized (9% and 16%) starches by α-amylase and glucoamylase.[a]

Starch	Duration (h)	α-Amylolysis			Glucoamylolysis		
		0%	9%	16%	0%	9%	16%
Common corn	1	11.9 ± 0.2b	12.7 ± 0.1a	12.3 ± 0.1ab	4.6 ± 0.1d	4.8 ± 0.0d	7.0 ± 0.1c
	5	16.8 ± 0.0d	23.2 ± 0.3b	24.2 ± 0.1a	18.4 ± 0.3c	18.6 ± 0.2c	18.3 ± 0.4c
	10	29.6 ± 0.7b	32.5 ± 1.0a	33.9 ± 0.4a	23.5 ± 0.7c	23.6 ± 0.1c	22.2 ± 0.0d
	24	38.2 ± 0.2d	42.5 ± 0.1b	45.7 ± 0.2a	40.4 ± 0.4c	38.1 ± 0.4d	37.9 ± 0.6d
Potato	1	6.9 ± 0.2c	7.6 ± 0.1b	8.1 ± 0.1a	3.1 ± 0.0f	4.4 ± 0.0e	6.1 ± 0.0d
	5	17.1 ± 0.2c	23.0 ± 0.1a	21.9 ± 0.2b	14.0 ± 0.1e	13.1 ± 0.0f	16.1 ± 0.1d
	10	23.5 ± 0.6d	33.9 ± 1.0b	41.0 ± 1.1a	22.5 ± 0.7d	23.3 ± 0.6d	26.7 ± 0.3c
	24	32.0 ± 0.0e	36.0 ± 0.7d	52.6 ± 0.4a	36.5 ± 0.5d	44.0 ± 0.0c	47.5 ± 0.1b

[a] Mean of two replicates ± standard deviation followed by a common letter in the same row are not significantly different (*$p < 0.05$)

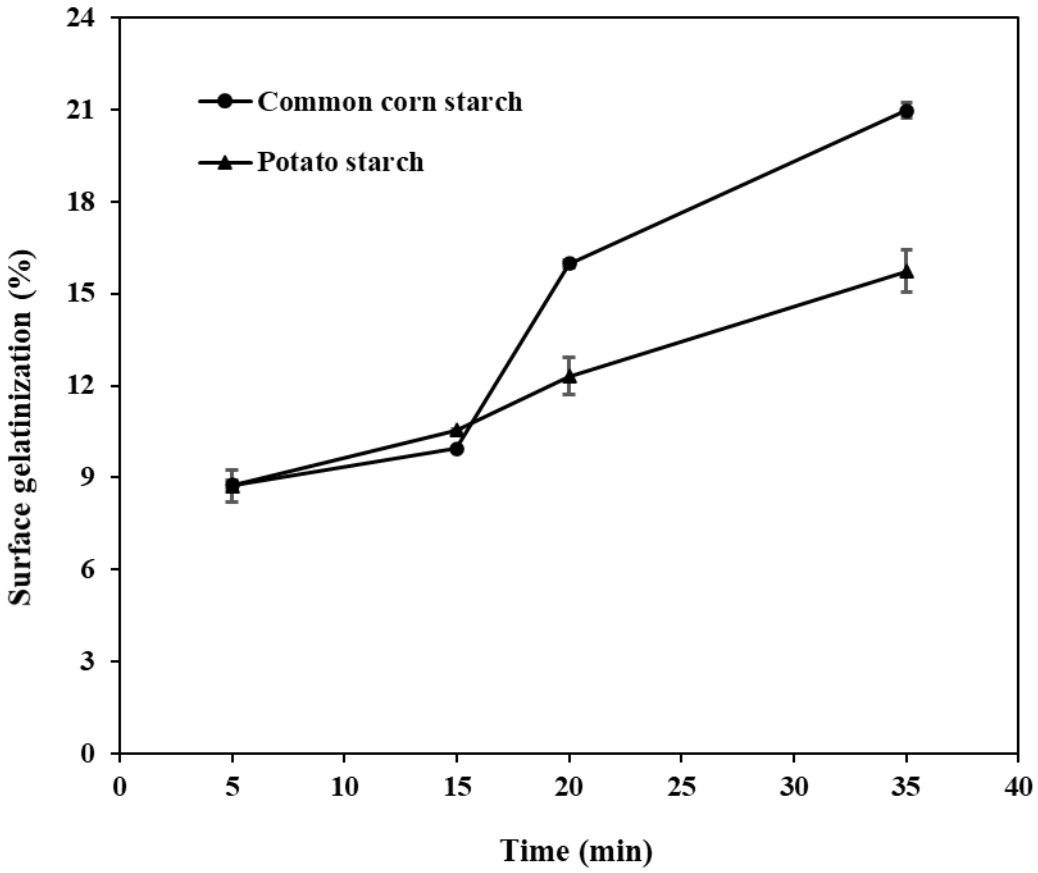

Figure 4.1. Surface gelatinization degree (%) of native potato and common corn starches by 13 M LiCl at room temperature over 35 min.

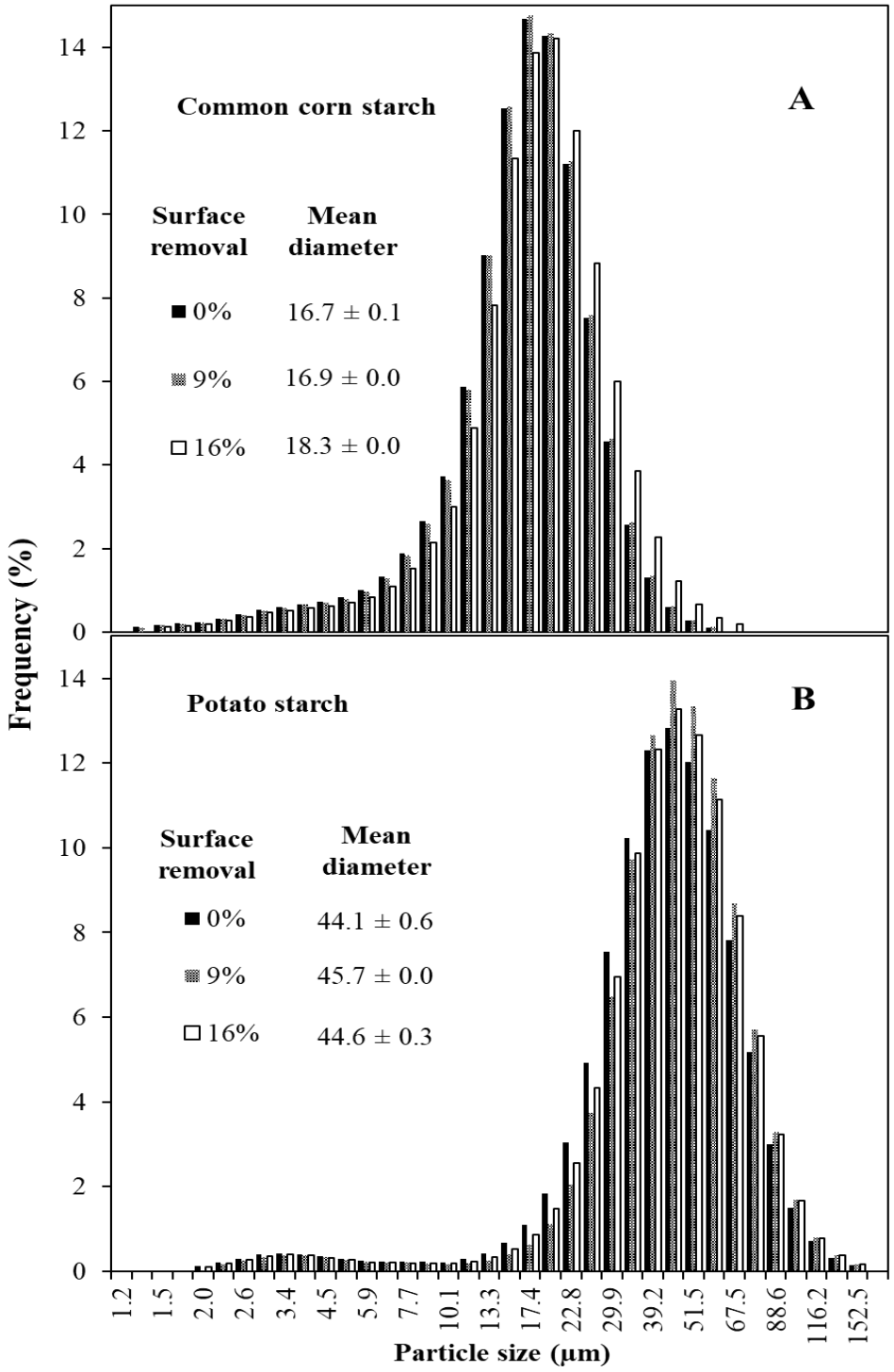

Figure 4.2. Particle size distribution and mean diameter values of common starch (A) and potato starch (B) after different degrees (0, 9, and 16%) of surface removal.

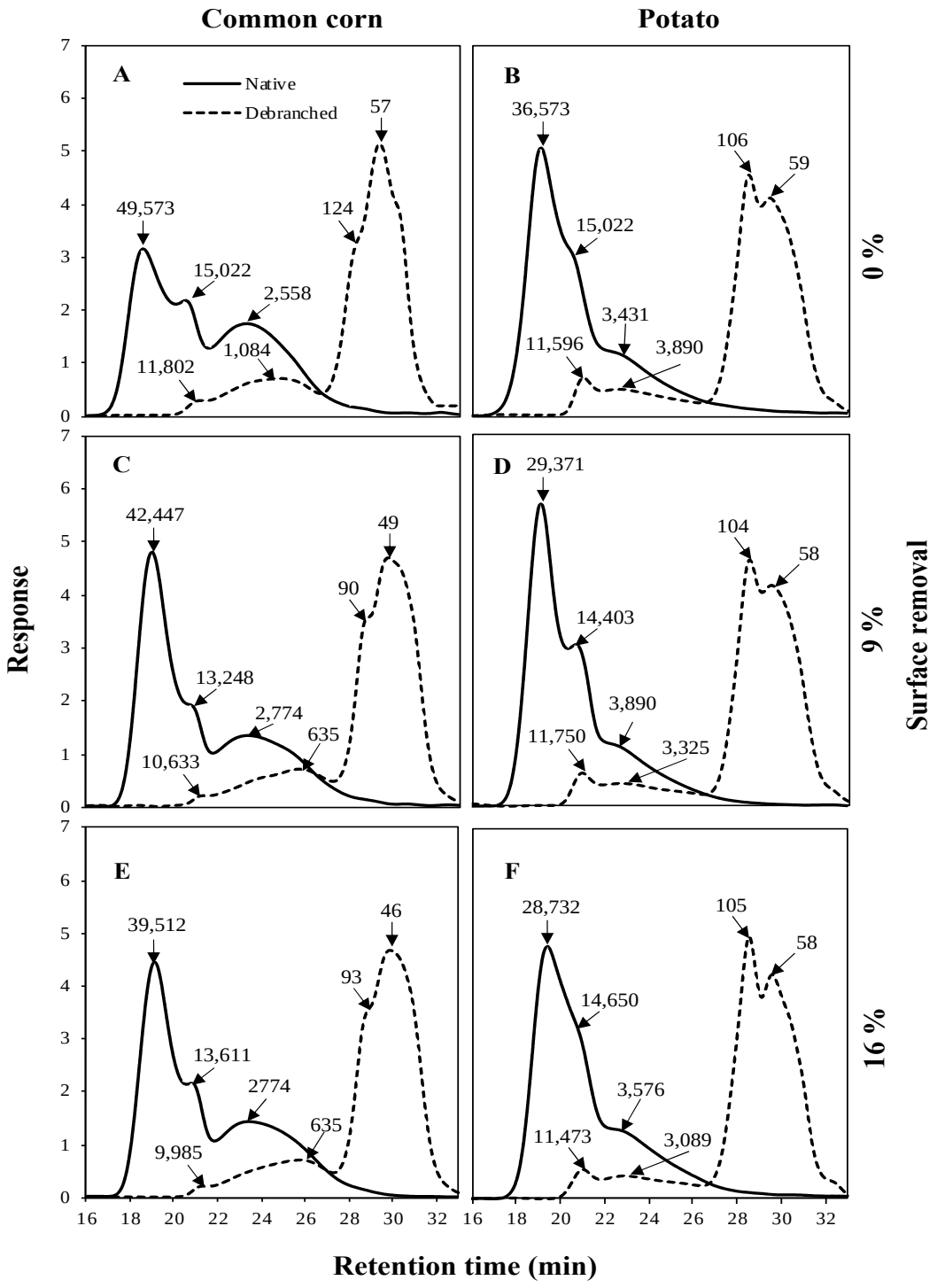

Figure 4.3. Normalized size-exclusion chromatograms of native and debranched common corn (A, C, E) and potato (B, D, F) starches after different degrees (0, 9, and 16%) of surface removal.

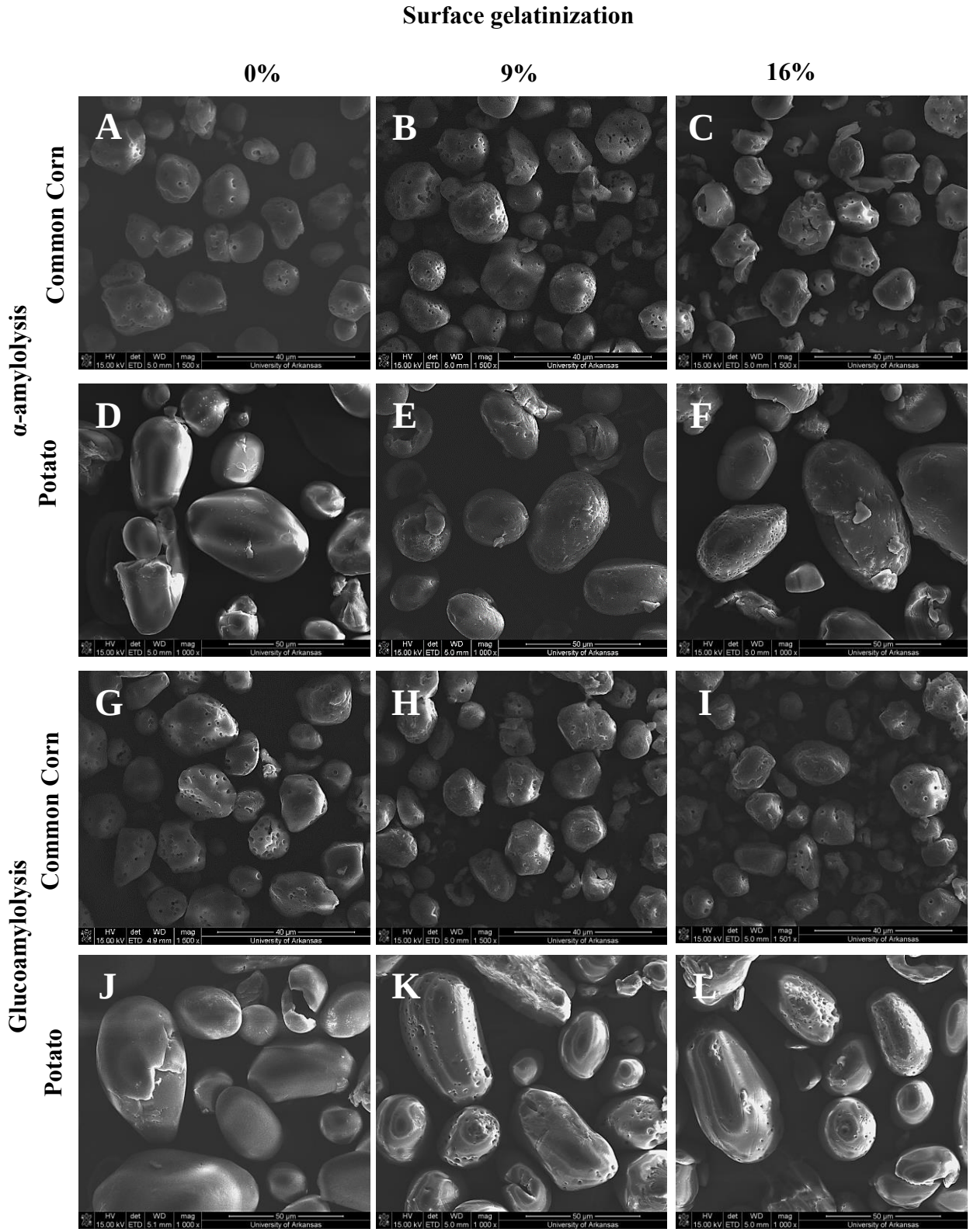

Figure 4.4. Scanning electron micrographs of native (0%) and surface removed (9% and 16%) common corn and potato starch after 10 h of α-amylase (A-F) and glucoamylase (G-L) digestion.

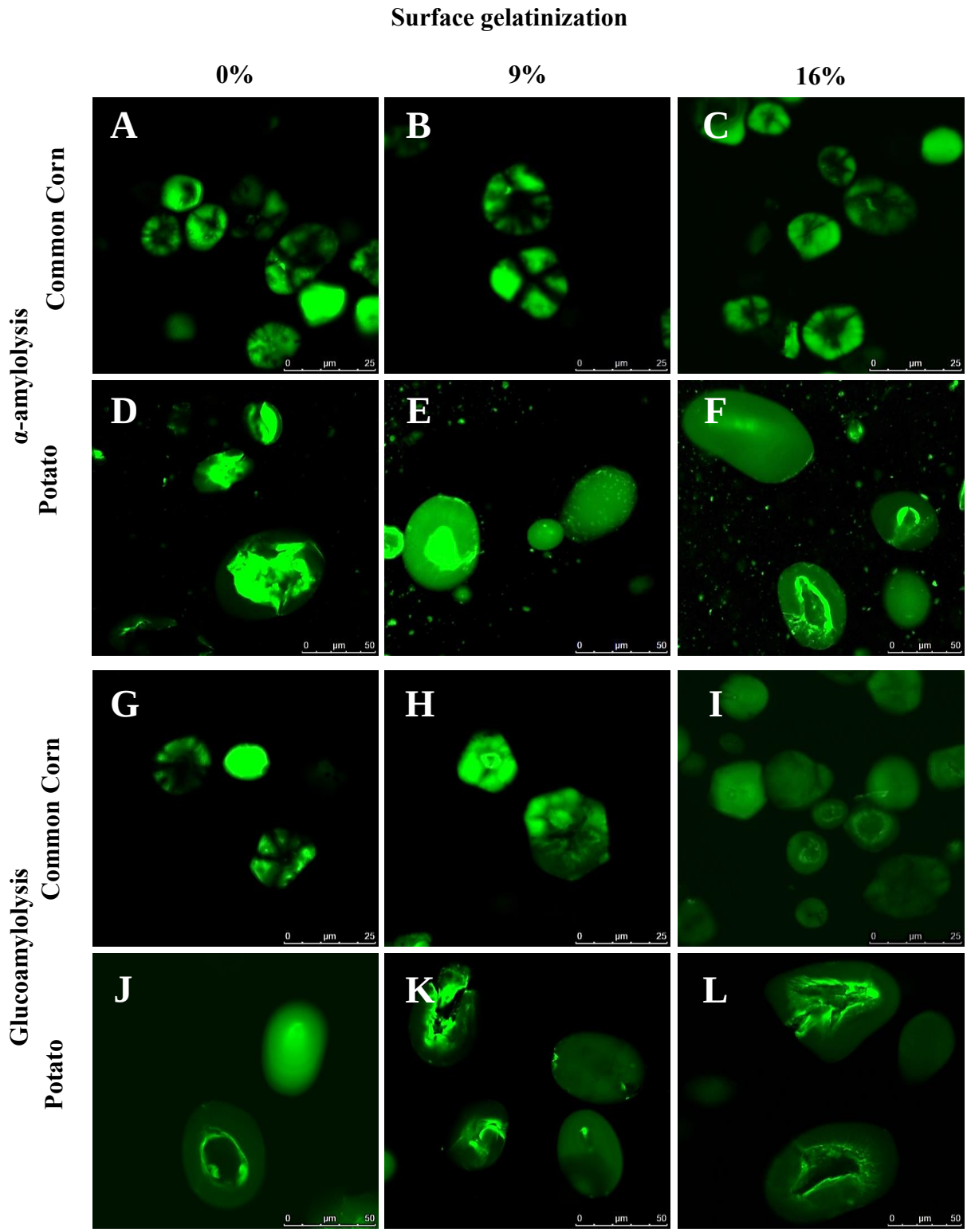

Figure 4.5. Confocal-laser **s**canning electron micrographs of native (0%) and surface removed (9% and 16%) common corn and potato starch after 10 h of α-amylase (A-F) and glucoamylase (G-L) digestion.

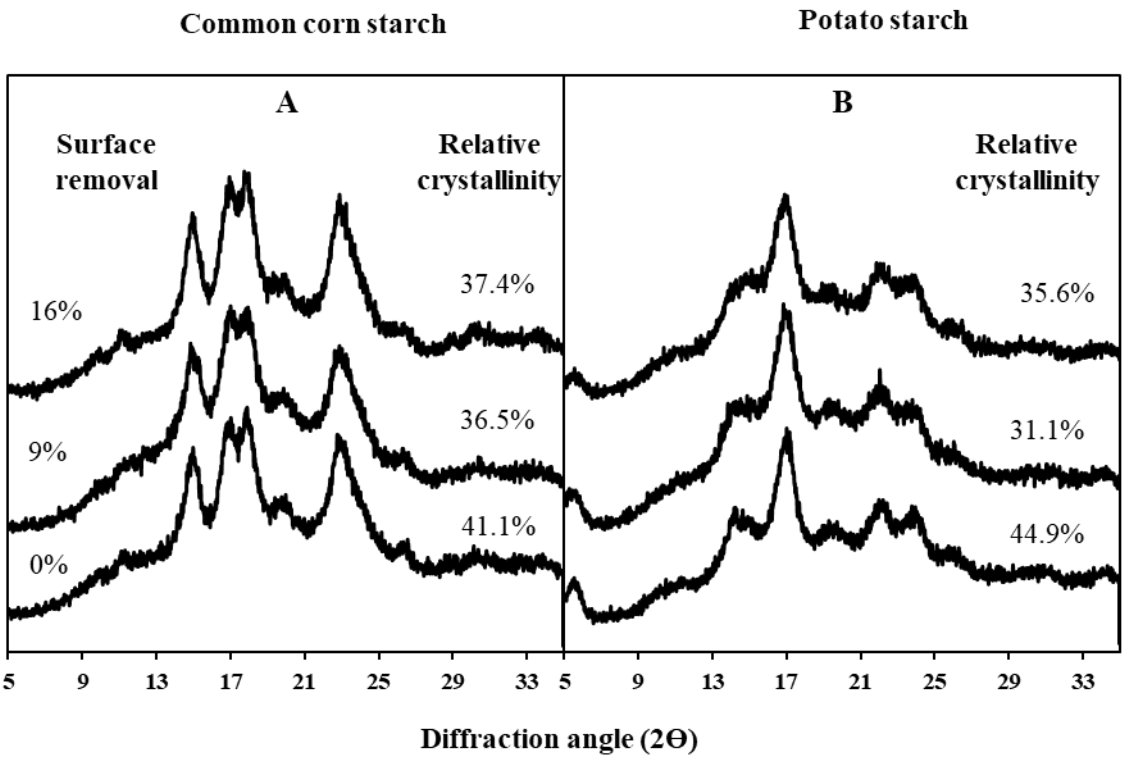

Supplemental Fig. 4.1. X-ray diffraction patterns and relative crystallinity values of common starch (A) and potato starch (B) after different degrees (0, 9, and 16%) of surface removal.

CHAPTER 5

EFFECTS OF ACID HYDROLYSIS LEVEL PRIOR TO HEAT-MOISTURE TREATMENT ON PROPERTIES OF STARCHES WITH DIFFERENT CRYSTALLINE POLYMORPHS

5.1 ABSTRACT

Highly crystalline starches find applications as delivery systems because of their improved thermal stability and reduced enzyme susceptibility. Both acid hydrolysis (AH) and heat-moisture treatment (HMT) have been used to alter starch gelatinization properties and digestibility. This study investigated the effects of varying AH levels (0-9%) prior to HMT on the structures and properties of starches with different crystalline polymorphs, including the A-type corn starch, the B-type potato starch, and the C-type pea starch. HMT resulted in significant increases in gelatinization temperatures and significant decreases in gelatinization enthalpy and α-amylase digestion for all three starches. When combined AH with HMT, all three starches generally displayed increases in gelatinization temperatures, gelatinization enthalpy and relative crystallinity with increasing AH level, but the susceptibility to α-amylase varied with starch type and AH level. Acid preferentially hydrolyzed the amorphous regions involving amylose and amylopectin branch points, and increased hydrolysis levels yielded greater amounts of linear chains that were capable of reorganizing into crystallites during HMT. The greater AH level, up to 9%, combined with HMT promoted the formation of more thermally stable crystallites for starches with different crystalline polymorphs.

Keywords: *acid hydrolysis, heat-moisture treatment, crystallinity, thermal stability, enzyme susceptibility.*

5.2 INTRODUCTION

The physicochemical properties of starch granules are determined by their molecular structure and complex hierarchical organization. Starch granules are organized in alternating amorphous and semi-crystalline growth rings. The semi-crystalline growth rings are comprised of repeating amorphous and crystalline lamellae, and the crystalline lamellae are formed by double helices of amylopectin chains organized into A-, B-, or C- polymorphic types. The A-type crystal, which is found in cereal starches, is characterized by monoclinic unit cells with 8 water molecules per unit cell and a greater proportion of short amylopectin chains. B-type crystals are found in tuber starches and consist of an open hexagonal unit cell containing 36 water molecules and a greater proportion of long amylopectin chains. The C-type crystal is a mixture of A- and B- types and is present in pulse starches (Zobel, 1988). Native starches are generally not suitable for industrial applications and therefore are conventionally chemically and/or physically modified to alter their physicochemical properties. Acid hydrolysis (AH) and heat-moisture treatment (HMT) are two of starch modification methods known to affect the amorphous and the crystalline lamellae, respectively (Chung, Hoover, & Liu, 2009; Wang, Blazek, Gilbert, & Copeland, 2012; Wang, Zhang, Chen, & Li, 2016).

In acid hydrolysis, the amorphous lamellae are preferentially hydrolyzed, whereas the crystalline lamellae are less accessible. The preferential hydrolysis of the amorphous lamellae by acid generates starches with increased crystallinity and decreased degrees of polymerization (DP) (Jayakody & Hoover, 2002; Wang, Blazek, Gilbert, & Copeland, 2012). Nevertheless, the extent and rate of hydrolysis varies with starch type (Hoover & Vasanthan, 1994). Jane, Wong, & McPherson (1997) subjected A- and B- type starches to AH using 15.3% H_2SO_4 at 22-25°C for 3 months and attributed the differences in the degree of hydrolysis of the two starch crystal

types to the distribution of the branching points. The branching points in the A-type starches are scattered in both the amorphous and crystalline lamellae, and those in the crystalline lamellae are protected during extended acid hydrolysis. In contrast, the branching points in the B-type starches are present in the amorphous lamellae and are more susceptible to acid hydrolysis. Other factors such as the amylose/amylopectin content, the granule size, the presence of pores on the surface, and the amount of amylose-lipid complexes have also been suggested to influence the extent and rate of hydrolysis (Jayakody & Hoover, 2002).

Heat-moisture treatment is a physical modification in which native starches at a low moisture content (< 35%) are subjected to a high temperature of 84–120°C for 15 min to 16 h (Gunaratne & Hoover, 2002). The three main changes that occur during HMT include disruption of the crystallites, increased interaction between starch chains, and disruption of the double-helical structures in the amorphous lamellae. Similar to AH, the effect of HMT varies with the starch crystal type. The B- and C-type starch crystals transition to the A-type, whereas no transition is observed for the A-type starches after HMT. The susceptibility of B-type crystals to HMT has been attributed to its less compact crystalline unit that facilitates the evaporation of the 36 water molecules followed by the lateral movement of amylopectin double helices into the space previously occupied by water (Chung, Hoover, & Liu, 2009; Jiranuntakul, Puttanlek, Rungsardthong, Puncha-arnon, & Uttapap, 2012; Klein et al., 2013; Wang, Blazek, Gilbert, & Copeland, 2012;). Nevertheless, the crystallinity of the treated starches will increase or decrease depending on the HMT conditions. Increased crystallinity is associated with high temperatures (>100°C) for long periods of time (>12 h) due to recrystallization of the amorphous lamellae into new crystallites (Shi, Gao, Liu, 2018; Vermeylen, Goderis, & Delcour, 2006). On the contrary, decreased crystallinity occurs under low temperatures (<100°C) for a shorter period of time (<12

h) due to the partial unwinding of the ends of the double helices (Sui et al., 2015; Wang, Zhang, Chen, & Li, 2016; Zhang et al., 2020).

When acid hydrolysis and HMT are combined, the resulting starches generally display increased gelatinization temperatures and thermally stable resistant starch fractions. These changes are ascribed to the decrease in the molecular size of starch chains from AH, which exhibit increased mobility and consequently realign into more thermally stable structures upon the addition of HMT (Brumovsky & Thompson, 2001; Kim & Huber, 2013; Lin, Singh, Wen, & Chang 2011; Shin, Byun, Park, & Moon, 2004; Xing, Liu, Li, & Wang, 2017a). However inconsistent results have been reported, and no study has compared the effects of combined AH and HM on changes in amylose and amylopectin of starches with different crystalline polymorphs. We hypothesized that the types of starch crystalline structure had impacts on the structure of acid hydrolysates, the quantity and quality of re-organized crystallites when combined AH with HMT, and consequently the properties of the resultant AH/HMT starches. Therefore, the objectives of this study were to compare the progressive changes in amylose and amylopectin structures of three starches with different crystalline polymorphs during AH prior to HMT to be correlated with their properties.

5.3 MATERIALS AND METHODS

Materials

Common corn and potato starches were obtained from Ingredion (Bridgewater, NJ). Pea starch N-753 was donated by Roquette (Portage la Prairie, Canada). Alpha-amylase from *B. licheniformis* (specific activity 55 U/mg protein) and glucoamylase from *A. niger* (specific

activity 36 U/mg protein) were purchased from Megazyme Ltd. (Wicklow, Ireland) and used without further dilution. All chemicals and reagents were of analytical grade.

Acid hydrolysis

Starches were hydrolyzed to different levels following the method of Ulbrich, Natan, & Flöter (2014) with modifications**.** Common corn starch (100 g, db) was dispersed in 250 mL of 0.36 M HCl; the mixture was incubated at 40°C with constant shaking (200 strokes/min), and samples were taken regularly over varying periods of time. The sample was vacuum filtered through a Whatman No. 2 filter paper, and the recovered starch residue was washed with 4-fold volumes of deionized water after adjusting the pH to 7 with 4 M NaOH, and then dried at 40°C for 24 h. The degree of hydrolysis was determined as the percentage of total solubilized carbohydrates in the filtrate by the phenol-sulfuric method (Dubois, Gilles, Hamilton, Rebers, & Smit, 1956) based on the initial starch dry weight. The same procedure was applied to potato and pea starches. Acid-treated common corn, potato, and pea starches of 2, 4, 6, and 9% hydrolysis levels were obtained and then subjected to the heat-moisture treatment (HMT).

Heat-moisture treatment

Unmodified and acid-hydrolyzed common corn, potato, and pea starches were subjected to HMT by following the method of Shi, Gao, & Liu (2018) with modifications. Starch samples (75 g, dry basis) were adjusted to a moisture content of 25% by adding the appropriate amount of deionized (DI) water. The starches were sealed in a hydrothermal reactor (model TOP-HT300, Toption Instruments Co. Ltd., China) and allowed to equilibrate at 4°C for 12 h. After equilibration, the hydrothermal reactor was placed in a forced air oven and held at 120°C for 12

h. The reactor was allowed to cool to room temperature, and the starch was dried at 40°C for 18 h, ground, and sieved through a 150-µm screen.

Starch structures

The molecular-size distribution of debranched starches was characterized by high-performance size exclusion chromatography (HPSEC) according to Arijaje, Wang, Shin, & Proctor (2014). The amylopectin chain length distribution was characterized by high-performance anion-exchange chromatography equipped with pulsed amperometric detection (HPAEC-PAD) according to Wong & Jane (1995). The chains were divided into degree of polymerization (DP) ranges and classified as A chains (DP 6–12), B1 chains (DP 13–24), B2 chains (DP 25–36), and B3+ chains (DP 37+) (Hanashiro, Abe, & Hizukuri, 1996).

Starch properties

The gelatinization properties were measured using a differential scanning calorimeter (DSC, model 4000, Perkin-Elmer, Norwalk, CT). Approximately 8 mg of starch was weighed into a stainless-steel pan, and then 16 µL of DI water was added. The pan was hermetically sealed and allowed to equilibrate for one hour at room temperature before scanning from 25 to 160°C at a rate of 5°C/min. The onset temperature (T_o), peak temperature (T_p), end temperature (T_e), and gelatinization enthalpy (ΔH) were calculated by Pyris data analysis software. The type of crystalline structure and relative crystallinity were characterized by a wide-angle powder X-ray diffraction pattern according to the method of Gonzalez & Wang (2021).

The α-amylase digestion was conducted by following the method of Gonzalez & Wang. (2021). The digestion degree was measured by the phenol-sulfuric method (Dubois, Gilles, Hamilton, Rebers, & Smit, 1956) and expressed as the percentage of hydrolyzed starch.

Statistical analysis

All experiments were replicated, and each analysis was conducted in duplicate. The treatments' effects were analyzed using analysis of variance (ANOVA). The means were compared using Tukey's honest significant difference (HSD) and expressed as mean ± standard deviation using JMP Pro16 Software (SAS Institute Inc., Cary, NC).

5.4 RESULTS AND DISCUSSION

5.4.1 Acid hydrolysis

The acid hydrolysis profiles of common corn, potato, and pea starches over the course of 18 days are presented in Figure 5.1. Acid hydrolysis takes place in two phases, an initial fast hydrolysis of the amorphous lamellae and a second phase of slow hydrolysis of the crystalline lamellae (Jenkins & Donald, 1997). All three starches displayed two hydrolysis phases, but the hydrolysis rate varied with starch type. Under the conditions used in this study (0.36 M HCl, 40°C), common corn starch displayed a higher initial hydrolysis rate, reaching a hydrolysis degree of 2% after 2 days, compared with potato and pea starches, which reached a hydrolysis degree of 2% after 3 days. After 3 days, the hydrolysis rate of pea starch became similar to that of common corn starch, whereas the hydrolysis rate of potato starch increased between Days 4 and 7. Pea starch reached a hydrolysis degree of 6% after 12 days and 9% after 18 days, compared with the 10 and 15 days for common corn and potato starch, respectively.

The type of acid used, the starch and acid concentrations, starch crystalline structure, and temperature all impact the rate and extent of acid hydrolysis (Bertoft, 2004; Pang et al., 2007; Wang, Truong, & Wang, 2003). The higher hydrolysis rate of common corn starch (A-type), which occurs through 2 days, is attributed to its inferior crystalline structure with shorter A-chains and less organized crystals derived from branch linkages located inside the crystalline region (Jane, Wong, & McPherson, 1997). The increase in the hydrolysis rate of potato and pea starches after 3 days implies an interplay between the distribution of branching points, the open structure, and the presence of more water molecules in the B-type crystalline units (Jane, 2006; Kim, Lee, Kim, Lim, & Lim, 2012). The lower hydrolysis level of pea starch after 4 days suggests amylose affects acid hydrolysis because pea starch has a higher amylose content than common corn and potato starches. Using atomic force microscopy, Ridout, Parker, Hedley, Bogracheva, & Morris (2003) suggested that pea starch with a high amylose content has hard layers of blocklets formed by a crystallized amylose matrix that affects its physicochemical properties. Therefore, it is possible that the presence of crystallized amylose within the granules contributed to the lower hydrolysis rate of pea starch after 4 days.

5.4.2 Structural characterization

The molecular-size distribution of debranched common corn, potato, and pea starches, after undergoing varying degrees of AH and the combination of AH with HMT are summarized in Table 5.1. The molecular-size distribution of the debranched starches consisted of three fractions including amylose, and long and short amylopectin chains. As the AH progressed, the amylose fraction of all three starches decreased considerably, with potato and pea starches showing the greatest decreases with less than 1% amylose present at 9% AH, which is attributed

to their significantly larger DP as evidenced by their molecular-size exclusion profiles (Supplemental Figure 5.1) (Hizukuri, Takeda, Uasuda, & Suzuki, 1981). The inherently amylose-lipid complex in common corn starch may impede the hydrolysis of the amylose fraction (Morrison, Tester, Gidley, & Karkalas, 1993). The fractions of long amylopectin chains in all three starches increased significantly at 2% AH and would increase or decrease upon further hydrolysis as affected by the starch type, indicating differences in the hydrolysis patterns of the amorphous and crystalline lamellae (Jane & Shen, 1993; Ridout, Parker, Hedley, Bogracheva, & Morris, 2003). The fractions of short amylopectin chains increased for all the starches, agreeing with Srichuwong, Isono, Mishsima, & Hisamatsu (2005).

When HMT was applied alone, the amylose fraction significantly decreased, with potato starch showing the greatest decrease (49%) followed by common corn starch (44%) and pea starch (19%), whereas the long amylopectin chains of potato and pea starches increased, and the short amylopectin chains increased for all three starches. When HMT was combined with AH, the amylose fractions of all starches further decreased, but the changes in the fractions of the long amylopectin chains varied with the starch type and AH level (Table 5.1). The short amylopectin chain fractions of all AH starches increased when combined with HMT, except common corn starch at 4% AH. Zhang et al. (2014) studied the structure of HMT potato starches with different amylose and phosphate contents. They observed the most significant changes to starch structure took place in the potato starch, which contained the lowest amylose content and the highest phosphate monoesters, and they concluded that amylose protected the starch structure while phosphate monoesters destabilized starch structure during HMT. Pea starch had a significantly higher amylose content than common corn and potato starches (Table 5.1). Therefore, the present results support the protection effect of amylose on starch structure during

HMT as proposed by Zhang et al. (2014), and further showed that the high molecular-weight amylose in potato and pea starches depolymerized to a greater extent during HMT possibly because it was not co-crystallized with amylopectin.

The amylopectin chain-length distributions of AH and AH/HMT starches are presented in Table 5.2. Prior to AH, common corn starch had a greater proportion of A chains (DP 6-12), potato starch had a greater proportion of B2 (DP 25-36) and B3+ (DP 37-65) chains, while pea starch had a greater proportion of B1 (DP13-24) chains. During AH, the average chain length and the proportion of B3+ chains decreased, whereas the proportion of A chains increased for all three starches, supporting the increase in short amylopectin chains (Table 5.1). The results indicate degradation in both the amorphous and crystalline lamellae because B3+ chains are located towards the edge of the crystalline lamellae (Li & Hu, 2021). HMT alone resulted in an increase in A chains, and a decrease in B3+ chains and an average chain length for all three starches. The changes were greater in potato starch, which is attributed to the sensitivity of its very long amylopectin chains to thermal depolymerization (Gunaratne & Hoover, 2002).

When HMT was combined with AH, the proportion of amylopectin A chains further increased, and that of the B chains and the average chain lengths generally decreased for all starches. Among the three starches, pea starch exhibited significantly greater changes in all chains from HMT, with significantly increased A chains and a reduction in all B chains. The B1 and B2 chains are located within the crystalline lamellae or segments of linear chains that connect different amylopectin clusters (Srichuwong, Isono, Mishsima, & Hisamatsu, 2005). The decrease in B1 and B2 chains suggests that HMT promoted depolymerizing the original amylopectin clusters, and the crystalline type affected the depolymerization. Common corn starch was more resistant to depolymerization from HMT because of the tightly packed A-type

crystallites (Jane, 2006). In contrast, the less compact B-type crystallites in potato and pea starches were more susceptible to depolymerization from HMT. Pea starch became more susceptible to HMT when AH was incorporated because of the higher amylose content and the extensive hydrolysis of amylose during AH (Table 5.1), thus decreasing the resistance of its amylopectin crystallites to depolymerization.

5.4.3 Gelatinization properties

The changes in the gelatinization properties of AH/HMT starches varied with the starch type and AH level (Table 5.3). The gelatinization temperatures increased, but the enthalpy significantly decreased for all three starches when HMT was applied alone, agreeing with previous reports on HMT starches (Hoover & Vasanthan, 1994; Kim & Huber, 2013). The gelatinization profiles of HMT potato and pea starches significantly changed with the appearance of shoulder peaks, whereas common corn starch showed a gelatinization peak and an amylose-lipid complex peak (Figure 5.2). The increase in gelatinization temperatures of HMT starches is ascribed to enhanced interactions between amylose and amylopectin from HMT. The greater increase in gelatinization temperature of HMT potato and pea starches is attributed to the longer branch chain-length of potato starch and the higher amylose content of pea starch compared with common corn starch (Jane, Wong, & McPherson, 1997). The decrease in enthalpy indicates partial starch gelatinization (Hoover, 2010; Lin, Singh, Wen, & Chang, 2011; Varatharajan, Hoover, Liu, & Seethararaman, 2010; Zavareze & Dias, 2011).

When AH was combined with HMT, the gelatinization temperatures further increased for all starches, while the intensity of the shoulder peaks in the gelatinization profiles was affected by both starch type and AH level. Because most of the branch linkages in the B-type crystalline

structures are clustered in the amorphous lamellae and more susceptible to AH (Jane, Wong, & McPherson, 1997), more linear chains were produced with increasing AH level of the potato and pea starches, and consequently, rearranged into structures with greater thermal stability when combined with HMT. These results suggest a synergistic effect between AH and HMT in the formation of thermally stable starch crystallites (Brumovsky & Thompson, 2001; Xing, Liu, Li, Wang, & Adhikari, 2017b), and more thermally stable starch was formed with increasing AH level. When comparing the amylopectin chain distribution of starches subjected to AH/HMT, potato starch displayed the smallest proportion of A chains and the largest proportion of B chains (Table 5.2). The depolymerization of long amylopectin chains resulted in a mixture of different DP chains in the AH potato starch, which thereafter formed crystallites of a wider range of melting temperatures upon HMT compared to common corn and pea starches.

The gelatinization enthalpy reflects the extent of the double helical order, while gelatinization temperatures reflect the perfection of the double helices (Cooke & Gidley, 1992). The gelatinization enthalpy of AH/HMT starch generally increased with increasing AH level for all starches. Mutungi, Rost, Onyango, Jaros, & Rohm (2009) and Trinh, Choi, & Moon (2013) subjected cassava and water yam starches, respectively, to debranching and repeated HMT and found that the gelatinization enthalpy increased gradually with each treatment repetition. They attributed the increased enthalpy to the extra linkage of linear chains within the amorphous region and/or perfection of partially unstable crystallites. The present results demonstrate that AH exerted similar impacts on starch structures as debranching, and higher AH levels resulted in the formation of more thermally stable crystallites.

5.4.4 X-ray diffraction pattern and relative crystallinity

The X-ray diffraction patterns and relative crystallinity (RC) values of all treated starches are displayed in Figure 5.3. HMT did not change the A-type pattern of common corn starch but changed the potato and pea starches from the B- and C-type, respectively, to the A-type, agreeing with previous works (Ambiagaipalan, Hoover, Donner, & Liu, 2014; ; Gunaratne & Hoover, 2002; Shi, Gao, & Liu, 2018). When HMT was applied alone, the RC of potato starch increased, whereas that of common corn and pea starches decreased. Most studies reported a reduction in RC upon HMT for various starch sources when HMT conditions were between 20-30% moisture content and 100°C for 2-16 h. The reduced RC is ascribed to the rearrangement of amylopectin crystallites that disrupt the original organization (Gunaratne & Hoover, 2002; Sui et al., 2015; Varatharajan, Hoover, Liu, & Seethararaman, 2010; Yang et al., 2019). HMT destabilized the orientation of native crystallites in all three starches, with potato starch being the most susceptible to depolymerization by HMT (Table 5.1). Therefore, the increase in RC with HMT alone could be associated with the susceptibility of the native crystallites to HMT and the proportion of long amylopectin chains (Tables 5.1 and 5.2). The greater proportion of long amylopectin chains in potato starch were capable of rearranging into larger A-type crystallites with increased crystallinity compared to corn and pea starches.

When AH was combined with HMT, the RC of all three starches generally increased with increasing AH level, and an increase in amylose-lipid complex in common corn starch was evident by the increased intensity at $2\theta = 20°$, presumably because of the increased mobility of starch chains from the combined AH and HMT. Pea starch had greater RC values than common corn and potato starches for the same treatment level, possibly because the hydrolysis of hard amylose layers allowed the formation of more organized crystallites upon HMT. Sui et al. (2015)

speculated that if starch branched chains gained sufficient mobilization during the HMT of common corn starch, the less stable helices would recombine into smaller crystals and promote the conversion of the amorphous lamellae into a more crystalline state. The increased crystallinity of all three AH/HMT starches confirms that AH increased the mobility of starch chains.

5.4.5 Alpha-amylase digestion

The α-amylase digestion degree of native starches after 24 h follows the order of common corn > pea > potato (Table 5.4), agreeing with Shi, Gao, & Liu (2018). When HMT was applied alone, the α-amylase digestion degree varied significantly with starch type and digestion time. The digestion degree of common corn and potato starches initially increased, whereas that of pea starch decreased and continued to decrease when compared with their native counterparts. The digestion degree at 24 h decreased by 16.8%, 42.7%, and 30.8% for common corn, potato, and pea starches, respectively, relative to their native counterparts. The susceptibility of starch to amylases may increase or decrease when subjected to HMT (Qi & Tester, 2016). The increased susceptibility to amylases has been attributed to the partial gelatinization of starch granules and changes in the crystalline organization of the granule surface during HMT (Gunaratne & Hoover, 2002). The decreased susceptibility is associated with increased interactions between starch chains and the compacting of the amorphous lamellae, which prevents α-amylase binding (Hoover & Vasanthan, 1994; Wang, Zhang, Chen, & Li 2016). In this study, the differences in the digestion degree among the HMT starches reflect their different susceptibility to partial gelatinization and increased interactions among starch chains from HMT. The initial increase in α-amylase digestion of HMT common corn and potato starches is ascribed to their greater

decreases in amylose fractions (Table 5.1) and greater increases in their gelatinization degrees (Table 5.3). In contrast, HMT pea starch exhibited reduced α-amylolysis despite displaying an increased gelatinization degree, demonstrating the important role of amylose on the initial stage of α-amylase digestion because its high amylose content organized into hard matrices (Ridout, Parker, Hedley, Bogracheva, & Morris, 2003). The decreased α-amylolysis of the three starches at 24 h supports the importance of increased interactions among starch chains as evidenced by their increased gelatinization temperatures. The larger decrease in the α-amylase digestion of HMT potato starch is attributed to its greater proportion of long amylopectin chains (Table 5.1), which re-organized to form highly crystalline structures as demonstrated by its higher gelatinization temperatures and enthalpy.

When AH was combined with HMT, further decreases in the α-amylase digestion degree were noted for all three starches, confirming that HMT promoted greater interactions among amylopectin chains after more amylose and branching points were removed from AH to form more thermally stable crystallites. However, the change in α-amylase digestion degree with increasing AH level varied with starch type, with corn, potato, and pea starches showing the lowest α-amylase digestion degree at 24 h at 6%, 9% and 2% AH, respectively, when combined with HMT. The α-amylase digestion degrees of AH/HMT corn starches decreased but remained greater than those of potato and pea starches, suggesting that their crystallite structure was less organized as shown by their lower gelatinization temperatures (Table 5.3). In contrast, the significantly lower α-amylase digestion degrees of AH/HMT potato and pea starches for all AH levels and digestions times are proposed to due to their greater proportions of long B chain (B2+) forming crystallites with higher gelatinization temperatures and enthalpies. The results indicate

the importance of the native crystalline structures on the α-amylase digestion of AH/HMT starches.

5.5 CONCLUSIONS

HMT resulted in decreased amylose fractions, gelatinization enthalpy, and α-amylase digestion but increased gelatinization temperatures and relative crystallinity for three starches with different polymorphs. HMT converted the B-type potato starch and the C-type pea starch into the A-type crystalline structure, while corn starch retained the A-type structure. Both amylose fractions and amylopectin branching points of the three starches were preferentially hydrolyzed during AH and become mobile, and subsequent HMT enhanced interactions among starch chains to form more thermally stable crystallites. Therefore, the combination of AH prior to HMT further increased the gelatinization temperatures and enthalpy and relative crystallinity, and decreased susceptibility to α-amylase digestion for all three starches. When subjected to combined AH and HMT, potato and pea starches exhibited significantly lower α-amylase digestion degree compared to corn starch. The greater proportions of long amylopectin chains in potato starch and the combined higher amylose and longer amylopectin chains in pea starch are proposed to be responsible for the lower susceptibility to α-amylase digestion of the AH/HMT potato and pea starches. The findings indicate that although all three starches displayed the A-type crystalline structure following HMT, their respective native starch structures responsible for the A-, B-, and C-type crystallites still exerted influences on the properties of the new crystallites. The increased depolymerization of amylose and long amylopectin chains from increasing AH level reorganized into more thermal stabile crystallites during HMT. Therefore,

incorporating higher levels of AH prior to HMT will result in starch with greater thermal stability.

5.6 REFERENCES

Ambiagaipalan, A., Hoover, R., Donner, R., & Liu, Q. (2014). Starch chain interactions within the amorphous and crystalline domains of pulse starches during heat-moisture treatment at different temperatures and their impact on physicochemical properties. *Food Chemistry*, *143*, 175–184.

Arijaje, E., Wang, Y.-J., Shin, S., Shah, U., & Proctor, A. (2014). Effects of chemical and enzymatic modifications on starch-stearic acid complex formation. *Journal of Agricultural and Food Chemistry*, *62*, 2963–2972.

Bertoft, E. (2004). Lintnerization of two amylose-free starches of A- and B-Crystalline types, respectively. *Starch – Stärke*, *56*, 167–180.

Brumovsky, J., & Thompson, D. (2001). Production of boiling-stable granular resistant starch by partial acid hydrolysis and hydrothermal treatments of high-amylose maize starch. *Cereal Chemistry*, *78*, 680–689.

Chung, H.-J., Hoover, R., & Liu, Q. (2009). The impact of single and dual hydrothermal modifications on the molecular structure and physicochemical properties of normal corn starch. *International Journal of Biological Macromolecules*, *44*, 203–210.

Cooke, D., & Gidley, M. J. (1992). Loss of crystalline and molecular order during gelatinization. Origin of the enthalpic transition. *Carbohydrate Research*, *227*, 103–112.

Dubois, M., Gilles, K., Hamilton, J., Rebers, P., & Smith, F. (1956). Colorimetric method for determination of sugars and related substances. *Analytical Chemistry*, *28*, 350–356.

Gonzalez, A., & Wang, Y.-J. (2021). Surface removal enhances the formation of a porous structure in potato starch. *Starch – Stärke*, *73*, 2000261.

Gunaratne, A., & Hoover, R. (2002). Effect of heat-moisture treatment on the structure and physicochemical properties of tuber and root starches. *Carbohydrate Polymers*, *49*, 425–437.

Hanashiro, I., Abe, J. I., & Hizukuri, S. (1996). A periodic distribution of the chain length of the amylopectin as revealed by high performance anion-exchange chromatography. *Carbohydrate Research*, *283*, 151–159.

Hizukuri, S., Takeda, Y., Yasuda, M., & Suzuki, A. (1981). Multibranched nature of amylose and the action of debranching enzymes. *Carbohydrate Research, 94,* 205–213.

Hoover, R. (2010). The impact of heat-moisture treatment on molecular structures and properties of starches isolated from different botanical sources. *Critical Reviews in Food Science and Nutrition, 50,* 835–847.

Hoover, R., & Vasanthan, T. (1994). Effect of heat-moisture treatment on the structure and physicochemical properties of cereal, legume, and tuber starches. *Carbohydrate Research, 252,* 33–53.

Jane, J.-L. (2006). Current understanding on starch granule structures. *Journal of Applied Glycoscience, 53,* 205–213.

Jane, J., & Shen, J. J. (1993). Internal structure of the potato starch granule revealed by chemical gelatinization. *Carbohydrate Research, 247,* 279–290.

Jane, J.-L., Wong, K.-S., & McPherson, A. (1997). Branch-structure difference in starches of A- and B-type X-ray patterns revealed by their Naegeli dextrins. *Carbohydrate Research, 300,* 219–227.

Jayakody, L., & Hoover, R. (2002). The effect of lintnerization on cereal starch granules. *Food Research International, 35,* 665–680.

Jenkins, P.J., & Donald, A.M. (1997). The effect of acid hydrolysis on native starch granule structure. *Starch – Stärke, 49,* 262–267.

Jiranuntakul, W., Puttanlek, C., Rungsardthong, V., Puncha-arnon, S., & Uttapap, D. (2012). Amylopectin structure of heat–moisture treated starches. *Starch – Stärke, 64,* 470–480.

Kim, H.-Y., Lee, J.H., Kim, J.-Y., Lim, W.-J., & Lim, S.-T. (2012). Characterization of nanoparticles prepared by acid hydrolysis of various starches. *Starch – Stärke, 64,* 367–373.

Klein, B., Pinto, V.Z., Vanier, N. L., Zavareze, E.D. R., Colussi, R., Evangelho, J. A.D., Gutkoski, L.C, & Dias, A.R.G. (2013). Effect of single and dual heat–moisture treatments on properties of rice, cassava, and pinhão starch. *Carbohydrate Polymers, 98,* 1578–1584.

Kim, J.-Y., & Huber, K. (2013). Heat–moisture treatment under mildly acidic conditions alters potato starch physicochemical properties and digestibility. *Carbohydrate Polymers*, *98*, 1245–1255.

Li, C., & Hu, Y. (2021). Effects of acid hydrolysis on the evolution of starch fine molecular structures and gelatinization properties. *Food Chemistry*, *353*, 129449.

Lin, J.-H., Singh, H., Wen, C.-Y., & Chang, Y.-H. (2011). Partial-degradation and heat-moisture dual modification on the enzymatic resistance and boiling-stable resistant starch content of corn starches. *Journal of Cereal Science*, *54*, 83–89.

Mutungi, C., Rost, F., Onyango, C., Jaros, D., & Rohm, H. (2009). Crystallinity, thermal and morphological characteristics of resistant starch type III produced by hydrothermal treatment of debranched Cassava Starch. *Starch – Stärke*, *61*, 634–645.

Morrison, W., Tester, R., Gidley, M., & Karkalas, J. (1993). Resistance to acid hydrolysis of lipid-complexed amylose and lipid-free amylose in lintnerised waxy and non-waxy barley starches. *Carbohydrate Research*, *19*, 289–302.

Pang, J., P., Wang, S., Yu, J., Y., Liu, H., Yu, J., & Gao, W. (2007). Comparative studies on morphological and crystalline properties of B-type and C-type starches by acid hydrolysis. *Food Chemistry*, *105*, 989–995.

Qi, X., & Tester, R.F. (2016). Heat and moisture modification of native starch granules on susceptibility to amylase hydrolysis. *Starch – Stärke*, *68*, 816–820.

Ridout, M., Parker, M., Hedley, C., Bogracheva, T., & Morris, V. (2003). Atomic force microscopy of pea starch granules: granule architecture of wild type parent, *r* and *rb* single mutants, and the *rrb* double mutant. *Carbohydrate Research*, *338*, 2135–2147.

Shi, M., Gao, Q., & Liu, Y. (2018). Corn, potato, and wrinkled pea starches with heat–moisture treatment: structure and digestibility. *Cereal Chemistry*, *95*, 603–614.

Shin, S., Byun, J., Park, K.-H., & Moon, T.-W. (2004). Effect of partial acid hydrolysis and heat-moisture treatment on formation of resistant tuber starch. *Cereal Chemistry*, *81*, 194–198.

Srichuwong, S., Isono, N., Mishsima, T., & Hisamatsu, M. (2005). Structure of lintnerized starch is related to X-ray diffraction pattern and susceptibility to acid and enzyme hydrolysis of starch granules. *International Journal of Biological Macromolecules*, *37*, 115–121.

Sui, Z., Yao, T., Zhao, Y., Ye, X., Kong, X., & Ai, L. (2015). Effects of heat–moisture treatment reaction conditions on the physicochemical and structural properties of maize starch: moisture and length of heating. *Food Chemistry, 173*, 1125–1132.

Trinh, K.-S., Choi, S.-J., & Moon, T.-W. (2013). Structure and digestibility of debranched and hydrothermally treated water yam starch. *Starch – Stärke, 65*, 679–685.

Ulbrich, M., Natan, C., & Flöter, E. (2014). Acid modification of wheat, potato, and pea starch applying gentle conditions–impacts on starch properties. *Starch – Stärke*, *66*, 903–913.

Varatharajan, V., Hoover, R., Liu, Q., & Seethararaman, K. (2010). The impact of heat-moisture treatment on the molecular structure and physicochemical properties of normal and waxy potato starches. *Carbohydrate Polymers, 81*, 466–475.

Vermeylen, R., Goderis, B., & Delcour, J. (2006). An X-ray study of hydrothermally treated potato starch. *Carbohydrate Polymers*, *64*, 364–375.

Wang, S., Blazek, J., Gilbert, E., & Copeland, L. (2012). New insights on the mechanism of acid degradation of pea starch. *Carbohydrate Polymers*, *87*, 1941–1949.

Wang, H., Zhang, B., Chen, L., & Li, X. (2016). Understanding the structure and digestibility of heat-moisture treated starch. *International Journal of Biological Macromolecules, 88*, 1–8.

Wang, Y.-J., Truong, V.-D., & Wang, L. (2003). Structures and rheological properties of corn starch as affected by acid hydrolysis. *Carbohydrate Polymers, 52*, 327–333.

Wong, K. S., & Jane, J. (1995). Effects of pushing agents on the separation and detection of debranched amylopectin by high performance anion-exchange chromatography with pulsed amperometric detection. *Journal of Liquid Chromatography and Related Technologies*, *18*, 63–80.

Xing, J.-j., Liu, Y., Li, D., Wang, L.-j., & Adhikari, B. (2017a). Heat-moisture treatment and acid hydrolysis of corn starch in different sequences. *LWT - Food Science and Technology, 79*, 11–20.

Xing, J.-j., Liu, Y., Li, D., Wang, L.-j., & Adhikari, B. (2017b). Multiple endothermic transitions of acid hydrolyzed and heat-moisture treated corn starch. *LWT - Food Science and Technology, 81*, 195–201.

Yang, X., Chi, C., Liu, X., Zhang, Y., Zhang, H., & Wang, H. (2019). Understanding the structural and digestion changes of starch in heat-moisture treated polished rice grains with varying amylose content. *International Journal of Biological Macromolecules*, *139*, 785–792.

Zavareze, E. d. R., & Dias, A. R. G. (2011). Impact of heat-moisture treatment and annealing in starches: A review. *Carbohydrate Polymers*, *83*, 317–328.

Zhang, B., Zhao, Y., Li, X., Zhang, P., Li, L., Xie, F., & Chen, L. (2014). Effects of amylose and phosphate monoester on aggregation structures of heat-moisture treated potato starches. *Carbohydrate Polymers*, *103*, 228–233.

Zhang, B.o., Zhao, K., Su, C., Gong, B., Ge, X., Zhang, Q., & Li, W. (2020). Comparing the multi-scale structure, physicochemical properties and digestibility of wheat A- and B-starch with repeated versus continuous heat-moisture treatment. *International Journal of Biological Macromolecules, 163*, 519–528.

Zobel, H. F. (1988). Starch crystal transformations and their industrial importance. *Starch – Stärke*, *40*, 1–7.

Table 5.1. Fraction distribution (%) of debranched acid hydrolyzed and acid hydrolyzed/heat-moisture treated common corn, potato, and pea starches.[a]

Starch	Fraction distribution (%)		Acid hydrolysis (%)									
			Without heat-moisture treatment					With heat-moisture treatment				
			0	2	4	6	9	0	2	4	6	9
Common corn	Amylose		18.8±0.1a	16.5±0.3b	3.8±0.1f	4.4±0.0ef	2.8±0.0g	10.5± .0d	11.7±0.4c	4.8±0.1e	2.9±0.1g	2.0±0.0h
	Amylopectin	Long chains	18.8±0.2h	22.9±0.0f	21.7±0.1g	27.3±0.1a	24.9±0.1cd	19.2±0.2h	23.9±0.3e	26.6±0.3b	25.5±0.1c	24.5±0.2de
		Short chains	62.4±0.1h	60.6±0.3i	74.5±0.0a	68.3±0.0f	72.3±0.1c	70.3±0.1e	64.4±0.0g	68.7±0.4f	71.5±0.2d	73.4±0.2b
Potato	Amylose		19.2±0.3a	12.1±0.1b	4.0±0.1e	1.8±0.0f	0.8±0.0 g	9.8±0.0c	5.7±0.3d	1.2±0.0g	0.2±0.0h	1.2±0.0g
	Amylopectin	Long chains	31.9±0.d	35.2±0.1b	36.4±0.1a	34.6±0.3bc	30.9± 0.1d	33.5±0.3c	34.7±0.1b	25.4±0.1f	22.6 ±0.5g	28.6±0.5e
		Short chains	48.9±0.0i	52.7±0.0h	59.6±0.2f	63.5±0.3e	68.3±0.1d	56.7±0.4g	59.6±0.4f	73.4± 0.0b	77.1±0.5a	70.2±0.5c
Pea	Amylose		30.0±0.1a	15.9±0.4c	5.0±0.2e	3.0±0.0f	0.6±0.0h	24.3±0.5b	6.6±0.3d	1.7±0.0g	1.4 ±0.0gh	1.3±0.0gh
	Amylopectin	Long chains	18.6±0.d	28.5±0.3b	32.9±0.0a	31.4±0.5a	16.6±0.1e	22.1±0.4c	27.8±0.9b	28.2 ±0.4b	16.5±0.1e	16.2±0.4e
		Short chains	51.4±0.3f	55.7±0.7e	62.1±0.d	65.6±0.4c	82.8±0.1a	53.5±0.9e	65.6±1.2c	70.1±0.4b	82.1±0.1a	82.5±0.4a

[a] Mean value of two measurements ± standard deviation in the same row with different letters are significantly different (*$p < 0.05$).

Table 5.2. Amylopectin chain-length distribution of acid hydrolyzed and acid hydrolyzed/heat-moisture treated common corn, potato, and pea starches.[a]

Starch	Chain length distribution (%)	Acid hydrolysis (%)									
		Without heat-moisture treatment					With heat-moisture treatment				
		0	2	4	6	9	0	2	4	6	9
Common corn	DP 6-12 (A chains)	23.0±0.1g	23.5±0.1fg	24.7±0.2e	25.1±0.1de	25.7±0.1d	23.7±0.0f	24.8±0.1e	27.6±0.2c	28.5±0.2b	29.3±0.1a
	DP 13-24 (B1 chains)	50.7±0.3d	51.2±0.1bcd	51.7±0.2ab	52.1±0.0a	51.6±0.1abc	50.8±0.1d	52.1±0.2a	51.2±0.2bcd	50.7±0.1d	50.9±0.3cd
	DP 25-36 (B2 chains)	17.0±0.0ab	16.8±0.1bc	17.3±0.0a	16.3±0.0de	16.9±0.0bc	16.7±0.0bc	16.5±0.1cd	16.0±0.0e	15.4±0.2f	14.8±0.1g
	DP 37-65 (B3+ chains)	9.4±0.1a	8.4±0.1b	6.3±0.0c	6.5±0.0c	5.8±0.0d	8.8±0.1b	6.5±0.0c	5.2±0.0ef	5.4±0.1e	4.9±0.1f
	Average chain length	20.6±0.0a	20.3±0.0b	19.4±0.1c	19.4±0.0c	19.2±0.0d	20.3±0.0b	19.4±0.1c	18.7±0.0e	18.7±0.1e	18.3±0.1f
Potato	DP 6-12 (A chains)	20.8±0.1fg	20.2±0.2gh	20.2±0.0h	20.9±0.1fg	21.1±0.1f	23.8±0.0c	22.2±0.1e	29.3±0.2a	27.9±0.0b	22.7±0.0d
	DP 13-24 (B1 chains)	48.6±0.1e	51.7±0.2b	51.0±0.1c	51.7±0.2b	52.8±0.1a	50.0±0.1d	49.6±0.1d	47.1±0.1f	47.5±0.2f	51.4±0.0bc
	DP 25-36 (B2 chains)	19.9±0.1a	19.4±0.1abc	19.4±0.1ab	17.7±0.1cd	18.3±0.0bcd	17.9±0.0d	19.4±0.0ab	17.4±0.3d	19.4±0.3ab	18.4±0.0bcd
	DP 37-65 (B3+chains)	10.8±0.1a	8.7±0.1c	9.4±0.0b	9.7±0.1b	7.8±0.1e	8.3±0.0d	8.8±0.0c	6.1±0.3f	5.2±0.1g	7.4±0.1e
	Average chain length	21.8±0.0a	20.8±0.0c	21.1±0.0a	20.9±0.1bc	20.5±0.1d	20.2±0.0de	20.7±0.0c	18.9±0.1f	19.0±0.0f	20.2±0.0e
Pea	DP 6-12 (A chains)	19.9±0.1g	21.4±0.1ef	21.4±0.3ef	21.8±0.2e	21.5±0.2ef	20.9±0.1f	24.2±0.2d	26.3±0.1c	31.5±0.3b	36.4±0.1a
	DP 13-24 (B1 chains)	52.7±0.0a	53.2±0.1a	51.1±0.2b	51.7±0.3b	51.1±0.2b	53.1±0.2a	51.8±0.2b	50.3±0.1c	47.3±0.3d	44.7±0.2e
	DP 25-36 (B2 chains)	17.6±0.0c	17.3±0.0c	19.0±0.1a	18.5±0.0b	19.3±0.0a	17.3±0.1c	16.8±0.0d	16.9±0.2d	15.2±0.0e	14.6±0.1f
	DP 37-65 (B3+ chains)	9.8±0.0a	8.0±0.0c	8.5±0.1b	8.0±0.1c	8.1±0.1c	8.7±0.2b	7.2±0.0d	6.5±0.2e	5.9±0.0f	4.3±0.0g
	Average chain length	21.0±0.0a	20.2±0.0c	20.6±0.0b	20.4±0.0bc	20.5±0.1bc	20.5±0.1b	19.6±0.0d	19.2±0.0e	18.3±0.1f	17.2±0.0g

[a] Mean value of two measurements ± standard deviation in the same row with different letters are significantly different (*$p < 0.05$). DP: degree of polymerization in glucose units.

Table 5.3. Gelatinization properties of acid hydrolyzed/heat-moisture treated common corn, potato, and pea starches.[a]

Starch	Property	Native	Acid hydrolysis (%)				
			0	2	4	6	9
Common corn	Onset (°C)	65.7±0.0d	77.4±0.0c	81.6±0.1b	84.2±0.2a	84.2±0.4a	84.4±0.2a
	Peak (°C)	70.3±0.1d	82.7±0.1c	87.6±0.1b	92.7±0.1a	92.7±0.1a	92.9±0.1a
	End (°C)	76.8±0.2e	90.2±0.1d	101.3±0.3c	107.1±0.1b	109.3±0.2a	110.2±0.1a
	Range[b]	11.1±0.2f	12.8±0.1e	19.7±0.1d	22.8±0.3c	25.1±0.3a	25.7±0.0b
	Enthalpy (J/g)	16.8±0.2ab	7.5±0.2f	10.4±0.1d	9.7±0.1e	14.2±0.0c	16.0±0.1b
Potato	Onset (°C)	61.8±0.1e	82.0±0.2d	84.4±0.0c	86.1±0.0b	84.5±0.1c	86.6±0.1a
	Peak (°C)	66.8±0.1d	87.0±0.1c	90.1±0.1b	94.7±0.1a	95.2±0.5a	95.3±0.5a
	End (°C)	74.9±0.0e	105.9±0.3d	109.3±0.1c	123.7±0.3a	121.8±0.1b	121.6±0.5b
	Range	13.1±0.1f	23.8±0.0e	25.0±0.1d	28.6±0.3c	37.3±0.2a	35.0±0.4b
	Enthalpy (J/g)	21.0±0.0c	12.9±0.1f	15.8±0.3e	19.7±0.2d	23.2±0.1b	24.2±0.1a
Pea	Onset (°C)	56.7±0.1f	76.2±0.1e	86.6±0.1c	89.4±0.1a	88.5±0.2b	84.2±0.1d
	Peak (°C)	63.3±0.0f	80.3±0.1e	91.3±0.2d	94.2±0.0b	94.9±0.1a	93.0±0.4c
	End (°C)	73.0±0.0f	98.2±0.3e	106.5±0.2d	111.0±0.1c	118.2±0.1b	124.6±0.4a
	Range	16.4±0.1e	22.2±0.1c	19.9±0.1d	21.7±0.2c	29.8±0.1b	40.4±0.3a
	Enthalpy (J/g)	15.6±0.5b	10.5±0.5e	14.2±0.1c	13.5±0.3d	14.7±0.2c	17.4±0.0a

[a] Mean value of two measurements ± standard deviation in the same row with different letters are significantly different (*$p < 0.05$). [b] Range = (End-Onset) gelatinization temperature.

Table 5.4. Alpha-amylase digestion degree (%) of acid hydrolyzed/heat-moisture treated common corn, potato, and pea starches. [a]

Starch	Digestion time (h)	Alpha-amylase digestion degree (%)					
		Native	Acid hydrolysis (%)				
			0	2	4	6	9
Common corn	1	12.6±0.4d	23.1±0.1a	20.5±0.2b	21.4±0.2b	19.1±0.0c	20.7±0.3b
	5	21.8±0.2e	29.3±0.2a	27.2±0.4b	27.7±01b	23.5±0.3d	25.3±0.1c
	10	31.4±0.4c	35.7±1.0a	34.0±0.0b	30.8±0.1d	31.2±0.4c	30.4±0.4d
	24	51.7±0.1a	43.0±0.1b	40.0±0.8d	40.0±0.2d	36.5±0.6e	41.2±0.1c
Potato	1	6.1±0.3e	8.4±0.1d	9.0±0.0d	17.8±0.2b	18.6±0.0a	12.0±0.0c
	5	17.7±0.2b	15.8±0.0c	14.1±0.3e	20.8±0.3a	20.8±0.3a	15.0±0.0d
	10	27.8±0.1a	19.5±0.0c	16.8±0.0d	23.1±0.2b	23.5±0.3b	17.2±0.3d
	24	48.5±0.8a	27.8±0.4c	26.8±0.2d	29.6±0.6b	27.5±0.1c	24.9±0.9e
Pea	1	15.6±0.1b	13.8±0.4c	7.7±0.1e	11.0±0.0d	15.6±0.1b	22.3±0.1a
	5	28.2±0.1a	20.7±0.1c	12.4±0.0f	13.9±0.2e	16.8±0.4d	23.6±0.6b
	10	38.8±0.6a	27.6±0.2b	15.1±0.0e	16.1±0.5e	19.1±0.7d	25.9±0.0c
	24	49.6±0.4a	34.3±0.5b	21.1±0.4e	24.0±0.3d	27.1±0.1c	27.9±0.8c

[a] Mean value of two measurements ± standard deviation in the same row within the same starch, with different letters are significantly different (*p <0.05).

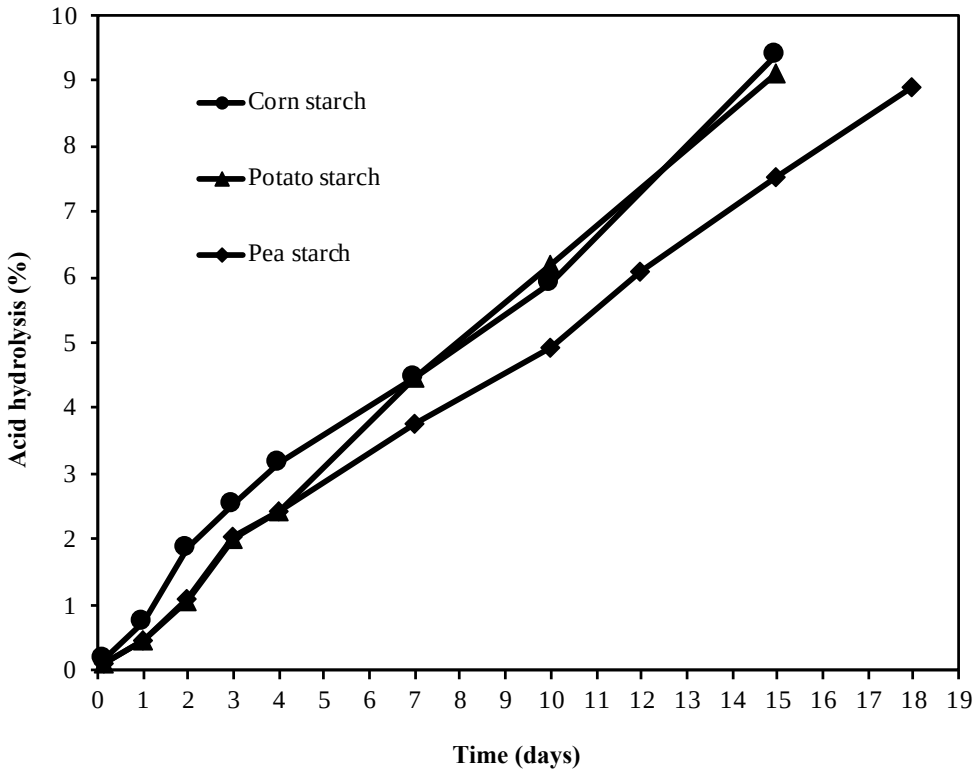

Figure 5.1. Acid hydrolysis profiles of native common corn, potato, and pea starches by 0.36 M HCl at 40 °C.

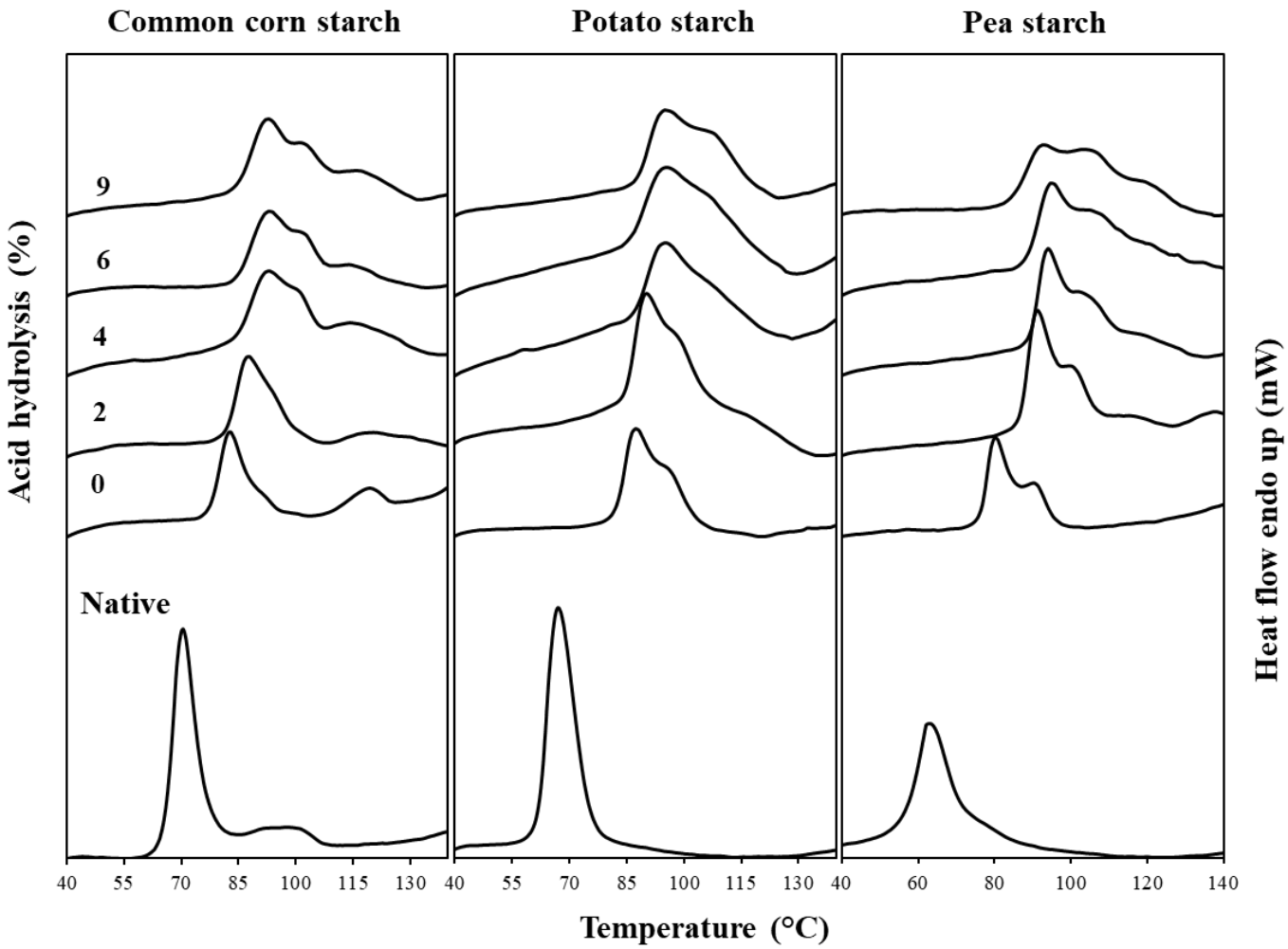

Figure 5.2. Gelatinization profiles of acid hydrolyzed/heat-moisture treated common corn, potato, and pea starches.

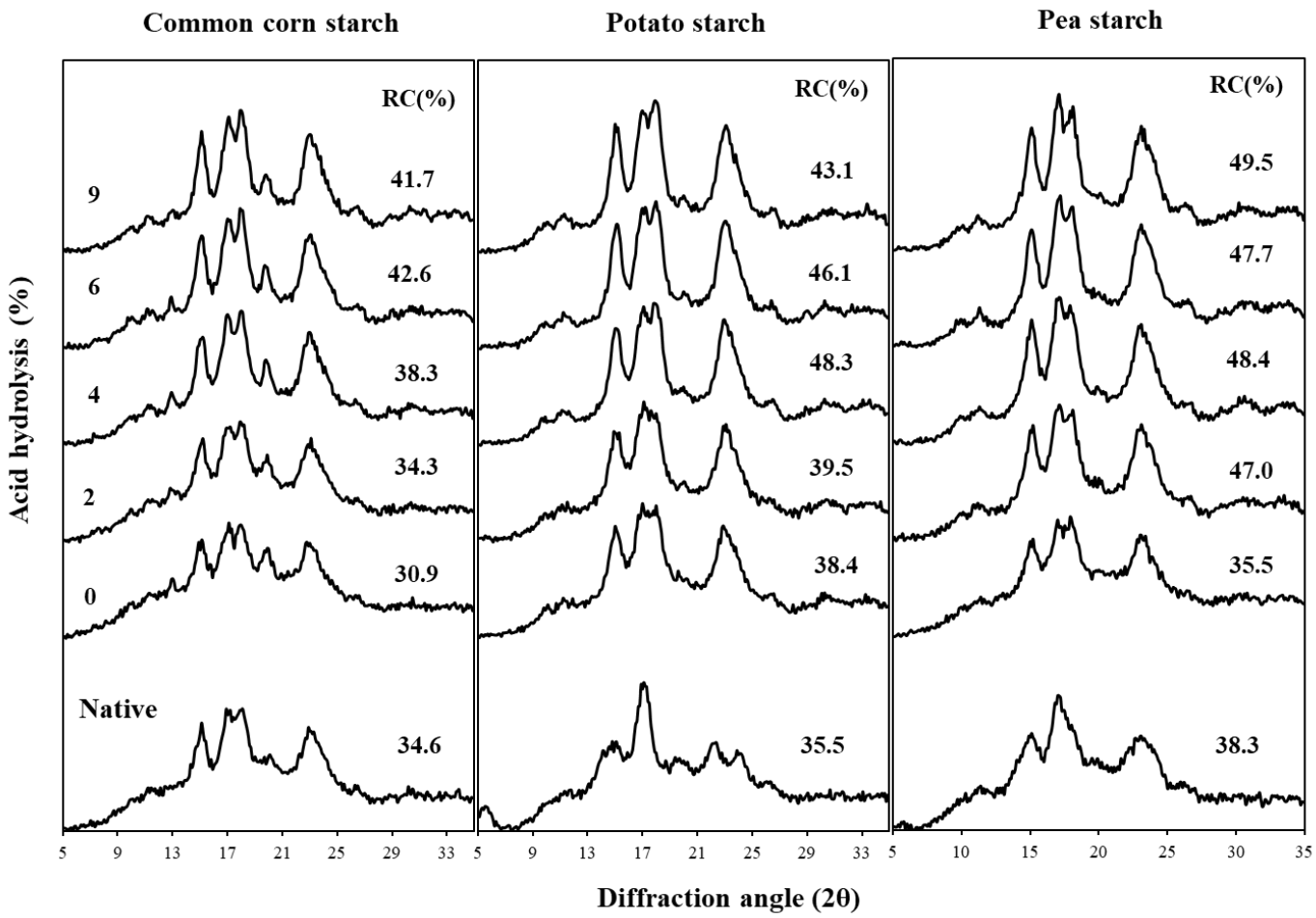

Figure 5.3. X-ray diffraction patterns and relative crystallinity (RC) of acid hydrolyzed and acid hydrolyzed/heat moisture treated common corn, potato, and pea starches.

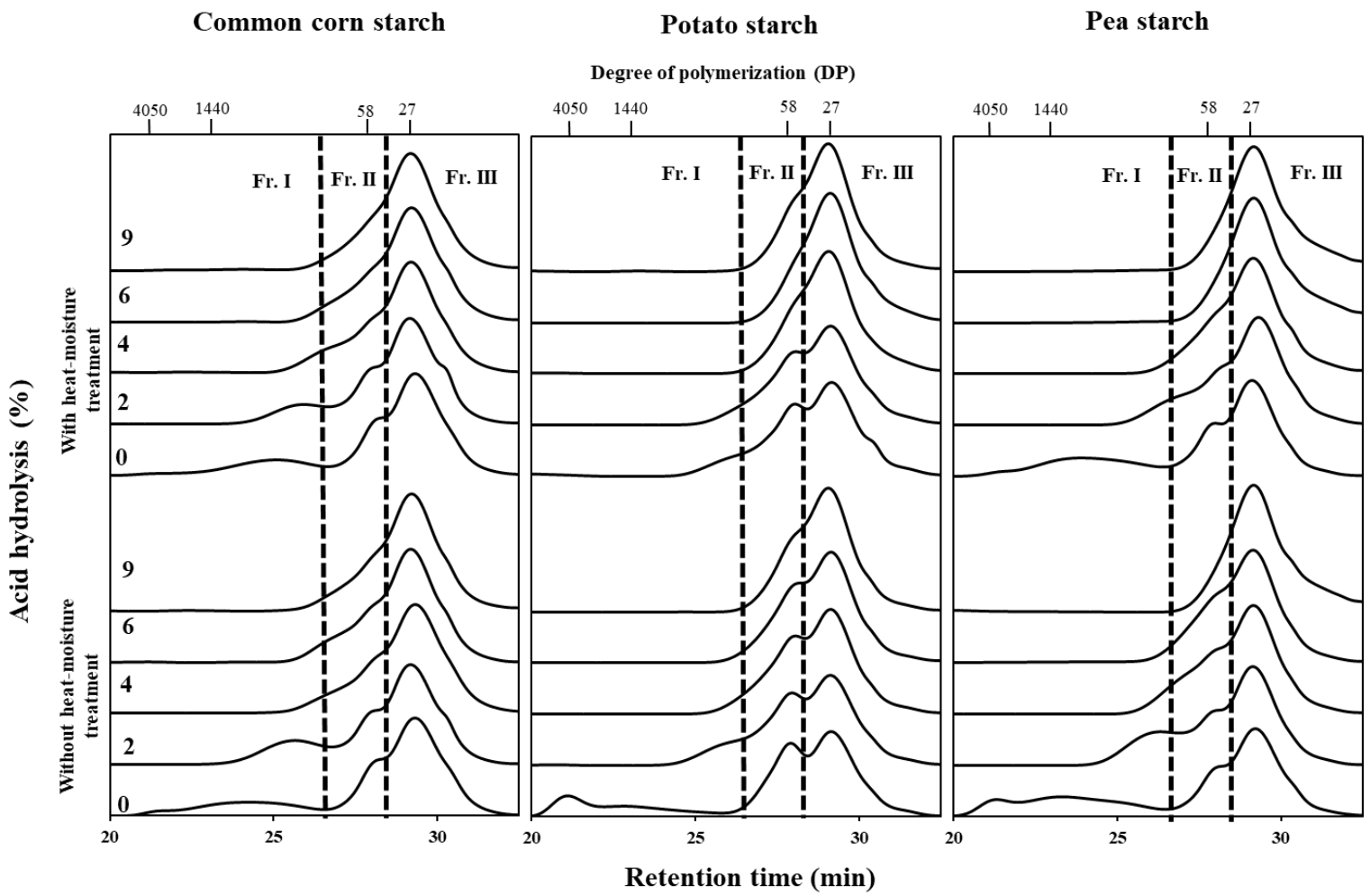

Supplemental Figure 5.1. Normalized size-exclusion chromatograms of acid hydrolyzed and acid hydrolyzed/heat-moisture treated common corn, potato, and pea starches.

CHAPTER 6

EFFECTS OF SUSPENSION MEDIA ON HIGH PRESSURE TREATED STARCHES WITH DIFFERENT CRYSTALLINE POLYMORPHS

6.1 ABSTRACT

High-pressure processing (HPP) is a starch modification method generally conducted in water, and little is known about the pressure-induced changes that occur when various suspension media are used. This study investigated the effects of water and sodium sulfate, at two ratios, on the structures and properties of HPP starches with different crystalline polymorphs. HPP in both media reduced gelatinization enthalpy and crystallinity for all three starches. HPP in sodium sulfate promoted the transition to C-type polymorphs for common corn and potato starches while water promoted the transition to B-type polymorphs. Electrostatic interactions between sodium sulfate and water molecules prevented the incorporation of water into the crystallites of common corn starch and competed for water in potato starch. All HPP starches in sodium sulfate displayed lower pasting temperatures due to diminished cross-linking among starch chains as a result of reduced water availability. The degree of alpha-amylase digestion increased for all HPP starches and was lower in sodium sulfate than in water. Only HPP common corn and potato starches in sodium sulfate displayed a porous structure after α-amylase digestion. The competition of sodium sulfate for water molecules in starch crystallites induced variations in the properties of HPP starches with different crystalline polymorphs.

Keywords: *high-pressure, gelatinization, crystallinity, enzyme susceptibility.*

6.2 INTRODUCTION

High-pressure processing (HPP) is a non-thermal technology that promotes gelatinization and physical modification of starches, which are different from those of heat-gelatinized starches (Liu et al., 2012). The extent of the changes varies with starch botanical origins and HPP parameters, including pressure-temperature combination, holding time, starch concentration, and suspending medium (Rubens and Haremans, 2000). A-type starch, such as cereal starches, is highly sensitive to high pressure treatments (Douzals et a., 1998; Rubens and Haremans, 2000), and transitions to a B-type structure at approximately 400-600 MPa (Hibi et al., 1993). In contrast, B-type starch, such as potato starch, is less sensitive to HPP, and the crystalline structure has been shown to remain unchanged (Bajaj et al., 2022). C-type starch, such as wrinkled pea, displays a susceptibility to HPP between that of the A- and B-type starches under similar conditions (Hibi et al., 1993; Bauer and Knorr, 2005; Kawai et al., 2007; Bajaj et al., 2022; Colussi et al., 2020; Liu et al., 2020; Shen et al., 2018). The effects of HPP on the physicochemical properties of starches have been extensively studied (Dominguez-Ayala et al., 2022), and water was used as the suspension medium in most studies. In general, HPP starches display decreased gelatinization temperatures and enthalpies when water is the medium due to the occurrence of gelatinization.

Katopo et al. (2002) subjected different starches, in dry powder form, to a pressure of 690 MPa, at ratios of 1:1 (v/w), and 2:1 (v/w) water to starch suspension, and 1:1 (v/w) ethanol to starch suspension for 5 min. They observed that the A-type crystalline structure of various starches changed to the B-type when water was used, but showed no change in the diffraction pattern and decreased in peak intensity when ethanol or a dry powder form was used. They also observed that when suspended in water, HPP common corn starch displayed increased pasting

temperatures and decreased pasting viscosity, which was attributed to amylose-lipid complexes that intertwined with amylopectin molecules as a result of the pressure treatment and disruption of the native structure. HPP potato starch exhibited a higher pasting temperature and a higher final viscosity but a slightly lower peak viscosity, which Katopo et al. (2002) proposed was due to the formation of a cross-linking network of amylose and amylopectin, which was induced by pressurization. More recently, Leite et al. (2017) observed no gelatinization peak for HPP pea starch when water was used as the medium at 500 and 600 MPa, but recorded decreased pasting temperatures and increased peak viscosity. The increased viscosity was attributed to increased particle size distribution from hydration and complete gelatinization. Liu et al. (2018) reported no gelatinization peak but a significantly lower peak viscosity for HPP pea starch suspended in water at 600 MPa, which was proposed to result from the rearrangement of starch molecules inhibiting hydration and swelling. In contrast, the HPP starches exhibited similar pasting profiles to their native counterparts when ethanol was the medium (Katopo et al., 2002; Leite et al., 2018).

Jane et al. (1993a) studied the effect of various salt solutions and their concentrations on starch gelatinization properties and concluded that the starch gelatinization mechanism is affected by salt solution. They observed that corn starch displayed increased onset gelatinization temperature when heated with sodium sulfate, which was attributed to a decrease of available water and a higher solution viscosity. Sodium sulfate is generally recognized as safe (GRAS) and is added during starch substitution modifications to prevent gelatinization at high temperatures and/or high pH and to enhance the reaction efficiency (Jane, 1993b; Mangels and Bailey, 1933; Shi and BeMiller, 2000). Sodium sulfate interacts strongly with water to form a cluster-like structure and its strong negative charge causes electrostatic repulsion from hydroxyl groups in

starch (Jane, 1993a), which not only stabilizes the granule at high pressure but also enhances the interactions between starch chains. Because more significant changes in the structure of HPP starch have been reported at a pressure ≥ 600 MPa, it is possible that the use of a salt solution for the HPP suspension medium may facilitate different types and/or extents of interactions between amylose and amylopectin, thus producing properties that are absent when water is used as the medium. Therefore, we hypothesized that the combination of an aqueous sodium sulfate solution and ultra-high pressure would promote the formation of different types of crystallites and properties, and these changes were affected by starch crystalline polymorphs. Therefore, the objectives of this study were to compare the changes in the molecular and granular structures of A-, B- and C-type starches during HPP in water versus in sodium sulfate and to correlate them with their morphological, physicochemical and digestion properties.

6.3 MATERIALS AND METHODS

Materials

Common corn and potato starches were purchased from Ingredion (Bridgewater, NJ). Pea starch N-753 was donated by Roquette (Portage la Prairie, Canada). Alpha-amylase from *B. licheniformis* (specific activity 55 U/mg protein) was purchased from Neogen® Megazyme (Wicklow, Ireland). All chemicals and reagents were of analytical grade.

High-pressure processing

Common corn, potato, and pea starches were treated with high hydrostatic pressure following the method of Katopo, Song, and Jane (2002) with modifications. Starch suspensions at a 1:1 1.5:1 (w/w) in water or 5% sodium sulfate were vacuum sealed into flexible

polyethylene bags and subjected to 690 MPa pressure at room temperature for 5 min in a 2 L pilot-scale high pressure processing equipment (Model FPG-9400, Stansted Fluid Power, Ltd., Essex, U.K.). After releasing the pressure in less than two seconds, the starches were washed four times with 1000 mL of deionized water, vacuum filtered through a Whatman No. 2 filter paper, and dried at 40°C for 24 h. The dried high-pressure treated starches were ground using a mortar and pestle and sieved through a 150-μm screen.

Starch structures

The molecular-size distribution of debranched starches was characterized by high-performance size exclusion chromatography (HPSEC) according to Arijaje, Wang, Shin, Shah, and Proctor (2014) with modifications. The HPSEC system consisted of an inline degasser, a Waters 515 HPLC pump with a 200-mL injector valve (model 7725i, Rheodyne, Cotati, CA), a Waters 2414 refractive index detector, a guard column (OHpak SB-G, 6.0×50 mm i.d×length), and two Shodex columns (OHpak SB×804 HQ and KB-802, 8.0×300 mm i.d×length). The molecular size distribution was calculated by comparing against dextran standards of molecular weight 180.16, 828.72, 1153 (Sigma–Aldrich), 5,200, 148,000, 872,300 (Waters Corp., Milford, MA), and 1,100,000 g/mol Sigma–Aldrich).

Starch properties

The morphology of native and HPP starches was characterized with scanning electron microscopy (SEM) according to the method of Gonzalez and Wang (2023, in review).

The pasting properties were determined with a Rapid ViscoAnalyser (RVA, model 4, Perten Instruments, Springfield, IL, U.S.). A slurry was prepared by mixing 3.0 g of starch (12%

moisture basis) with 25.0 mL of DI water. The slurry was stirred at 960 rpm for 10 s, stirred at 120 rpm for 1.0 min at 50°C, heated from 50 to 95°C at 11.2°C/min, held at 95°C for 2.5 min, cooled to 50°C at 11.2°C/min, and held at 50°C for 1.0 min. The pasting properties quantified included peak viscosity, final viscosity, breakdown, total setback, and pasting temperature.

The gelatinization properties were measured using a differential scanning calorimeter (DSC, model 4000, Perkin-Elmer, Norwalk, CT). Eight mg of starch was weighed into a stainless-steel pan and added with 16 µL of DI water. The hermetically sealed pan was equilibrated for one hour at room temperature before scanning from 25 to 125°C at a rate of 5°C/min. The onset temperature (To), peak temperature (Tp), end temperature (Te), and gelatinization enthalpy (ΔH) were calculated by Pyris data analysis software.

The crystalline structure was characterized by a wide-angle powder X-ray diffraction pattern using a Philips PW 1830 MPD diffractometer (Almelo, the Netherlands). Prior to measurement, the starch samples were equilibrated in a 100% RH chamber for 18 h. The X-ray generator was set at 45 kV and the current tube at 40 mA at the scanning 2θ angle from 5° to 35° with a step size of 0.0999° at 1 s per step. The relative crystallinity (%) was calculated as the ratio of the sum of single individual peak area divided by the total area using the X'Pert HighScore software.

The extent of α-amylase digestion of both native and HPP starches was evaluated after 1, 5, 10, and 24 h following the method of Gonzalez and Wang (2021).

Statistical analysis

All the experiments were replicated, and each analysis was conducted twice. The means were compared using Tukey's honest significant difference (HSD) and expressed as mean ± standard deviation using JMP Pro16.0 Software (SAS Institute Inc., Cary, NC).

6.4 RESULTS AND DISCUSSION

6.4.1 Structural characterization

The fractions (%) and peak degree of polymerizations (DP) of amylose and long and short amylopectin chains of debranched common corn, potato, and pea starches before and after HPP in different suspension media are summarized in **Table 6.1**. The amylose fraction of common corn starch and the respective peak DP decreased, and the fractions of long and short amylopectin chains slightly increased but their peak DP did not change when suspended in both media at 1:1 ratio and at 1.5:1 starch:water. The increase in the fractions of both long and short amylopectin chains is attributed to the depolymerization of amylose from pressure induced gelatinization. There were no changes in the fractions or their peak DPs at 1.5:1 starch:sodium sulfate, indicating little depolymerization of corn starch chains under limited water conditions. In contrast, HPP potato starch showed no change in all three fractions in water, but the amylose fraction increased, and the long amylopectin chain fraction decreased in sodium sulfate at both ratios. The results of HPP potato starch in water agree with the resistance of B-type starches to HPP (Katopo, Song, and Jane, 2002), however, the increased amylose fraction in sodium sulfate suggest that some amylose chains interacted with amylopectin chains under limited water condition. The contrast in structural changes between potato and corn starches in sodium sulfate versus in water suggests that starch crystalline structure determines its responses to HPP.

HPP pea starch exhibited decreased amylose fraction in water, increased long amylopectin chains in both media, and decreased short amylopectin chains in sodium sulfate. The changes in the amylose and long amylopectin chain fractions of HPP pea starch as affected by the suspension medium were more similar to those of common corn starch. However, the differences between the suspension media were more pronounced for pea starch presumably because of its high amylose content and the presence of B-type crystallites. The peak DP of long and short amylopectin chains increased more significantly at 1.5:1 starch:sodium sulfate, suggesting the depolymerization of amylose and long amylopectin chains.

6.4.2 X-ray diffraction pattern and relative crystallinity

The X-ray diffraction pattern and relative crystallinity (%) of HPP common corn, potato and pea starches and their native counterparts are presented in Figure 6.1. Except for corn starch at 1.5:1 starch:sodium sulfate, all three starches decreased in relative crystallinity after HPP, and there was no significant difference between the suspension media. HPP common corn starch changed from the A-type to a less defined B-type when suspended in water as evidenced by the appearance of a small peak at 5.5° but transitioned to the C-type when suspended in sodium sulfate as evidenced by the disappearance of the peak at 5.5° and the partial fusion of the split peaks at 17°. Potato starch changed from the B-type to a C-like pattern following HPP, and the change was more pronounced in sodium sulfate with the disappearance of the peak at 5.5° and the partial fusion of the peaks at 22-24°. Common corn starch was more susceptible to HPP treatment in water because of the scattered branching points in both the amorphous and crystalline lamellae and transformed into the B-type by allowing the incorporation of water (Wang, Zhu, Li., Wang, and Wang, 2017, Zhang, Wang, Liu, Xue, and Zhao, 2023). The

occurrence of C-type common corn starch in sodium sulfate is proposed to be a transitional state in which the water was sufficient to allow starch chain movement but not available to be incorporated into the helical structure to form the B-type crystallites. The diffraction pattern of pea starch did not change, but the intensity of major peaks decreased after HPP in both media. The decrease in relative crystallinity and the change from the B-type to the C-like pattern of potato starch when suspended in sodium sulfate are different from previous reports stating that potato starch was more resistant to pressure treatments at a pressure < 800 MPa (Hibi, Matsumoto, and Hagiwara, 1993; Yang, Gu, and Hemar, 2013). The B-type crystalline structure comprises clustered branching points in the amorphous lamellae and 36 water molecules located in the unit cell between the six double helices (Gallant, Bouchet, Buleon, and Perez, 1992), and both stabilize the crystalline structure by preventing the inclusion of more water molecules in the unit space during HPP (Wang, Zhu, Li., Wang, and Wang, 2017). Water is a mixture of hydrogen-bonded clusters and unbonded free water (Luck, 1980), and strong electrostatic interactions between sulfate ions and water molecules create additional cluster-like structures that reduce the free water (Jane, 1993a). Therefore, it is proposed that sodium sulfate solution exerted strong electrostatic interactions with water molecules in the B-type crystallites, which resulted in reduced water availability to stabilize its crystalline structure. Consequently, potato starch became more susceptible to pressure, and thus more depolymerization occurred, which is supported by the decreases in peak DP of amylose and amylopectin fractions, particularly at 1.5:1 starch:sodium sulfate (Table 6.1)

6.4.3 Gelatinization properties

HPP common corn starches displayed both retrogradation and gelatinization peaks as well as amylose-lipid complex peak when water was the medium and when sodium sulfate solution was used at 1:1 ratio, whereas potato and pea starches only showed the gelatinization peak regardless of medium and ratio (Supplemental Figure 6.1). Katopo, Song, and Jane (2002) reported a retrogradation peak in HPP corn starch when water was used, but no peak when pure ethanol was used. Therefore, the absence of the retrogradation peak at 1.5:1 starch:sodium sulfate is attributed to stabilization effect of sodium sulfate on starch crystallites (Jane, 1993; Stute, Klinger, Boguslawski, Eshtiaghai, and Knorr, 1996), and supported by its higher relative crystallinity (Figure 6.1). Most HPP starches suspended in both media displayed similar or decreased gelatinization temperatures and increased gelatinization range (Table 6.2). A decrease in onset gelatinization temperature indicates a reduction in the stability of starch double helices from pressure induced starch gelatinization. Some HPP corn and pea starches displayed increased peak and end gelatinization temperatures, which implies that some crystallites became more thermally stable from the rearrangement of the amorphous lamellae.

All HPP starches exhibited decreased ΔH, with potato starch displaying the highest ΔH, followed by pea starch, and corn starch the lowest for both media and ratios, agreeing with previous reports that the B-type starch is more resistant to HPP, and the A-type is the least resistant (Błaszczak, Valverde, and Fornal, 2005; Bajaj, Singh, Ghumman, Kaur, and Niwas-Mishra, 2022; Zhang, Wang, Liu, Xue, and Zhao, 2023). All HPP starches suspended in sodium sulfate displayed higher ΔH than those suspended in water at both ratios, except common corn starch at 1:1 ratio, supporting the role of sodium sulfate in reducing the extent of gelatinization by decreasing water availability. The C-type starches comprising a greater proportion of the A-

type crystallites tend to display higher gelatinization temperatures (Yu et al., 2013). Therefore, the higher onset gelatinization temperature at 1.5:1 than at 1:1 starch:sodium sulfate of pea starch indicates a greater proportion of A-type crystals remained in the granule at a pressure > 600 MPa and reduced moisture content, supporting the instability of B-type crystallites from their interactions with sodium sulfate during HPP.

6.4.4 Pasting properties

The pasting properties and profiles of native and HPP treated starches are presented in Table 6.3 and Figure 6.2, respectively. Following HPP, common corn and pea starches showed significant increases in pasting temperatures, whereas no change or decrease was observed for potato starch. Most HPP starches displayed decreased pasting viscosities compared with their native counterparts, but the differences varied significantly with starch type and suspension medium and ratio. Katopo, Song, and Jane (2002) observed similar changes in pasting properties for HPP common corn starch in water and attributed the changes to the formation of more amylose-lipid complex and amylopectin intertwining during HPP, thus limiting the granule swelling power. Comparing the suspension media, HPP common corn and pea starches in sodium sulfate generally exhibited higher pasting viscosities than in water; however, the opposite was noted for HPP potato starch. Most HPP starches exhibited higher pasting viscosities at 1.5:1 ratio than at 1:1 ratio for both suspension media. The limited water content from sodium sulfate repulsion and at a higher starch content at 1.5:1 ratio may limit the reassociation of gelatinized starch, and thus starch granule swelled to a greater extent but also disintegrated readily. The higher water contents in HPP common corn and pea starches suspended in water and at 1:1 ratio encouraged amylose forming cross-linking network with amylopectin to strengthen the granule

structure, thus resulting in higher pasting temperatures and lower peak viscosities. Furthermore, the high amylose content in pea starch played a role in the gradual change in pasting temperature by enhancing this network formation with increasing water availability.

The pasting profiles of potato starch only changed slightly because of the more resistance nature of the B-type crystalline structure to HPP (Figure 6.2B). The significantly higher peak DP of amylose and a greater proportion of long amylopectin chains in potato starch (Table 6.1) responsible for the B-type crystalline structure may also contribute to its opposite trend in pasting viscosities compared to common corn and pea starches following HPP. The decreased pasting temperature of potato starch in sodium sulfate is consistent with the depolymerization of long amylopectin chains (Table 6.1) that allowed a slightly faster swelling compared to corn and pea starches.

6.4.5 Alpha-amylase digestion and morphology

The degrees of α-amylase digestion for native and HPP treated starches, over a 24 h period, are presented in Table 6.4. Compared to their native counterparts, with the exception of pea starch at 24 h, the digestion degree of all HPP starches increased when suspended in water, and the digestion degree was lower at a ratio of 1.5:1 than at 1:1 for most digestion times. The increased digestion degree is supported by the lower ΔH values of the HPP starches compared to that of their native counterparts and is also consistent with the lower ΔH values at a ratio of 1:1 (Table 6.2).

Except for common corn at a ratio of 1:1 starch:sodium sulfate, the digestion degree at 1 and 5 h for all three starches tended to be lower when suspended in sodium sulfate than in water. After 5 h, common corn starch displayed a significantly lower digestion degree at a ratio of 1.5:1

starch:sodium sulfate after 24 h, but there was little difference for the potato and pea starches under similar conditions. The initial stages of enzyme digestion require that amylase binds to the starch surface, and thus, the lower digestion degree at early hours suggests that the surfaces of the three starches had a diminished capacity to bind when in sodium sulfate compared to when in water, likely due to their lower degrees of gelatinization and/or some changes in their structures from HPP. HPP-induced gelatinization of common corn starch was suggested in one study, to start at the less organized hilum area (Liu et al., 2020), and amylase digestion of common corn starch was shown to initiate at the surface pores and channels and proceed from the inside towards the surface (Dhital et al., 2010). Therefore, it is proposed that the reduced digestion degree of common corn starch at a ratio of 1.5:1 versus 1:1 sodium sulfate is a result of the rearranged amylose-lipid complexes and amylose-amylopectin cross-linking network concentrated towards the interior. In contrast, Dhital et al. (2010) suggests that B-type starch digestion takes place from the surface towards the granule interior, and more recently Gonzalez and Wang (2021) demonstrated that the destabilization of B-type crystallites in the outermost 10% granule surface of potato starch increased the a-amylase binding and digestion degree. Consequentially, it is proposed that disruption of the potato starch surface crystallites by HPP in both media is partly responsible for the significant increase in digestibility. Compared to common corn, pea starch only showed decreased digestion at 24 h in water at both ratios and at a ratio of 1:1 sodium sulfate. Pea starch displays both A- and B-type polymorphs, significantly higher amylose content, and a stronger cross-linking network as shown by its significantly lower pasting viscosities (Figure 6.2C). Therefore, it is suggested that similar to common corn starch, the cross-linking network located towards the hilum, restricted α-amylase activity. However, the

destabilization of the B-type crystallites in HPP pea starch disrupted the cross-linking network effect and thus increased the digestion degree.

When treated with amylase, common corn starch typically forms a porous structure with enlarged pores (Gonzalez and Wang, 2021). After 1 h of digestion, HPP common corn starch displayed a less defined porous structure when suspended at a ratio of 1.5:1 starch:sodium sulfate (Figure 6.3A), but no porous structure was observed at the other conditions. Similarly, HPP potato starch displayed a porous structure only in sodium sulfate, and the pores became more evident after 10 h and at the ratio of 1.5:1 sodium sulfate (Figure 6.3B). In contrast, pea starches did not exhibit a porous structure after HPP regardless of the suspension media (Figure 6.3C). The cross-section of HPP potato starch at a ratio of 1.5:1 starch:sodium sulfate, after 10 hours of α-amylase digestion, consisted of concentric starch layers and spaces between the layers (Figure 6.3E). The spaces may represent the partial gelatinization of the granule during HPP due to limited water availability as a result of the sodium sulfate. The incomplete gelatinization caused separation of the crystalline and the amorphous lamellae and created a channel-like structure that allowed for the formation of pores. The spaces were not observed in the cross-sections of the corn (Figure 6.3D) or pea starches (Figure 6.3F), presumably because the corn and pea starches were more gelatinized and re-organized, forming a stronger structure. Differences in the strength of the network, as evidenced by the pasting profiles (Figure 6.2), could also account for the less defined or absence of porous structures in the corn and pea starches in both water and sodium sulfate.

6.5 CONCLUSIONS

When sodium sulfate was used as the suspension medium in HPP, it exerted strong electrostatic interactions with water and induced the formation of cluster-like structures that decreased the water availability. As it competed for the water molecules in the crystalline units, sodium sulfate destabilized the B-type crystalline structure of potato starch and promoted the depolymerization of starch chains and consequently, the transition to the C-type polymorph. HPP common corn starch displayed the B-type polymorph when suspended in water, but displayed the C-type when suspended in sodium sulfate as water was unavailable and thus not incorporated in the helical structure. Due to its strong interaction with water, when sodium sulfate served as the suspension medium, it generally resulted in decreased gelatinization and the formation of cross-linking among starch chains and amylose-lipid complexes. The crosslinking of amylose-amylopectin and amylose-lipid complexes increased the pasting temperatures of HPP common corn and pea starches. The partial gelatinization and destabilization of the B-type crystallites in potato starch created channels that increased the α-amylase digestion and allowed for the formation of a porous structure. However, the strength and distribution of the crosslinked network, in combination with a greater amylose content, limited the presence of a porous structure in corn starch and prevented its formation in pea starch. This study demonstrates that sodium sulfate, in combination with ultra-high pressure, modified the properties of HPP starches by reducing free water and promoting the destabilization and rearrangement of the crystallites.

6.6 REFERENCES

Arijaje, E., Wang, Y.-J., Shin, S., Shah, U., & Proctor, A. (2014). Effects of chemical and enzymatic modifications on starch-stearic acid complex formation. *Journal of Agricultural and Food Chemistry*, 62, 2963–2972.

Bajaj, R., Singh, N., Ghumman, A., Kaur, A., & Niwas-Mishra, H. (2022). Effect of high-pressure treatment on structural, functional, and in-vitro digestibility of starches from tubers, cereals, and beans. *Starch – Stärke*, 74, 2100096.

Bauer, B. A. & Knorr, D. (2005). The impact of pressure, temperature and treatment time on starches: pressure-induced starch gelatinization as pressure time temperature indicator for high hydrostatic pressure processing. *Journal of Food Engineering*, 68, 329–334.

Błaszczak, W., Valverde, S., & Fornala, J. (2005). Effect of high pressure on the structure of potato starch. *Carbohydrate Polymers*, *59*, 377–383.

Colussi R., Kringel, D. Kaur, L., Zavareze, E.d.R., Guerra-Dias, A. R., & Singh, J. (2020). Dual modification of potato starch: Effects of heat-moisture and high pressure treatments on starch structure and functionalities. *Food Chemistry*, 318, 126475.

Dhital, S., Shrestha, A. K., & Gidley, M. (2010). Relationship between granule size and *in vitro* digestibility of maize and potato starches. *Carbohydrate Polymers*, *82*, 480–488.

Dominguez-Ayala, J., Soler, A., Mendez-Montealvo, G., & Velzquez, G. (2022). Supramolecular structure and techno functional properties of starch modified by high hydrostatic pressure (HHP): A review. *Carbohydrate Polymers.* 291, 119609.

Douzals, J.P., Perrier Cornet, J.M., Gervais, P., & Coquillet, J.C. (1998). High-pressure gelatinization of wheat starch and properties of pressure-induced gels. *Journal of Agricultural and Food Chemistry*, 46, 4824–4829.

Gallant, D.J., Bouchet, B., Buleon, A., & Perez, S. (1992). Physical characteristics of starch granules and susceptibility to enzymatic degradation. *European Journal of Clinical Nutrition*, *46*, S3–S16.

Gonzalez, A., & Wang, Y.-J. (2021). Surface removal enhances the formation of a porous structure in potato starch. *Starch – Stärke, 73*, 2000261.

Gonzalez, A., & Wang, Y.-J. (2023, in review). Effects of acid hydrolysis level prior to heat-moisture treatment on properties of starches with different crystalline polymorphs.

Hibi, Y., Matsumoto, T., & Hagiwara, S. (1993). Effect of high pressure on the crystalline structure of various starch granules. *Cereal Chemistry*, 70, 671–676.

Jane, J.-L. (1993a). Mechanism of starch gelatinization in neutral salt solutions. *Starch–Stärke*, 45, 161–168.

Jane, J.-L. (1993b). ^{13}C-NMR study of interactions between amylodextrin and neutral salts. *Starch – Stärke*, 45, 172–175.

Katopo, H., Song, Y., & Jane, J.-L. (2002). Effect and mechanism of ultrahigh hydrostatic pressure on the structure and properties of starches. *Carbohydrate Polymers*, 47, 233–244.

Kawai, J., Fukami, K., & Yamamoto, K. (2007). Effects of treatment pressure, holding time, and starch content on gelatinization and retrogradation properties of potato starch-water mixtures treated with high hydrostatic pressure. *Carbohydrate Polymers*, 69, 590–596.

Leite, T.S., de Jesus, A.L.T., Schmiele, M., & Tribst, A.A.L. (2017). High pressure processing (HPP) of pea starch: Effect on the gelatinization properties. *LWT - Food Science and Technology*, *76*, 361–369.

Liu, Z., Wang, C., Liao, X., & Shen, Q. (2020). Measurement and comparison of multi-scale structure in heat and pressure treated corn starch granule under the same degree of gelatinization. *Food Hydrocolloids*, 108, 106081.

Liu, P.-L., Qing, Z., Qun, S., Hu, X.-S., & Wu, J.-H., (2012). Effect of high hydrostatic pressure on modified non crystalline granular starch of starches with different granular type and amylase content. *LWT - Food Science and Technology*, 47(2), 450–458.

Liu, M., Wu, N.-N., Yu, G.-P., Zhai, X.-T., Chen, X., Zhang, M., Tian, X.-H., Liu, Y.-X., Wang, L.-P., & Tan, B. (2018). Physicochemical properties, structural properties, and in vitro digestibility of pea starch treated with high hydrostatic pressure. *Starch – Stärke*, 70, 1700082.

Mangels, C. E., & Bailey, C. H. (1933). Relation of concentration to action of gelatinization agents on starch. *Journal of the American Chemical Society*, 55, 1981–1988.

Rubens, P., & Heremans, K. (2000). Pressure-temperature gelatinisation phase diagram of starch: An in situ fourier transform infrared study. *Biopolymer*, 54, 524–530.

Shen X., Shang, W., Strappe, P., Chen, L., Li, X., Zhou, Z., & Blanchard, C. (2018). Manipulation of the internal structure of high amylose maize starch by high pressure treatment and its diverse influence on digestion. *Food Hydrocolloids*, 77, 40–48.

Shi, X., & BeMiller, J. N. (2000). Effect of sulfate and citrate salts on derivatization of amylase and amylopectin during hydroxypropylation of corn starch. Carbohydrate Polymers, 43, 333–336.

Stute R., Klinger, R.W., Boguslawski, S., Eshtiaghai, M.N., & Knorr, D. (1996). Effect of high pressures treatment on starches. *Starch – Stärke*, 48, 399–408.

Luck, W. A. P. (1980). The structure of aqueous systems and the influence of electrolytes. In Stanley P. Rowland (Ed.), *Water in Polymers* (pp.43–71), ACS. Washington, D.C.

Wang, J., Zhu, H., Li, S., Wang, S., & Wang, S. (2017). Insights into structure and function of high pressure-modified starches with different crystalline polymorphs. *International Journal of biological Macromolecules*, 102, 414–424.

Yang, Z., Gu, Q., & Hemar, Y. (2013). *In situ* study of maize starch gelatinization under ultra-high hydrostatic pressure using X-ray diffraction. *Carbohydrate Polymers*, *97*, 235–238.

Yu, H., Cheng, L., Yin, J., Yan, S., Liu, K., Zhang, F., Xu, B., & Li, L. (2013). Structure and physicochemical properties of starches in lotus (*Nelumbo nucifera Gaertn*.) rhizome. *Food Science & Nutrition*, 1, 273–283.

Zhang, X., Wang, C., Liu, Z., Xue, Y., & Zhao, Q. (2023). Four stages of multi-scale structural changes in rice starch during the entire high hydrostatic pressure treatment. *Food Hydrocolloids*, 134, 108012.

Table 6.1. Fraction distribution (%) and degree of polymerization (DP) of debranched high-pressure treated common corn, potato, and pea starches.[a]

Starch	Starch:suspension media (w/w)		Amylose		Amylopectin			
					Long chains		Short chains	
			Fraction (%)	Degree of polymerization	Fraction (%)	Degree of polymerization	Fraction (%)	Degree of polymerization
Common corn	Native		22.0 ± 0.5a	1394 ± 11a	18.8 ± 0.0c	107 ± 0a	59.2 ± 0.5c	41 ± 0ab
	Water	1:1	15.7 ± 0.3b	1123 ± 43b	19.5 ± 0.2ab	106 ± 1a	64.8 ± 0.1a	40 ± 0b
		1.5:1	17.7 ± 0.7b	1195 ± 17b	19.6 ± 0.2ab	107 ± 0a	62.7 ± 0.5b	41 ± 0ab
	Sodium	1:1	16.2 ± 0.1b	1178 ± 25b	19.8 ± 0.2a	107 ± 0a	64.0 ± 0.1ab	41 ± 0ab
	sulfate	1.5:1	21.3 ± 0.7a	1340 ± 4a	19.1 ± 0.0bc	107 ± 0a	59.6 ± 0.7c	41 ± 1a
Potato	Native		17.7 ± 0.2b	7771 ± 141a	34.3 ± 0.1ab	125 ± 0a	48.1 ± 0.2a	56 ± 0a
	Water	1:1	16.8 ± 0.5b	7868 ± 23a	34.5 ± 0.4ab	125 ± 0a	48.7 ± 1.0a	56 ± 0a
		1.5:1	16.7 ± 0.3b	7177 ± 1b	35.5 ± 0.4a	126 ± 0a	47.7 ± 0.8a	56 ± 0a
	Sodium	1:1	19.3 ± 0.1a	7156 ± 126b	33.4 ± 0.6b	126 ± 0a	47.3 ± 0.5a	56 ± 0a
	sulfate	1.5:1	19.1 ± 0.2a	6644 ± 0c	31.6 ± 0.1c	116 ± 0b	49.3 ± 0.3a	51 ± 0b
Pea	Native		29.8 ± 0.5a	1996 ± 17ab	14.5 ± 0.1c	101 ± 0d	55.7 ± 0.4b	44 ± 1c
	Water	1:1	22.1 ± 0.7c	1914 ± 78b	18.2 ± 0.2b	100 ± 0e	59.7 ± 0.8a	40 ± 0d
		1.5:1	25.9 ± 1.2b	2089 ± 2ab	17.3 ± 0.2b	103 ± 0b	56.8 ± 1.4ab	47 ± 0b
	Sodium	1:1	29.8 ± 0.4a	2133 ± 90ab	20.8 ± 0.0a	102 ± 0c	49.4 ± 0.4c	48 ± 0ab
	sulfate	1.5:1	30.2 ± 0.1a	2173 ± 28a	20.5 ± 0.7a	110 ± 0a	49.3 ± 0.8c	49 ± 0a

[a] Mean value of two measurements ± standard deviation in the same column, within the same starch, with different letters are significantly different (*$p < 0.05$).

Table 6.2. Gelatinization properties of high-pressure treated common corn, potato, and pea starches.[a]

Starch	Suspension media (w/w)		Retrogradation Peak					Gelatinization Peak				
			Onset (°C)	Peak (°C)	End (°C)	Range	Enthalpy (J/g)	Onset (°C)	Peak (°C)	End (°C)	Range	Enthalpy (J/g)
Common corn		Native	ND	ND	ND	ND	ND	66.3 ± 0.0b	70.7 ± 0.2b	76.9 ± 0.1c	10.6 ± 0.1c	13.5 ± 0.3a
	Water	1:1	47.8 ± 0.3b	56.1 ± 0.0a	62.7 ± 0.5a	14.9 ± 0.3a	1.6 ± 0.0a	66.8 ± 0.2ab	72.8 ± 0.6a	78.9 ± 0.0a	12.1 ± 0.2b	1.0 ± 0.0d
		1.5:1	50.6 ± 0.3a	56.3 ± 0.1a	62.6 ± 0.2a	12.1 ± 0.1c	0.4 ± 0.0c	63.7 ± 0.1c	70.7 ± 0.5b	78.4 ± 0.1b	14.7 ± 0.0a	3.0 ± 0.0c
	Sodium sulfate	1:1	48.4 ± 0.5b	55.5 ± 0.2b	62.1 ± 0.1a	13.7 ± 0.3b	1.5 ± 0.0b	67.3 ± 0.2a	73.4 ± 0.3a	79.2 ± 0.2a	11.9 ± 0.0b	0.7 ± 0.0d
		1.5:1	ND	ND	ND	ND	ND	64.0 ± 0.3c	69.3 ± 0.0b	76.0 ± 0.1d	12.0 ± 0.4b	9.6 ± 0.2b
Potato		Native	ND	ND	ND	ND	ND	62.0 ± 0.2a	66.8 ± 0.1a	74.8 ± 0.0a	12.8 ± 0.2b	16.7 ± 0.2a
	Water	1:1	ND	ND	ND	ND	ND	61.1 ± 0.0b	66.3 ± 0.0b	75.0 ± 0.3a	13.9 ± 0.3a	12.2 ± 0.2d
		1.5:1	ND	ND	ND	ND	ND	61.2 ± 0.0b	66.2 ± 0.1b	74.5 ± 0.0a	13.3 ± 0.0ab	13.1 ± 0.1c
	Sodium sulfate	1:1	ND	ND	ND	ND	ND	60.4 ± 0.1c	65.1 ± 0.0c	74.4 ± 0.3a	14.0 ± 0.2a	14.4 ± 0.2b
		1.5:1	ND	ND	ND	ND	ND	60.3 ± 0.1c	65.2 ± 0.0c	74.3 ± 0.2a	14.0 ± 0.1a	14.8 ± 0.2b
Pea		Native	ND	ND	ND	ND	ND	56.6 ± 0.0b	62.8 ± 0.4ab	71.9 ± 0.4ab	15.3 ± 0.4c	11.8 ± 0.2a
	Water	1:1	ND	ND	ND	ND	ND	50.6 ± 0.2d	61.8 ± 0.1b	73.6 ± 0.3ab	22.9 ± 0.4a	6.9 ± 0.0d
		1.5:1	ND	ND	ND	ND	ND	54.7 ± 0.0c	63.6 ± 0.0a	73.6 ± 0.4ab	18.9 ± 0.5b	6.2 ± 0.2e
	Sodium sulfate	1:1	ND	ND	ND	ND	ND	55.3 ± 0.3c	63.9 ± 0.3a	73.9 ± 1.0a	18.6 ± 0.7b	8.7 ± 0.1c
		1.5:1	ND	ND	ND	ND	ND	58.1 ± 0.2a	63.5 ± 0.2a	71.6 ± 0.2b	13.5 ± 0.3c	9.7 ± 0.2b

[a] Mean value of two measurements ± standard deviation in the same column, within the same starch, with different letters are significantly different (*$p < 0.05$). ND = Not detected

Table 6.3. Pasting properties of high-pressure treated common corn, potato, and pea starches.[a]

Starch	Starch:suspension media (w/w)		Pasting properties				
			Pasting temperature (°C)	Peak viscosity (cp)	Final viscosity (cp)	Breakdown (cp)	Total setback (cp)
Common corn	Native		75.3 ± 0.1c	2805 ± 17a	2824 ± 18a	1043 ± 13b	1061 ± 14a
	Water	1:1	84.0 ± 0.0b	1815 ± 22c	1652 ± 21d	376 ± 1d	213 ± 0d
		1.5:1	84.4 ± 0.4ab	1970 ± 3b	1824 ± 2c	485 ± 11c	338 ± 16c
	Sodium sulfate	1:1	84.7 ± 0.0a	1899 ± 5bc	1726 ± 6cd	396 ± 10d	224 ± 9d
		1.5:1	73.7 ±0.0d	2742 ± 58a	2309 ± 57b	1247 ± 35a	814 ± 34b
Potato	Native		68.9 ± 0.1a	11077 ± 90a	4079 ± 88b	7826 ± 16a	828 ± 18c
	Water	1:1	68.1 ± 0.0a	9856 ± 5bc	4481 ± 11a	6518 ± 17c	1144 ± 33a
		1.5:1	68.5 ± 0.6a	10324 ± 18b	4009 ± 8b	7242 ± 24b	928 ± 15b
	Sodium sulfate	1:1	66.6 ± 0.0b	9255 ± 335c	3068 ± 88c	6869 ± 265bc	681 ± 18d
		1.5:1	67.5 ± 0.0b	9440 ± 53c	3165 ± 45c	6974 ± 112bc	699 ± 15d
Pea	Native		69.8 ± 0.1e	3687 ± 24a	5132 ± 32a	1317 ± 23a	2761 ± 33a
	Water	1:1	85.2 ± 0.6a	2275 ± 38e	3272 ± 56e	- 3 ± 0e	993 ± 18e
		1.5:1	76.9 ± 0.0b	2401 ± 14d	3479 ± 3d	65 ± 5d	1143 ± 6d
	Sodium sulfate	1:1	73.7 ± 0.0c	2608 ± 33c	3856 ± 48c	368 ± 6c	1616 ± 8c
		1.5:1	71.3 ± 0.1d	3185 ± 29b	4590 ± 37b	863 ± 13b	2268 ± 5b

[a] Mean value of two measurements ± standard deviation in the same column, within the same starch, with different letters are significantly different (*$p < 0.05$).

Table 6.4. Degree of alpha-amylase digestion (%) in high-pressure treated common corn, potato, and pea starches.[a]

Starch	Digestion time (h)	Alpha-amylase digestion degree (%)				
		Starch: suspension media (w/w)				
		Native	Water		Sodium Sulfate	
			1:1	1.5:1	1:1	1.5:1
Common corn	1	12.9 ± 0.0d	44.4 ± 0.2a	32.1 ± 0.1b	44.5 ± 0.1a	18.4 ± 0.3c
	5	23.1 ± 0.2e	50.3 ± 0.0b	39.5 ± 0.1c	52.0 ± 0.2a	27.5 ± 1.1d
	10	32.4 ± 0.1d	55.9 ± 0.6a	49.9 ± 0.3b	56.1 ± 0.4a	35.2 ± 0.1c
	24	53.2 ± 0.5c	62.6 ± 0.3a	59.3 ± 0.2b	62.3 ± 0.6a	37.5 ± 0.3d
Potato	1	6.3 ± 0.0e	23.6 ± 0.2a	14.1 ± 0.4b	7.2 ± 0.0d	10.7 ± 0.0c
	5	20.1 ± 0.3c	42.5 ± 0.7a	25.9 ± 0.2b	20.2 ± 0.6c	20.0 ± 0.4c
	10	34.9 ± 0.2b	54.8 ± 0.3a	35.3± 0.1b	34.1 ± 0.7b	32.3 ± 1.1c
	24	49.0 ± 0.6d	64.4 ± 0.3a	60.4 ± 0.3b	57.4 ± 0.8c	58.4 ± 0.3c
Pea	1	15.3 ± 0.3d	35.0 ± 0.2a	23.1 ± 1.0b	18.9 ± 0.2c	18.2 ± 0.0c
	5	29.9 ± 0.2d	44.3 ± 0.5a	33.1 ± 0.5b	32.1 ± 0.3c	30.8 ± 0.5d
	10	37.6 ± 0.5c	45.5 ± 1.0a	45.0 ± 0.2a	40.5 ± 0.7b	39.9 ± 1.0b
	24	55.6 ± 0.8a	45.6 ± 0.6c	46.9 ± 0.3c	49.5 ± 0.4b	55.4 ± 0.1a

[a] Mean value of two measurements ± standard deviation in the same row with different letters are significantly different (*$p < 0.05$).

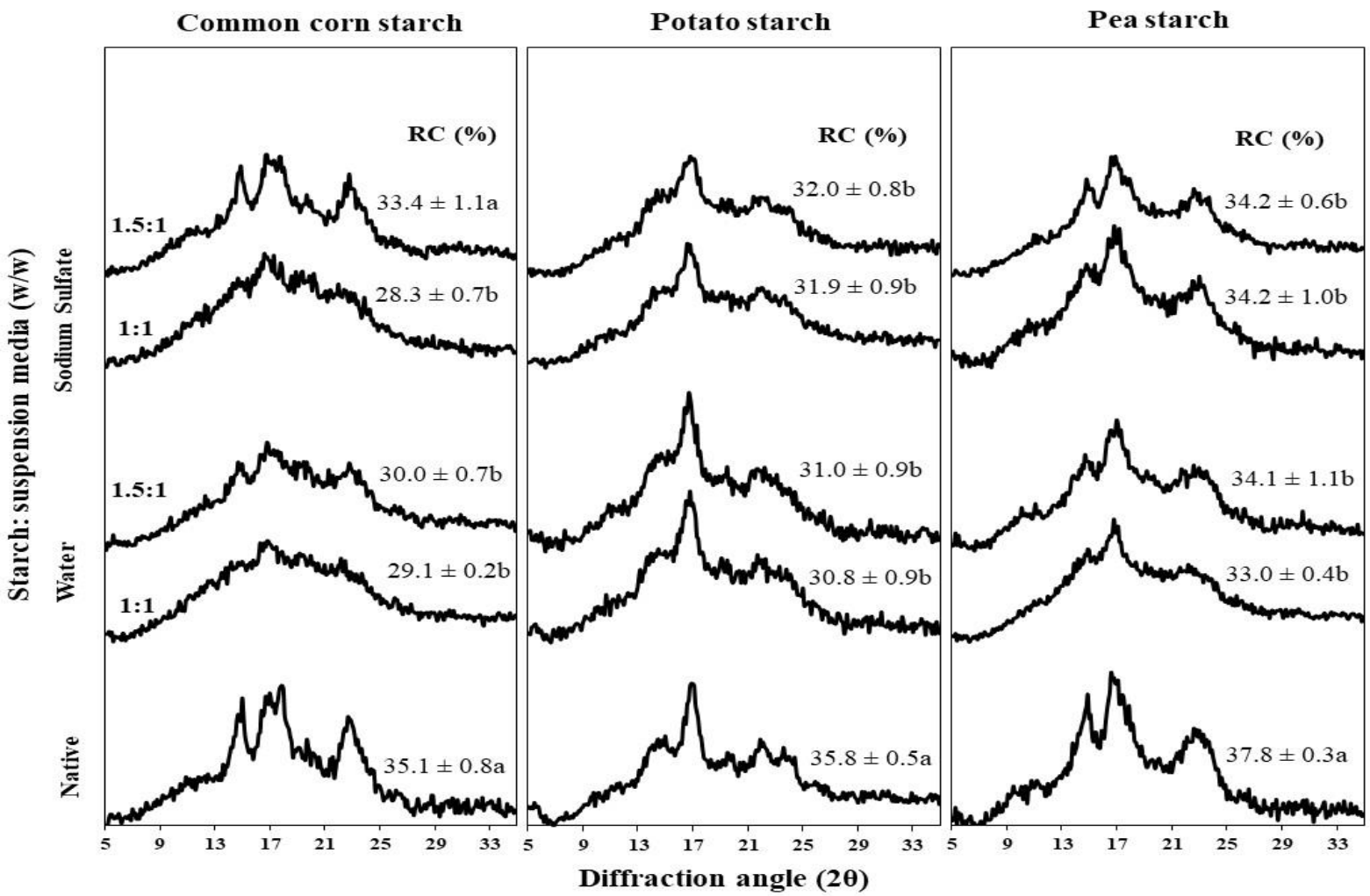

Figure 6.1. X-ray diffraction patterns and relative crystallinity (RC) of high-pressure treated common corn, potato, and pea starches.

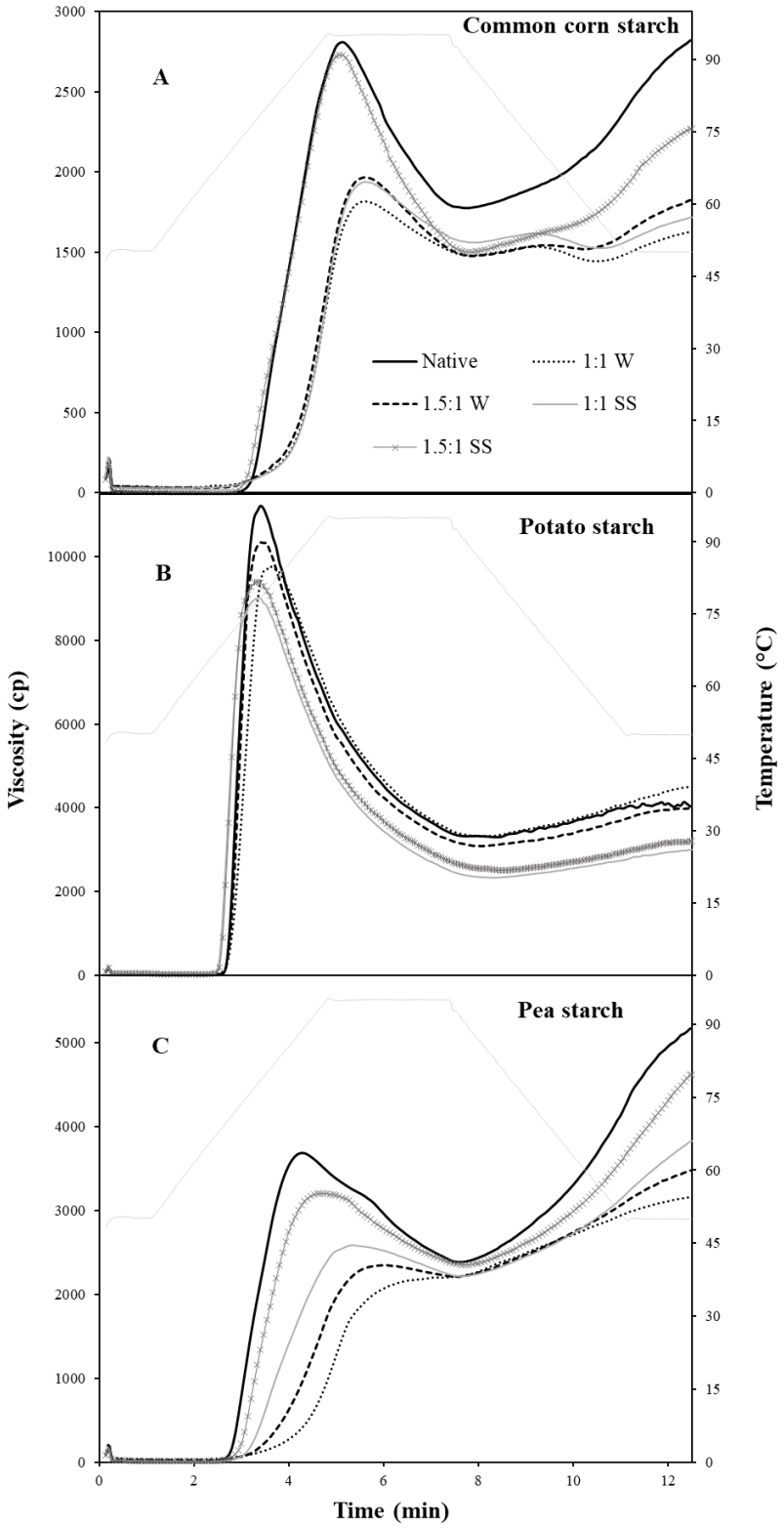

Figure 6.2. Pasting properties of high-pressure treated common corn, potato, and pea starches.

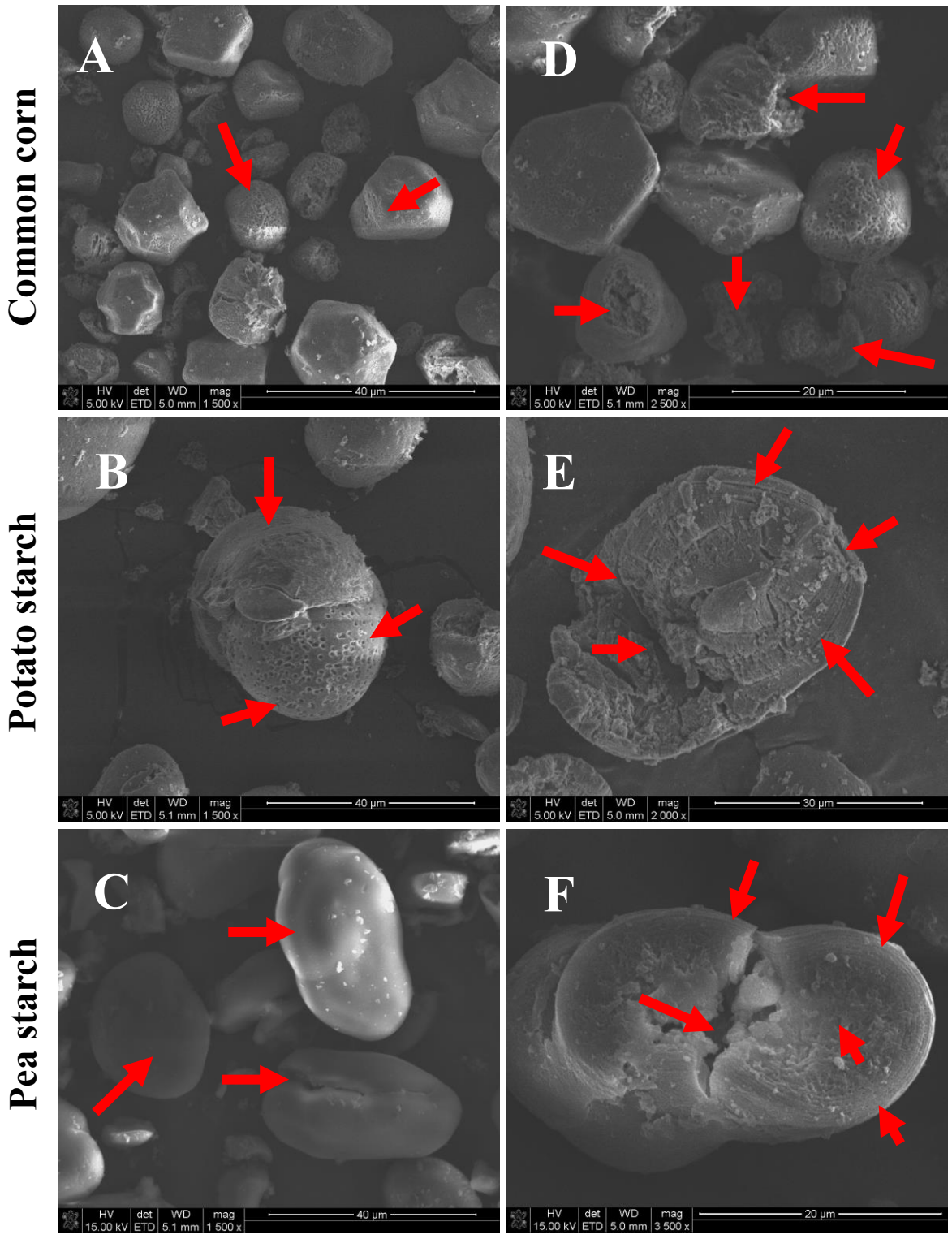

Figure 6.3. Scanning electron micrographs of high-pressure treated corn (A, D), potato (B, E), and pea starches (C, F) in a 1.5:1 starch: sodium sulfate ratio (w/w) after 10 h of α-amylase digestion.

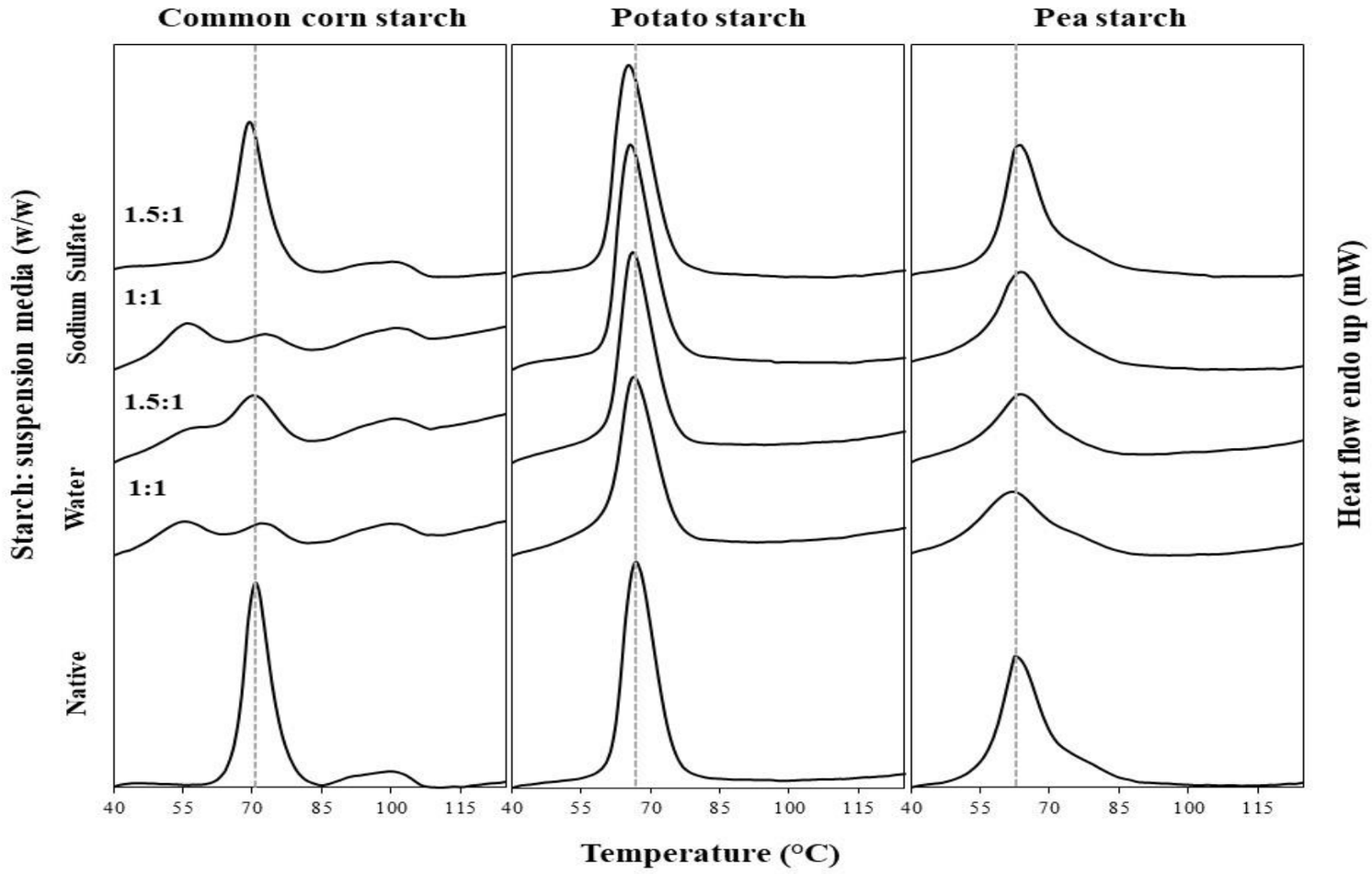

Supplemental Figure 6.1. Gelatinization profiles of high-pressure treated common corn, potato, and pea starches.

CHAPTER 7

OVERALL CONCLUSION

There is a complex relationship between starch crystalline structure and their susceptibility to amylase digestion. High levels of acid hydrolysis destabilized the tightly packed crystalline lamella, which improved the enzyme binding and allowed a better access to starch chains. The increased binding and catalytic activity resulted in the formation of a porous structure in common corn starch, and for the first time in potato starch. Starch granule surface removal by LiCl increased amylases digestion of common corn and potato starches, and confirms that the outermost surface layer in potato starch is composed of densely packed crystallites restricting amylase activity. Nevertheless, the pores of potato starch were mostly superficial compared to a deeper structure in corn starch after combined surface gelatinization and amylase digestion. Heat-moisture treatment promoted the transformation of the B-type potato and the C-type pea starches into the A-type crystalline structure. When acid hydrolysis was combined prior to HMT, acid hydrolyzed the amorphous regions, including amylose and amylopectin branching points, thus resulting in more linear chains that formed more thermally stable crystallites upon HMT. High-pressure processing in different suspension media gradually transformed the A- and B-type starches into a C-like type. The pressure-induced gelatinization and reorganization decreased when HPP starches suspended in sodium sulfate compared to in water due to its ability to form a cluster-like structure with water. The ability of sodium sulfate to compete for the water molecules in the B-type crystallites destabilized the crystalline structure of potato starch, thus increasing the α-amylase binding and promoting the formation of a porous structure. The results from this study contributed to the understanding of the role of starch surface and crystalline

structure on its susceptibility to amylases, and combined chemical or physical modifications with amylase digestion to achieve starches with increased thermal stability and crystallinity.